Identification of novel sirtuin inhibitors and activators

Inaugural-Dissertation

zur

Erlangung des Doktorgrades

Dr. rer. nat.

der Fakultät für

Biologie

an der

Universität Duisburg-Essen

vorgelegt von

Gesine Hoffmann

geboren in Cottbus

Dezember 2012

Die der vorliegenden Arbeit zugrunde liegenden Experimente wurden an der Fakultät für Biologie in der Abteilung Genetik der Universität Duisburg-Essen durchgeführt.

1. Gutachter: Prof. Dr. Ann E. Ehrenhofer-Murray

2. Gutachter: Prof. Dr. Martin Schuler

3. Gutachter:

Vorsitzender des Prüfungsausschusses: Prof. Dr. Markus Kaiser

Tag der mündlichen Prüfung: 15.04.2013

TABLE OF FIGURES

LIST OF TABLES

ABBREVIATIONS

1. INTRODUCTION 5

1.1 CHROMATIN IN EUKARYOTES 5
1.2 HISTONE MODIFICATIONS 5
1.3 HISTONE DEACETYLASES 6
1.4 SIRTUINS 6
1.4.1 *S. CEREVISIAE* HOMOLOGUE SIR2 7
1.4.2 MAMMALIAN SIRTUINS 8
1.4.3 DEACETYLATION REACTION OF SIRTUINS 15
1.4.4 STRUCTURAL CHARACTERISTICS OF SIRTUINS 17
1.5 SIRTUIN DEACETYLASE ASSAYS 18
1.6 SIRTUIN MODULATORS 19
1.6.1 ENDOGENOUS MODULATORS 20
1.6.2 SMALL-MOLECULE ACTIVATORS OF SIRTUINS 20
1.6.3 SMALL-MOLECULE INHIBITORS OF SIRTUINS 22
1.7 SIRTUINS AND DISEASE 29
1.8 AIM OF THIS THESIS 32

2. MATERIAL & METHODS 33

2.1 MEDIA AND GROWTH CONDITIONS 33
2.2 *E. COLI* STRAINS 33
2.3 SACCHAROMYCES CEREVISIAE STRAINS 33
2.4 HUMAN CANCER CELL LINES 34
2.5 MOLECULAR CLONING 34
2.6 SILENCING ASSAYS IN *SACCHAROMYCES CEREVISIAE* 36
2.7 PROTEIN PURIFICATION OF RECOMBINANT SIRT1 37
2.8 PROTEIN EXTRACTION FROM HUMAN CELLS 38
2.9 ACID EXTRACTION OF HISTONES FROM HUMAN CELLS 38
2.10 SDS-PAGE AND WESTERN BLOTTING 39
2.11 FLUORESCENCE BASED DEACETYLASE ASSAY 39
2.12 HIGH PERFORMANCE LIQUID CHROMATOGRAPHY (HPLC)-BASED DEACETYLASE ASSAY 41
2.13 FLOW CYTOMETRY 41
2.14 CELL PROLIFERATION AND VIABILITY ASSAY (MTT ASSAY) 41

3. RESULTS 43

3.1 IDENTIFICATION OF NOVEL SIRTUIN MODULATORS 43
3.1.1 ESTABLISHMENT OF MAL DEACETYLATION ASSAY 43
3.1.2 HIGH THROUGHPUT SCREENING OF COMPOUND LIBRARIES 46
3.1.3 ESTABLISHMENT OF AN HPLC-BASED P53 DEACETYLATION ASSAY 49
3.1.4 EFFECT OF INHIBITORS ON SIRT1-DEPENDENT P53 DEACETYLATION 51
3.2 *IN VITRO* CHARACTERIZATION OF POTENTIAL SIRT1 INHIBITORS 52
3.2.1 GENERATION OF N-TERMINAL TRUNCATIONS OF SIRT1 52
3.2.2 DEACETYLASE ACTIVITY OF FURTHER SIRTUIN FAMILY MEMBERS IN THE MAL DEACETYLATION ASSAY 55

3.2.3 INFLUENCE OF INHIBITORS ON FURTHER SIRTUIN FAMILY MEMBERS 56
3.2.4 SIRTUIN INHIBITION BY DERIVATES OF COMPOUNDS H AND L 59
3.3 CHARACTERIZATION OF SIRTUIN INHIBITORS *IN VIVO* 62
3.3.1 INCREASED APOPTOSIS AFTER INHIBITOR TREATMENT 62
3.3.2 SIRTUIN INHIBITORS DECREASED CELL VIABILITY AND PROLIFERATION 65
3.3.3 INDUCED APOPTOSIS WAS PARTLY DEPENDENT ON P53 67
3.3.4 INHIBITORS DID NOT CHANGE THE ACETYLATION LEVEL OF SIRTUIN TARGETS 70
3.3.5 YSIR2 INHIBITORS DID NOT INHIBIT SILENCING IN YEAST 72
3.4 VALIDATION AND CHARACTERIZATION OF POTENTIAL SIRTUIN ACTIVATORS 73

4. DISCUSSION 76

4.1 IDENTIFICATION OF SIRT1 INHIBITORS 76
4.2 THE INHIBITORY ACTIVITY OF SIRTUIN INHIBITORS IS INFLUENCED BY THE N-TERMINAL REGION OF SIRTUINS 79
4.3 COMPOUND L IS A POTENT INHIBITOR OF SIRT2 81
4.4 *IN VIVO* EFFECT OF SIRTUIN INHIBITORS 82
4.5 A SIRT1 ACTIVATOR IS AN INHIBITOR OF SIRT2 AND YSIR2 86
4.6 SUMMARY AND OUTLOOK 87

5. ABSTRACT 88

6. ZUSAMMENFASSUNG 89

7. APPENDIX 91

8. LITERATURE CITED 95

Table of figures

FIGURE 1.1: SCHEMATIC VIEW OF HUMAN SIRTUINS 8
FIGURE 1.2: DEACETYLATION REACTION OF SIRTUINS 16
FIGURE 1.3: STRUCTURE OF HUMAN SIRT2 18
FIGURE 1.4: CHEMICAL STRUCTURE OF SIRTUIN ACTIVATORS 21
FIGURE 1.5: CHEMICAL STRUCTURES OF SIRT1 ACTIVATORS 22
FIGURE 1.6: STRUCTURE OF SPLITOMICIN AND ITS ANALOGUE HR73 23
FIGURE 1.7: STRUCTURE OF SPLITOMICIN DERIVATES 24
FIGURE 1.8: STRUCTURE OF SIRTINOL AND ITS DERIVATES 24
FIGURE 1.9: SCHEMES OF PROPOSED INTERACTIONS FOR SIRTINOL AND SALERMIDE WITH SIRT2 25
FIGURE 1.10: STRUCTURE OF CAMBINOL 26
FIGURE 1.11: STRUCTURE OF SURAMIN 27
FIGURE 1.12: STRUCTURE OF TENOVIN 28
FIGURE 1.13: STRUCTURE OF THE INDOLE, EX527 28
FIGURE 2.1: FLUORESCENCE-ASSAY TO MEASURE DEACETYLASE ACTIVITY OF SIRTUINS 40
FIGURE 3.1: PURIFICATION OF RECOMBINANT HUMAN SIRT1 44
FIGURE 3.2: DEACETYLASE ACTIVITY OF PURIFIED RECOMBINANT HUMAN SIRT1 45
FIGURE 3.3: SIRT1 CATALYTIC MUTANTS SHOWED NO DEACETYLATION ACTIVITY 45
FIGURE 3.4: IDENTIFICATION OF POTENTIAL SIRT1 INHIBITORS FROM THE BIOMOL LIBRARY 47
FIGURE 3.5: IDENTIFICATION OF POTENTIAL SIRT1 INHIBITORS FROM THE CHEMBIONET LIBRARY 49
FIGURE 3.6: SEPARATION OF P53 (AA 368-386) AND AC-P53 (AA 368-386) BY HPLC 50
FIGURE 3.7: INFLUENCE OF INHIBITORS ON SIRT1-DEPENDENT P53 DEACETYLATION 51
FIGURE 3.8: GENERATION OF TRUNCATED SIRT1 CONSTRUCTS 53
FIGURE 3.9: DEACETYLASE ACTIVITY OF SIRT1 TRUNCATIONS 53
FIGURE 3.10: SIRT1 TRUNCATIONS HAD DIFFERENT DEACETYLASE ACTIVITY 54
FIGURE 3.11: INFLUENCE OF RESVERATROL AND SURAMIN ON SIRT1 TRUNCATIONS 55
FIGURE 3.12: PURIFICATION AND DEACETYLASE ACTIVITY OF YSIR2 55
FIGURE 3.13: DEACETYLASE ACTIVITY OF HUMAN SIRTUINS IN THE MAL DEACETYLATION ASSAY 56
FIGURE 3.14: INFLUENCE OF INHIBITORS ON FURTHER SIRTUIN MEMBERS 57
FIGURE 3.15: COMPOUND L IS A POTENT SIRT2 INHIBITOR 58
FIGURE 3.16: INHIBITORY EFFECT OF COMPOUND L IN THE P53 DEACETYLATION ASSAY 59
FIGURE 3.17: INHIBITORY EFFECT OF H DERIVATES ON SIRT1 DEPENDENT MAL DEACETYLATION 60
FIGURE 3.18: INHIBITORY EFFECT OF L DERIVATES ON SIRT2 DEPENDENT MAL DEACETYLATION 61
FIGURE 3.19: COMPOUND L AS WELL AS L-I INHIBITED P53 DEACETYLATION 62
FIGURE 3.20: CELL DEATH OF A549 CELLS AFTER INHIBITOR TREATMENT 63
FIGURE 3.21: INFLUENCE OF COMPOUND B, C AND F ON THE CANCER CELL LINE A549 64
FIGURE 3.22: COMPOUND H INDUCED APOPTOSIS OF CANCER CELLS 64
FIGURE 3.23: INFLUENCE OF COMPOUND L ON THE CANCER CELL LINES A549 AND H1299 65
FIGURE 3.24: CELL PROLIFERATION WAS DECREASED AFTER INHIBITOR TREATMENT 66
FIGURE 3.25: CELL VIABILITY WAS REDUCED AFTER INHIBITOR TREATMENT 67
FIGURE 3.26: H1299 (MS48) CELLS EXPRESSED P53 PROTEIN 68

FIGURE 3.27: INFLUENCE OF COMPOUND L AND L-I ON H1299 (MS48) 69
FIGURE 3.28: INFLUENCE OF COMPOUND L AND L-I ON H1299 (MS48) AFTER TAMOXIFEN TREATMENT 70
FIGURE 3.29: NO ADDITIONAL INCREASE OF THE P53 ACETYLATION SIGNAL AFTER INHIBITOR TREATMENTS 71
FIGURE 3.30: NO ACETYLATION SIGNAL OF A-TUBULIN AFTER TREATMENT WITH L OR L-I 71
FIGURE 3.31: YSIR2 INHIBITORS HAD NO INFLUENCE ON *HMR* SILENCING 73
FIGURE 3.32: CHEMICAL STRUCTURES OF POTENTIAL SIRT1 ACTIVATORS 73
FIGURE 3.33: IDENTIFICATION OF SIRT1 ACTIVATORS 74
FIGURE 3.34: INFLUENCE OF COMPOUND 1 ON SIRT1 TRUNCATIONS 74
FIGURE 3.35: INHIBITORY EFFECT OF COMPOUND 1 ON SIRT2 AND YEAST SIR2 75
FIGURE 7.1: SIR2 CHIMERAS INDUCED TELOMERIC SILENCING 92
FIGURE 7.2: SIR2 CHIMERAS INDUCED *HMR* SILENCING 92
FIGURE 7.3: CLONING STRATEGIES OF THE SIRT1 CHIMERAS 93
FIGURE 7.4: SIRT1 CHIMERAS DID NOT INDUCE TELOMERIC SILENCING 93
FIGURE 7.5: SIRT1 CHIMERAS DID NOT INDUCE *HMR* SILENCING 94

List of tables

TABLE 2.1: *E. COLI* STRAINS USED IN THIS STUDY
TABLE 2.2: *S. CEREVISIAE* STRAINS USED IN THIS STUDY
TABLE 2.3: PLASMIDS USED IN THIS STUDY
TABLE 2.4: OLIGONUCLEOTIDES USED FOR CLONING AND MUTAGENESIS
TABLE 2.5: ANTIBODIES USED IN THIS STUDY

Abbreviations

5-FOA	5-fluoro-orotic acid
aa	amino acid
Ac	acetylated
AK	antibody
APS	ammoniumpersulfat
ATP	adenosine triphosphate
bp	base pairs
BSA	bovine serum albumin
DNS	desoxyribonucleic acid
E.coli	*Escherichia coli*
EDTA	ethylen-diamin-tetraacetat
EGTA	ethylen-glycol-tetraacetat
FACS	fluorescence associated cell sorting
FCS	fetal calf serum
HAT	histone acetyltransferase

HEPES	N-(2-Hydroxyethyl)-piparazin-N´-2-ethansulfonsäure
HDAC	histone deacetylase
HMR / HML	homotallic mating right / left
HP1	Heterochromatin Protein 1
HPLC	High Performance Liquid Chromatography
HRP	horseradish peroxidase
Hst	homologe of Sir two
kDa	kilo Dalton
LB	Luria-Bertani
NAD^+	nicotinamide adenine dinucleotide
NF-κB	nuclear factor-κB
nm	nano metre
NP-40	Nonidet-P40
OD	optical density
PBS	phosphat buffered saline
PCR	polymerase chain reaction
rDNA	ribosomal DNA
rpm	rounds per minute
RNA	ribonucleic acid
RT	room temperature
Sir	silent information regulator
siRNA	small interfering RNA
mRNA	messenger RNA
SDS	sodium dodecyl-sulfate
SDS-PAGE	SDS polyacrylamide gel electrophoresis
TBST	tris buffered saline with Tween 20
TCA	trichloroacetic acid
TEMED	tetramethylendiamin
TFA	trifluoroacetic acid
TRIS	tris-(hydroxymethyl)-aminomethan
Tween-20	polyoxyethylen-(20)-sorbitan-monolaurat
v/v	by volume
wt	wild-type
YM	yeast minimal medium
YPD	yeast peptone medium

Yeast genes were named according to nomenclature conventions of *Saccharomyces cerevisiae* genome database (SGD).

Amino acids were given in the single letter code, e.g. K = lysine

1. Introduction

1.1 Chromatin in eukaryotes

The structure of chromatin plays an important role in the regulation of gene transcription, replication and DNA repair. In eukaryotic cells, the DNA is organized into long linear structures called chromosomes. DNA in combination with specialized proteins forms chromatin, which allows the long DNA molecules to fit into the cell nucleus. The basic repeat element of chromatin is the nucleosome, where 147 base pairs of DNA are wrapped around a histone octamer consisting of two molecules of each histone type, H2A, H2B, H3 and H4 (Kornberg 1974; Luger et al. 1997). This structure is repeated every 200 ± 40 base pairs and forms a "beads-on-a-string" fibre structure with a diameter of 10 nm. With the addition of linker histone H1 in mammals (Contreras et al. 2003), the "beads-on-a-string" structure coils into a further condensed 30 nm-diameter helical structure known as the 30 nm fibre.

1.2 Histone modifications

Histone proteins consist of a globular domain and a more flexible, charged N-terminal region known as the histone tail. Histone tails are rich in lysine residues and are targets for covalent modifications, especially the strongly conserved histone tails of H3 and H4. Such posttranslational modifications are the acetylation, methylation and ubiquitination of lysine (K) residues, the methylation of arginines (R) and the phosphorylation of serine (S) and threonine (T) residues. These modifications regulate interactions with DNA and other proteins. They are deposited during cell cycle progression, DNA replication, DNA damage and repair and influence overall chromosome stability (reviewed in (Jenuwein and Allis 2001)). Furthermore, histones can be sumoylated, with the consequence of transcriptional repression (Nathan et al. 2006).

The acetylation status of histone proteins plays a role in protein-protein interactions, nuclear transport, DNA-binding affinity, and it alters gene transcription. The reversible acetylation of ε-amino groups of lysines in histone proteins neutralizes the positive charge and therefore weakens the interaction with the negatively charged DNA phosphate backbone. This allows different transcription factors to gain access to the promoters of target genes (reviewed in (Turner 1991)). This characterizes euchromatin, which is transcriptionally active and tends to

be hyperacetylated. Removal of acetyl groups from lysine residues results in stronger histone-DNA contact and compaction of chromatin, called heterochromatin. This chromatin structure represses gene transcription and tends to be hypoacetylated (Braunstein et al. 1993). This histone modification depends on the activity of histone acetyltransferases (HATs) and histone deacetylases (HDACs).

1.3 Histone deacetylases

HDACs are a group of enzymes that remove acetyl groups from a ε-N-acetyl lysine amino acid on histones. So far, there are eighteen different histone deacetylases known in humans. They are divided into four groups based on their functions and protein sequence similarity to yeast transcriptional repressors. Class I and class II are considered "classical" HDACs whose activities are inhibited by Trichostatin A (TSA). HDACs of class I (HDAC1, -2, -3 and -8) are homologues of the yeast transcription factor Rpd3 (reduced potassium dependency 3). They have a conserved structure and are located preferentially in the nucleus. Class II HDACs (HDAC4, -5, -6, -7, -9 and -10) are homologues of yeast Hda1 (histone deacetylase 1), and they are able to shuttle in and out of the nucleus, depending on different signals (de Ruijter AJ, 2003). HDAC11 is the only member of class IV HDAC that has characteristics of both class I and II. Class III HDACs are a family of nicotinamide adenine dinucleotide (NAD^+)-dependent histone deacetylases, so called sirtuins. In contrast to class I, II and IV they are not Zn^{2+}-dependent, although a Zn^{2+}-binding domain exists in the catalytic core domain, and they cannot be inhibited by TSA.

1.4 Sirtuins

The founding member of sirtuins is the yeast transcriptional repressor Sir2 (**s**ilent **i**nformation **r**egulator 2). It was originally identified in *Saccharomyces cerevisiae* as a factor involved in regulation of mating type (Rine and Herskowitz 1987). Meanwhile, more than 60 homologues of sirtuins have been found in plants, bacteria, vertebrates and invertebrates. Each sirtuin has a protein core domain of approximately 270 amino acids, and most of them contain NAD^+-dependent deacetylase activity. This catalytic core domain defines the sirtuin family, which is conserved from bacteria to eukaryotes (Frye 2000). In addition to the core domain, each sirtuin contains a unique N- and/or C-terminal region that varies in length and sequence.

1.4.1 *S. cerevisiae* homologue Sir2

The discovery of the Sir2 protein from the budding yeast *S. cerevisiae* resulted from studies of how the yeast cell type, known as mating type, is regulated (Rine and Herskowitz 1987). Mating type in yeast is determined by a single locus, *MAT*, which regulates the sexual behaviour of both haploid and diploid cells. Haploid cells contain only one allele of *MAT*, *MAT***a** or *MAT*α, which determines their mating type. *MAT***a** cells can mate only with *MAT*α cells, which produces *MAT***a**/α diploid cells. Furthermore, yeast cells also contain two silenced copies of the mating type information, *HML* and *HMR*. The *HML* (**h**omothallic **m**ating **l**eft) locus carries a silenced copy of the α allele, and the *HMR* (**h**omothallic **m**ating **r**ight) locus carries a copy of the **a** allele.

Sir2 is required for all known types of silencing in yeast: (I) repression of the mating-type loci *HML* and *HMR*, (II) telomeric repression, (III) rDNA silencing (reviewed in (Stone and Pillus 1998)). Even though it is required at all three silenced regions, the repressive mechanism differs. At telomeric DNA regions and at the silent mating type loci, Sir2, together with Sir3 and Sir4, builds the SIR complex, which is an essential structural component of heterochromatin. Additionally, at the *HM* loci, Sir1 is necessary for the SIR complex to assemble at the silencers. Sir2 deacetylates the histones H3 and H4 in a NAD^+-dependent fashion and thereby creates new high-affinity binding sites for Sir3 and Sir4 at adjacent nucleosomes. They bind to the deacetylated tails of H3 and H4 as well as to unmethylated H3K79 and spread throughout the silent locus. At the ribosomal DNA locus (rDNA), Sir2, together with Net1 and Cdc14, builds the RENT complex (regulator of nucleolar silencing and telophase exit) to silence integrated reporter genes (reviewed in (Rusche et al. 2003)).

One reason of aging in yeast is the accumulation of circular species of rDNA, so-called extrachromosomal rDNA circles (ERCs). They are able to replicate and preferentially segregated to mother cells during cell division. As a result, aging mother cells accumulate vast amounts of ERCs (Sinclair and Guarente 1997). In 1999, it was shown that the addition of an extra copy of the *SIR2* gene extend lifespan by suppressing rDNA recombination and decreasing ERC formation, while deletion of *SIR2* has the opposite effect (Kaeberlein et al. 1999). Also in *Caenorhabditis elegans* (Tissenbaum and Guarente 2001) and *Drosophila melanogaster* (Rogina and Helfand 2004) an extension of lifespan could be observed through increased dosage of a *SIR2* gene. However, recent studies have called the effect of increased *SIR2* dosage in both *C. elegans* and *D. melanogaster* to question (Burnett et al. 2011). Nonetheless, these findings have led to widespread interest in mammalian sirtuins.

1.4.2 Mammalian sirtuins

The mammalian sirtuins consist of seven members, SirT1 to SirT7 (displayed in **Figure 1.1**). They can be localized in different cell compartments, have distinct substrates and a broad range of functions. Their expression level differs and can be modulate through different environmental or pathological conditions. Similar to the yeast transcription factor Sir2, some of them deacetylate histones, but several sirtuins also have targets such as enzymes or transcription factors that regulate stress, metabolism and survival pathways. Because of their sequence similarity, they are divided into subgroups. Class I sirtuins including SirT1 to SirT3 have a robust deacetylase activity compare to the other sirtuins, which have either no detectable or very weak deacetylase activity. Class II comprises only SirT4 and Class III only SirT5, whereas SirT6 and SirT7 belong to Class IV (Frye 2000).

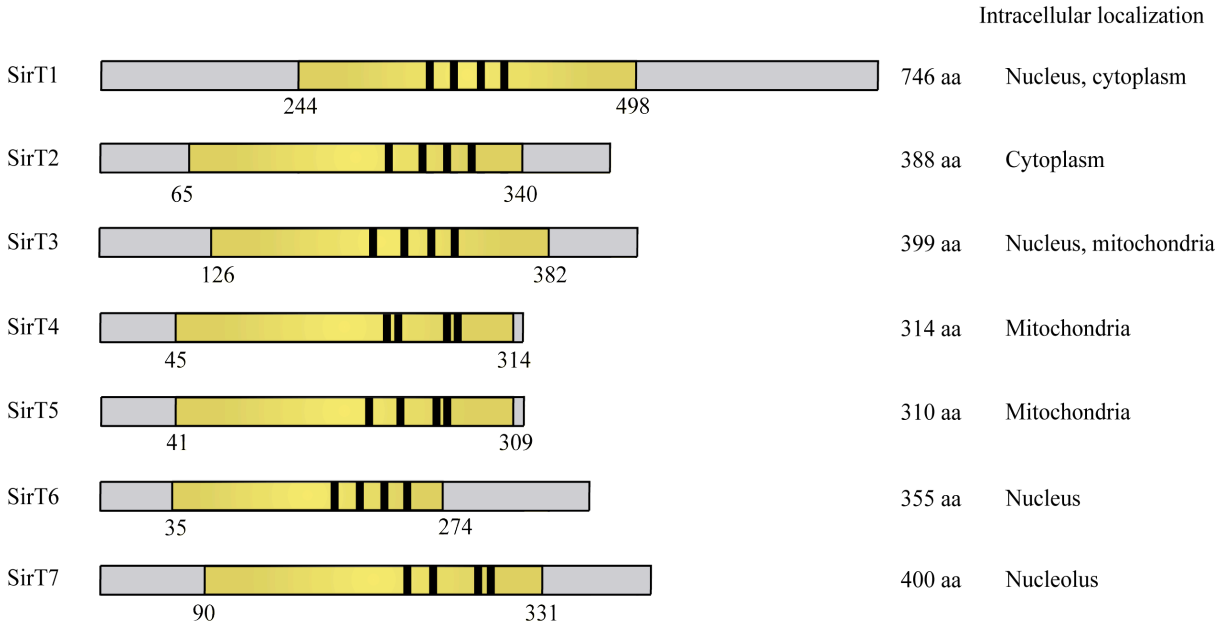

Figure 1.1: Schematic view of human sirtuins
The illustration shows the domain architecture of human sirtuins (SirT1-SirT7) and their intracellular localization. The NAD^+-dependent conserved catalytic core domain (yellow) is flanked by variable N- and C-terminal segments. Zn^{2+}-binding domains (black) are located in the catalytic core domain. The picture is modified from (Rajendran et. al, 2011).

SirT1 is the closest homolog of the Sir2 protein of *S. cerevisiae* (Voelter-Mahlknecht and Mahlknecht 2006), and it is the best-characterized mammalian sirtuin so far. It plays an important role in many biological processes like cancer development, calorie restriction and aging associated diseases. SirT1 is mainly located at the nucleus, but apart from 2 NLSs (nuclear localisation signal), it also contains 2 NES (nuclear export signal) domains. Through these domains, SirT1 can shuttle between the cytoplasm and the nucleus (Tanno et al. 2007). The nuclear-cytoplasmic distribution and enzymatic activity of SirT1 is regulated by different

modifications. For instance, JNK (c-**J**un **N**-terminal **k**inase) interacts directly with SirT1 upon oxidative stress and phosphorylates SirT1 at Ser^{27}, Ser^{47} and Thr^{530}, thereby enhancing its nuclear localisation and enzymatic activity (Nasrin et al. 2009). In contrast to this, mTOR-dependent phosphorylation of Ser^{47} alone results in inhibition of SirT1 deacetylase activity (Back et al. 2011). All in all, Sasaki *et al.* identified 13 phosphorylation sites on SirT1, which are located in the N- and C-terminal region. Two of these sites, Thr^{530} and Ser^{540}, are substrates of CDK (cyclin B/cyclin-dependent kinase 1) complexes. Further analyses show that phosphorylation of these two sites are required for normal cell cycle progression (Sasaki et al. 2008). In murine SirT1, four more phosphorylation sites of protein kinase CK2 were identified, whereby two of them were also described in human SirT1 at the corresponding amino acids Ser^{659} and Ser^{661} (Kang et al. 2009; Zschoernig and Mahlknecht 2009). Ser^{659} and Ser^{661} lie within the ESA (**e**ssential for **S**irT1 **a**ctivity) motif of SirT1, which comprises a small region from amino acids 641-665 (Kang et al. 2011). ESA interacts with the catalytic core domain, activates the catalytic activity and increases the affinity for substrates.

The binding site of ESA in the catalytic core domain is also the interaction site of DBC1 (**d**eleted in **b**reast **c**ancer 1), the endogenous inhibitor of SirT1 (Kim et al. 2008). It is possible that the two phosphorylation sites within ESA modulate the interaction of the C-terminaus with the catalytic core domain, and thereby control the SirT1 activity and substrate recognition through an allosteric mechanism (Flick and Luscher 2012).

In addition to phosphorylation, SirT1 is modified by sumoylation, which increases catalytic activity. SUMO is a small ubiquitin-related protein that can be attached to the C-terminal end of SirT1 at Lys^{734}. Upon stress, SirT1 becomes associated with the nuclear desumoylase SENP1, which reduces SirT1 activity and promotes p53 activation and cell death (Yang et al. 2007). The mechanism is not fully understood, but it is suggested that the sumoylation enhances the interaction of ESA with the catalytic core domain (Flick and Luscher 2012).

Liu *et al.* identified an additional modification of SirT1. The methyltransferase Set7/9 interacts with and methylates SirT1 at Lys^{233}, Lys^{235}, Lys^{236} and Lys^{238} of the N-terminal region. It is currently not known whether the methylation of SirT1 affects its activity, but the interaction of Set7/9 with SirT1 disrupts the binding of SirT1 with p53. Thus, p53 remain acetylated and in the activated state (Liu et al. 2011).

Furthermore, nuclear SirT1 is transnitrosylated by nitrosylated GAPDH at two cysteines, Cys^{387} and Cys^{390}, within the catalytic core domain. Upon nitrosylation of SirT1, an increase of acetylated PGC-1α (**p**eroxisome proliferator-activated receptor **g**amma **c**oactivator 1-alpha), a substrate of SirT1, was observed. This indicates that the deacetylase activity of SirT1 is inhibited by nitrosylation (Kornberg et al. 2010).

As mentioned above, the expression level is tissue-specific and can be influenced by environmental conditions. For example, SirT1 is up-regulated by calorie restriction (CR), external cold temperature or oxidative stress (Cohen et al. 2004; Crujeiras et al. 2008). It is also up-regulated in different cancer cells such as murine and human lung caner, prostate cancer, leukaemia, lymphomas and colon cancer compare to the normal tissue (Lim 2006; Fraga and Esteller 2007; Stunkel et al. 2007). Furthermore, Kim *et al.* have shown that SirT1 and AROS (**a**ctive **r**egulator **o**f **S**irT1) are co-expressed in nearly equal amounts in the majority of cancer cell lines that were screened, suggesting that AROS might be a tumour cell survival factor and maybe a target for tumour therapy (Kim et al. 2007b). Intriguingly, SirT1 protein level was also found reduced in some cancer types, including various forms of ovarian cancers, prostate carcinoma, bladder carcinoma and glioblastoma (Wang et al. 2008).

Similar to the yeast Sir2, SirT1 mediates heterochromatin formation through deacetylation of the histone tails (H1K26, H3K9 and H4K16) and through recruitment and deacetylation of H1 (Vaquero et al. 2004). Further, SirT1 modifies histones indirectly through deacetylation of the histone acetylase p300, which is sumoylated and rapidly degraded upon lysine deacetylation (Bouras et al. 2005). The acetylase p300 is a rate-limiting co-activator for a broad range of transcription factors. SirT1 also deacetylates a number of important transcription factors, most importantly p53 (Vaziri et al. 2001). The tumour suppressor p53 is acetylated and activated in response to cellular stress and DNA damage, and induces cell death. The deacetylation of p53 by SirT1 inactivates its transcriptional activity and therefore promotes cell survival. Further substrates of SirT1 are members of the forkhead box O (FOXO) family (Brunet et al. 2004). These transcription factors are homologs of *C. elegans* DAF-16 and regulate several mammalian cell functions, including cell metabolism and cell cycle progression. As for p53, the deacetylation of FOXO by SirT1 inhibits its transcriptional activity and promotes cell survival. SirT1 also deacetylates and inhibits the transcription factor NF-κB, a master regulator of inflammatory processes (Yeung et al. 2004). Furthermore, SirT1 interacts with several components of the DNA repair machinery such as NBS1 and Ku70 (Cohen et al. 2004; Yuan et al. 2007; Li and Luo 2011). Whereas NBS1 operates in the homologous recombination pathway of **d**ouble-**s**trand **b**reak (DSB) repair, Ku70 operates in the **n**on-**h**omologous **e**nd-**j**oining (NHEJ) pathway.

SirT2 is expressed in at least two isoforms, a longer variant consisting of 389 amino acids and a shorter variant of 352 amino acids (Voelter-Mahlknecht et al. 2005). In contrast to SirT1, SirT2 is predominantly localized in the cytoplasm and co-localizes with microtubules, but it can also be found in the nucleus (North et al. 2003; Bae et al. 2004). North *et al.*

identified a Crm-1 dependent NES domain located in the N-terminus of SirT2, and through this domain it is actively exported from the nucleus. Although they were unable to identify a functional NLS domain, they could show that SirT2 constantly shuttles between nucleus and cytoplasm during interphase. During G2/M transition and in mitosis, SirT2 is predominantly nuclear or chromatin-associated. Additionally, SirT2 is hyperphosphorylated during G2/M transition and in M phase, which correlates with the nuclear translocation of SirT2 (Dryden et al. 2003; North and Verdin 2007). This suggests that Cyclin B/CDK1 and other mitosis-specific kinases regulate the cell cycle-dependent nuclear localisation (Flick and Luscher 2012). So far, two phosphorylation sites are known on SirT2 (long and short variant), $Ser^{368/331}$ and $Ser^{372/335}$, which are located in the C-terminal region (Nahhas et al. 2007). $Ser^{368/331}$ is part of a Cyclin/CDK consensus motif and has been identified as a substrate of Cyclin B/CDK1, Cyclin E/CDK2, Cyclin A/CDK2, Cyclin D3/CDK4 and p53/CDK5 (North and Verdin 2007; Pandithage et al. 2008). Phosphorylation of SirT2 at $Ser^{368/331}$ reduces its deacetylase activity and occurs when cells enter S phase, suggesting that this modification does not play a role in nuclear accumulation of SirT2 (Pandithage et al. 2008). So far, nothing is known about the phosphorylation at $Ser^{372/335}$, neither the responsible kinase nor the influence on SirT2 function (Flick and Luscher 2012). A further modification of SirT2 is the acetylation by the HAT p300. Although this modification has not been mapped, it interferes with the catalytic activity of SirT2 (Han et al. 2008).

One important target of SirT2 is lysine 40 of α-tubulin both *in vitro* and *in vivo*. Tubulin regulates different cellular events such as mitosis, cellular organisation, transport and motility. Acetylated tubulin is abundant in stable microtubules, but is absent in dynamic cellular structures, thus the acetylation status of α-tubulin serves as a marker for the presences of stable microtubules (Piperno et al. 1987; Robson and Burgoyne 1989). It was shown that knockdown of endogenous SirT2 via siRNA results in hyperacetylation of α-tubulin. Despite the fact that SirT2 co-localises and interacts with HDAC6, another tubulin deacetylase, SirT2 is a bona fide tubulin deacetylase (North et al. 2003). However, the group of G. Bates has recently shown that reduction or loss of SirT2 has no effect on the acetylation of α-tubulin in the brains of wild type mice. Therefore, they postulate that HDAC6, and not SirT2, is the major tubulin deacetylase in the brain (Bobrowska et al. 2012).

Furthermore, SirT2 deacetylates the histone tails H4K16, H3K9 and H3K56 (Vaquero et al. 2006; Vempati et al. 2010). It has been hypothesized that SirT2 functions in mitotic regulation, because SirT2 deacetylates H4K16 at a global level during mitosis, which may facilitate the generation of condensed chromatin (Vaquero et al. 2006). However, the loss of Hst2, a yeast homologue of SirT2, does not affect viability, and SirT2 knockout mice also

seem to be normal (Perrod et al. 2001; Kim et al. 2011). Similar to SirT1, SirT2 also deacetylases the forkhead transcription factors FOXO1 and FOXO3a (Wang et al. 2007; Wang and Tong 2009) and the tumour suppressor p53 (Peck et al. 2010). Therefore, SirT2 is also connected with multiple cellular processes such as cell cycle progression, apoptosis, metabolism and aging. Furthermore, SirT2 is suspected to play a role in blood glucose homeostasis by deacetylating and stabilizing the phosphoenolpyruvate carboxykinase 1 (PEPCK1), which is an important enzyme in gluconeogenesis (Jiang et al. 2011). When SirT2 is activated by low glucose conditions, PEPCK1 becomes deacetylated and stabilized, and enhances the gluconeogenesis, which is the generation of glucose from non-carbohydrate carbon substrates such as pyruvate and lactate.

SirT3 is one of three sirtuins that are located in the mitochondria (Michishita et al. 2005). It is present in the mitochondrial inner membrane (Onyango et al. 2002; Schwer et al. 2002; Lombard et al. 2007). Two distinct isoforms of SirT3 are known. A long form of approximately 44 kDa contains an NH_2-terminal cleavable presequence, a so-called mitochondrial localization sequence (MLS), which is important for the mitochondrial import. This long isoform is synthesized as an inactive precursor within the cytoplasm. Upon translocation into the mitochondria, SirT3 is cleaved at arginines 99/100 by MPP (matrix processing peptidase) to the short isoform of 28 kDa. This proteolytic cleavage of SirT3 activates its NAD^+-dependent deacetylates activity (Schwer et al. 2002; Jin et al. 2009; Bao et al. 2010). Six phosphorylation sites of SirT3 have been identified, between amino acid 101 and 118 (Olsen et al. 2010), but their biological function or influence on SirT3 has not been analyzed yet. Due to the fact that the phosphorylation sites are close to the mitochondrial cleavage site, it is possible that they modulate the SirT3 enzyme activity (Flick and Luscher 2012).

Analysis of the acetylation status of mitochondrial proteins in SirT3, SirT4 and SirT5 knockout mice showed that SirT3 is the main deacetylase in mitochondria (Lombard et al. 2007). SirT3 has a large number of important mitochondrial proteins as substrates, for instance subunits of oxidative phosphorylation complexes (Ahn et al. 2008), metabolic enzymes such as acetyl-CoA synthetase 2 (Hallows et al. 2006; Schwer et al. 2006), long-chain acyl CoA dehydrogenase (LCAD) (Hirschey et al. 2010) and 3-hydroxy-3-methylglutaryl CoA (HMG-CoA) synthase 2 (Shimazu et al. 2010), as well as the oxidative stress reducing enzymes isocitrate dehydrogenase 2 (IDH2) (Someya et al. 2010), superoxide dismutase 2 (SOD2) (Qiu et al. 2010) and manganese superoxide dismutase (MnSOD) (Tao et al. 2010). Because of this large number of substrates, SirT3 is associated with diverse

metabolic processes such as ATP production, energy metabolism, fatty acid oxidation, ketogenesis and the urea cycle. Furthermore, it was shown that SirT3 functions as a tumour suppressor in response to stress (Kim et al. 2010), and it can delay the onset of a number of oxidative stress-mediated pathologies in multiple tissues (Qiu et al. 2010; Someya et al. 2010). All observations so far suggest that SirT3 may be a novel target for age-associated diseases as well as aging itself, but much work is needed to completely understand the function of SirT3.

SirT4 is another sirtuin located in the mitochondria (Michishita et al. 2005). It is the sole sirtuin that has no detectable NAD^+-dependent deacetylase activity. Only an ADP-ribosyltransferase activity is known. Similar to SirT3 and other typical mitochondrial matrix proteins, SirT4 is proteolytically processed to remove the N-terminal 28 amino acids upon translocation into the mitochondria (Ahuja et al. 2007). In contrast to SirT3, it is not known whether this proteolytic cleavage of SirT4 influences its enzymatic activity. In SirT4, three phosphorylation sites have been identified at Ser^{255}, Ser^{261} and Ser^{262} (Yu et al. 2007). However, no functional relevance has been determined yet.
Very little is known about the functions of SirT4, but in SirT4 knockout mice an increased insulin secretion in response to glucose and amino acids was observed. Through its ADP-ribosylation activity, it represses the activity of glutamate dehydrogenase (GDH), which promotes insulin secretion (Haigis et al. 2006). Ahuja *et al*. identified two additional targets of SirT4, insulin-degrading enzyme (IDE) and the ADP/ATP carrier protein adenine nucleotide translocator (ANT), which support the role of SirT4 in the control of insulin secretion in pancreatic β-cells (Ahuja et al. 2007).

SirT5 is the third mitochondrial sirtuin located in the intermembrane space. Two transcriptional splice variants of SirT5 exist, which encode proteins with distinct C-terminal regions. Similar to SirT3 and SirT4, both isoforms are cleaved after the first 36 amino acids upon entry into the mitochondria (Michishita et al. 2005; Nakamura et al. 2008). The cleaved shorter isoform seems to be exclusively in the mitochondria, in contrast to the longer isoform, which is additionally found in the cytoplasm. The reason for this could be the different C-terminal regions of the two isoforms. The short isoform has a hydrophobic C-terminus and functions as a mitochondrial membrane insertion signal (Matsushita et al. 2011). So far, no posttranslational modifications on SirT5 are known. SirT5 has only weak deacetylase activity and was recently identified as a protein lysine desuccinylase and demalonylase (Du et al. 2011). Du *et al.* have shown that the catalytic efficiencies for demalonylation and

desuccinylation were much higher (29- to >1000-fold) than that for deacetylation. The reason for this phenomenon is an arginine residue (Arg^{105}) and tyrosine residue (Try^{102}) in the active site of SirT5, which interact with succinyl and malonyl groups. Du *et al.* identified several mammalian proteins that carry succinyl or malonyl lysine modifications (Du et al. 2011).
It has furthermore been shown that SirT5 binds and deacetylases carbamoyl phosphate synthetase (CPS1), which catalyses the rate-limiting and first step of the urea cycle. SirT5 knockout mice show increased acetylation of CPS1 and elevated levels of ammonia after prolonged fasting, whereas SirT5 overexpression in mice leads to increased CPS1 activity (Nakagawa et al. 2009; Ogura et al. 2010). Du *et al*. identified three lysine residues on CPS1 that are both acetylated and succinylated (Lys^{44}, Lys^{287} and Lys^{1291}). Additionally, it was shown that the succinylation level of Lys^{1291} increases dramatically in SirT5 knockout mice in comparison to wild-type mice (Du et al. 2011).

SirT6 is a broadly expressed nuclear protein with deacetylase activity, but robust auto-ADP-ribosyltransferase activity (Liszt et al. 2005). Tennen *et al.* showed that the conserved core domain of SirT6 alone is not sufficient for the deacetylase activity, but that it requires the N-terminal region. Thus is similar to other sirtuins, which require either N- or C-terminal regions to activate catalytic function. In the C-terminal region, two phosphorylation sites at Tyr^{294} and Ser^{303} were identified (Dephoure et al. 2008), but their influence on SirT6 function still needs to be determined. Furthermore, an NLS signal between amino acids 345 and 351 in the distal region of the C-terminal has been identified (Tennen et al. 2010).
Human SirT6 was characterized as a NAD^+-dependent H3K9Ac deacetylase that modulates telomeric chromatin. Its depletion leads to telomere dysfunction with end-to-end chromosomal fusions and premature cellular senescence (Michishita et al. 2008). Under physiologic conditions, SirT6 interacts with the transcription factors NF-κB and HIF1α, and is transported to their target gene promoters, where it deacetylates H3K9Ac or H3K56Ac (Kawahara et al. 2009; Yang et al. 2009). SirT6 binds to many promoters, which are highly enriched for NF-κB, SP1, STAT1/3, ELK1, E2F1 and FOXO1/4 binding motifs (Kawahara et al. 2011). As a result, SirT6 seems to have widespread activities as a regulator of transcription of genes involved in glucose and lipid metabolism. Additionally, SirT6 has been established as a key component of base excision repair (BER). It directly stabilises DNA-dependent protein kinase at the site of dsDNA breaks. This allows the formation of the DNA repair complex and the initiation of repair mechanism (McCord et al. 2009).

SirT7 is a widely expressed nucleolar protein that is associated with active ribosomal RNA (rRNA) genes and histones (Michishita et al. 2005). It is proposed to be an active regulator of RNA polymerase I (Pol I) and therefore required for cell viability in mammals. Its expression level correlates with growth, it is abundant in tissues with high proliferation, such as liver and spleen, and absent or low in non-proliferating tissues like heart, brain and muscle (Ford et al. 2006). It is suggest that SirT7 is phosphorylated during mitosis by a CDK complex, but neither have any sites been mapped, nor are any functional consequences known (Grob et al. 2009).

Indirect evidence has led to the assumption that SirT7 deacetylates the tumour suppressor p53 (Vakhrusheva et al. 2008), but this has not been confirmed so far. Recent data have shown that SirT7 has a specific NAD^+-dependent H3K18Ac deacetylase activity (Barber et al. 2012). Previously it was shown that low levels of H3K18Ac predict a higher risk of prostate cancer recurrence and poor prognosis in lung, kidney and pancreatic cancers (Manuyakorn et al. 2010).

1.4.3 Deacetylation reaction of sirtuins

Although sirtuins have been known for many years, their deacetylation activity was many years after their initial discovery. Studies of the *Salmonella* Sir2-like protein (CobB) gave the first hint that Sir2-like proteins are ADP-ribosyltransferases, because they transfer ADP-ribose from NAD^+ to substrate molecules (Tsang and Escalante-Semerena 1998; Frye 1999). From there, several studies followed showing that Sir2-like proteins also have a NAD^+-dependent histone deacetylase activity (Imai et al. 2000; Landry et al. 2000; Smith et al. 2000). In contrast to the classical zinc-dependent histone deacetylases, sirtuins cleave the nicotinamide ribosyl bond of NAD^+ and transfer the acetyl group from proteins to their cosubstrate NAD^+. This generates deacetylated protein, nicotinamide (NAM) and 2´-*O*-acetyl-ADP-ribose (*O*-AADPr) (Tanner et al. 2000; Tanny and Moazed 2001; Lee et al. 2008) (Figure 1.2). Two different possible mechanism of deactylation reaction are discussed, an S_N1- or an S_N2-like reaction, but recent evidence strongly supports the S_N2-like mechanism. In the first chemical step, the acetyl oxygen undergoes nucleophilic attack of the 1`-carbon of the nicotinamide ribose to form an *O*-alkylamidate intermediate through elimination of NAM. Subsequently, the 2`-hydroxyl of the nicotinamide ribose is activated by an active-site histidine for attack of the *O*-alkylmediate carbon, forming a 1`, 2`-cyclic intermediate (Sauve et al. 2006; Smith and Denu 2006). The reaction occurs in a highly conserved region of sirtuins. Crystallographic studies indicate that bound acetyl-lysine changes the NAD^+

conformation and forces the nicotinamide ring of NAD^+ deep within a conserved hydrophobic pocket, the so-called C-pocket. This forms a more reactive conformation of NAD^+ (Avalos et al. 2004; Zhao et al. 2004b). The elimination of deacetylated protein followed by water addition generates a mixture of 2`- and 3`-*O*-Acetyl-ADP-ribose, whereby 3`-*O*-Acetyl-ADP-ribose is formed by intramolecular transesterification (Sauve et al. 2001; Jackson and Denu 2002). It is thought that these two unique metabolites (2`- and 3`-*O*-AADPr) play an important role in cell signalling and metabolism (Borra et al. 2002; Kustatscher et al. 2005; Grubisha et al. 2006).

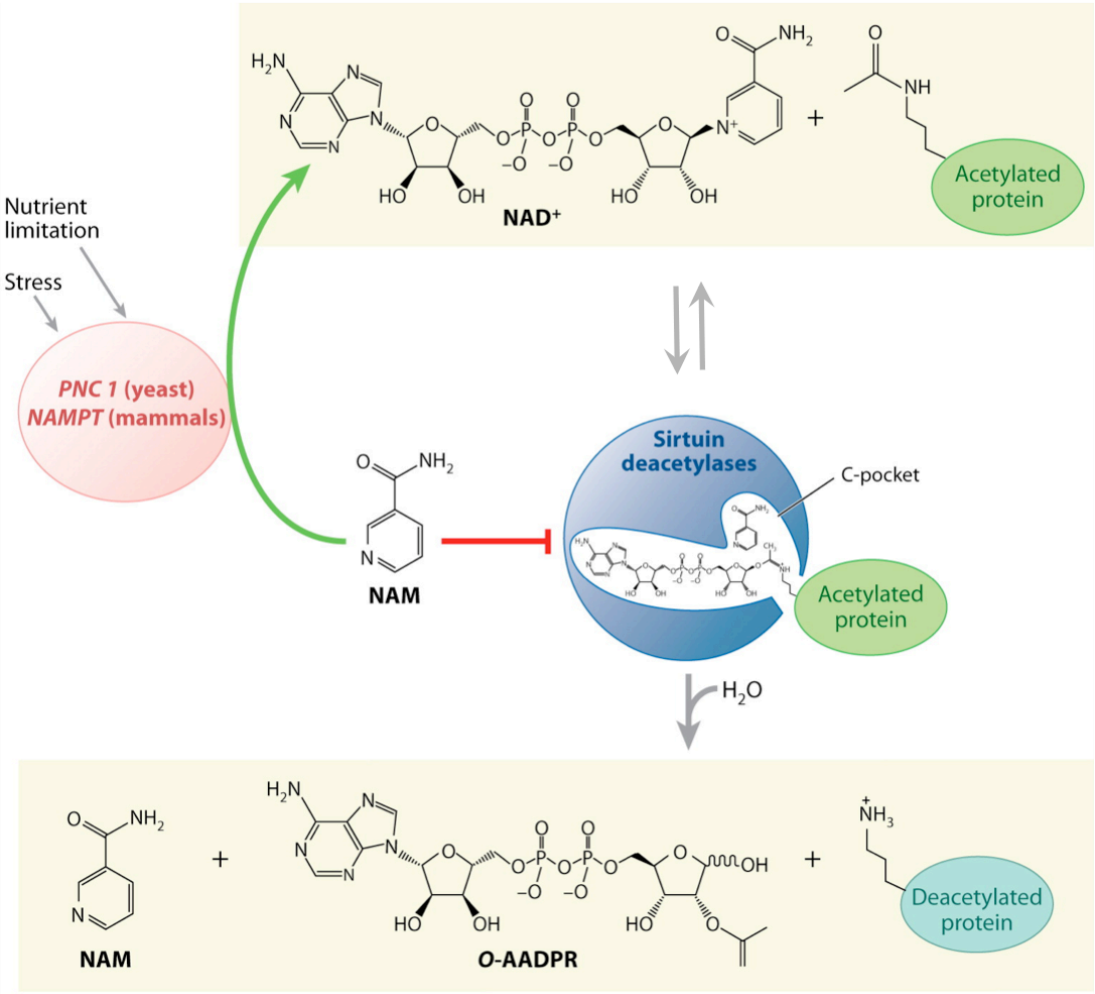

Figure 1.2: Deacetylation reaction of sirtuins
Sirtuins deacetylate NAD^+-dependent acetylated lysine residues to form nicotinamide (NAM), *O*-acetyl-ADP-ribose (*O*-AADPR) and deacetylated protein. The reaction occurs in a highly conserved region of sirtuins and can be inhibited by NAM, which reacts with the intermediate and regenerate NAD^+. NAM is also recycled back to NAD^+ in further different mechanism. In yeast, worms and flies the reaction is catalyzed by PNC1 (nicotinate phosphoribosyltransferase) and in mammals by NAMPT (NAM phosphoribosyltransferase). Both enzymes can be influenced by environmental stress. (Haigis and Sinclair 2010)

Furthermore, it was reported that sirtuins are inhibited by NAM, the endogenous sirtuin inhibitor (Bitterman et al. 2002; Sauve and Schramm 2003). It reacts with the *O*-alkylamidate intermediate and regenerates NAD^+. It is thought to be a major mechanism for *in vitro* control

of sirtuin activity. NAM can also be recycled back to NAD^+ in further different reactions. In yeast, worms and flies, the first step is catalyzed by Pnc1 (nicotinate phosphoribosyltransferase) to produce nicotinic acid. In the case of environmental stress, such as heat or calorie restriction (CR), Pnc1 is up-regulated, and this leads to increased stress resistance and life span extension in *S. cerevisiae* and *D. melanogaster* (Anderson et al. 2003; Gallo et al. 2004; Balan et al. 2008). Thus, it seems that Pnc1 promotes survival and life span in response to environmental stress. In mammals, the first step is catalyzed by NAM phosphoribosyltransferase, known as NAMPT, which converts NAM to nicotinamide mononucleotide (Rongvaux et al. 2002; Revollo et al. 2004). Consistent with the ability of Pnc1 to regulate Sir2 in yeast, mammalian NAMPT is one of the main regulators of sirtuin activity (Yang et al. 2006).

1.4.4 Structural characteristics of sirtuins

Most of the information on the structure of the catalytic core domain of sirtuins and its binding to ligands was obtained from crystallographic studies of the archaeal sirtuins, Sir2Af1 (Garcia-Salcedo et al. 2003) and Sir2Af2 (Avalos et al. 2002; Avalos et al. 2004; Avalos et al. 2005), human SirT2 (Finnin et al. 2001), yeast Hst2 (Zhao et al. 2003b; Zhao et al. 2004b) and the bacterial sirtuins, cobB (Zhao et al. 2004a) and Sir2Tm (Avalos et al. 2005).

The catalytic core domain of sirtuins consists of two characteristic domains (**Figure 1.3**). The larger domain (residues 53-89, 146-186 and 241-356 of SirT2) is a variant of the Rossmann fold, the classic pyridine dinucleotide binding fold, which is present in many diverse NAD(H)/NADP(H) binding enzymes (Rossmann and Argos 1978). The smaller domain is composed of two structural modules (residues 90-145 and 187-240 of SirT2) that result from two insertions within the Rossmann fold domain. One module contains a structural zinc atom coordinated by four cysteine residues, which has the same topology as the RING finger motif and mediates protein-protein interactions. The other module forms a helical module that includes a small groove, lined with hydrophobic residues, that intersects the large groove. This small groove forms a pocket that may be a class-specific binding site for a protein, possibly recognizing portions of the substrate. The large groove partially corresponding to the large domain contains residues (Gly^{84}, Gly^{86}, Arg^{97}, Gln^{167}, Asn^{168}, Asp^{170} and His^{187} of SirT2) invariant across the Sir2 family members and includes the NAD^+ binding site. Mutations of these residues disrupt the deacetylase activity of sirtuins, suggesting that the large groove is the catalytic site (Finnin et al. 2001). This NAD^+ binding pocket can be divided into three regions: site A, where the adenine-ribose moiety of NAD^+ is bound; site B,

where the nicotinamide-ribose moiety is bound; and site C, which is deep inside the pocket and is directly involved in catalysis (Min et al. 2001). Furthermore, it has been proposed that the N-terminal extension is not required for the deacetylase activity *in vitro* (Finnin et al. 2001).

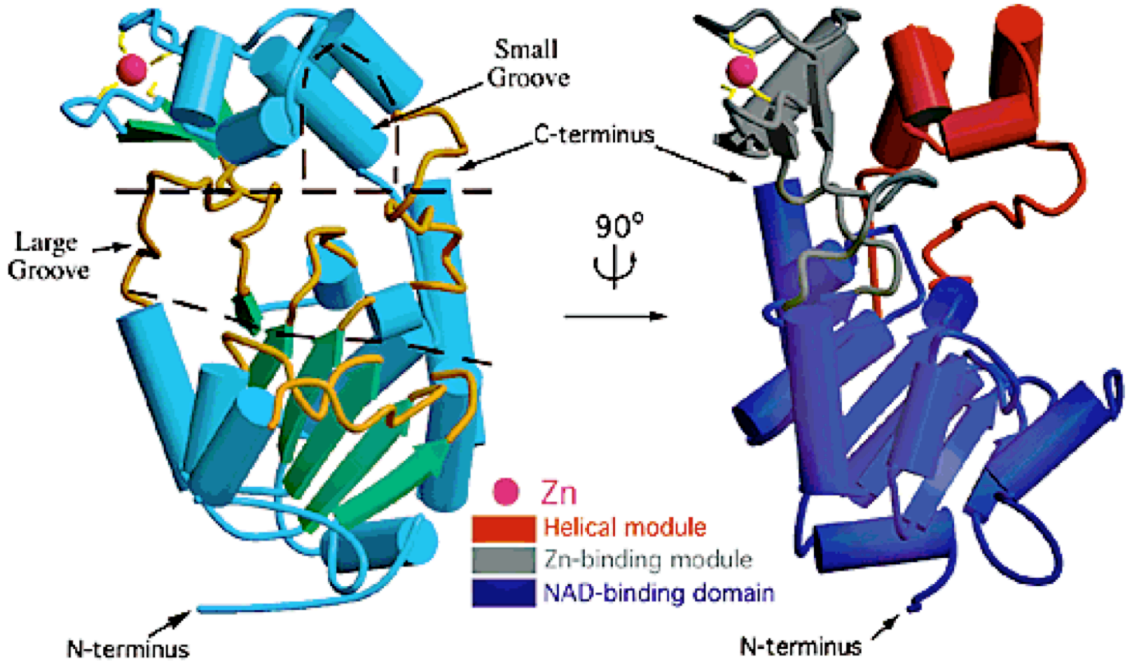

Figure 1.3: Structure of human SirT2
The picture shows two views of the structure of human SirT2 catalytic core domain rotated by 90 °. SirT2 consists of two domains, which are connected by several loops. The loops, which are the major structural components of the large groove (left panel; yellow), connect the small and large domain. The large NAD^+ binding domain consists of a Rossmann fold domain (right panel; dark blue). The small domain contains two modules; one (right panel; gray) binds a zinc-atom (right panel; magenta) and the other (right panel; red) forms a helical module and contains a hydrophobic pocket. (Finnin et al. 2001)

1.5 Sirtuin deacetylase assays

In early sirtuin studies, different radioactive assays were used to determine the deacetylase activity of sirtuins. In these assays either, the acetyl group of the histone H4 lysine substrate is radiolabeled with ^3H, or the nicotinamide group of NAD^+ is labeled with ^{14}C and the released ^{14}C-nicotinamide during the deacetylation reaction can be quantified (Kolle et al. 1998; Nare et al. 1999; Borra and Denu 2004; Borra et al. 2004). However, all these assays are time-consuming and require the use of radioactivity. For this reason, several fluorescence-based assays were developed, where a fluorophore covalently conjugated to the substrate was detected (Hoffmann et al. 1999; Heltweg et al. 2003; Wegener et al. 2003). The fluorophores that were used and the quantification of deacetylated substrate differ, and not all of these assays are suitable for high-throughput analysis.

The most popular high-throughput fluorescence assay is the 'Fluor the Lys' assay (available from Biomol), whose substrate is based on an acetylated p53 peptide conjugated with a coumarin derivative (Marcotte et al. 2004). However, this assay is controversial, and data from several groups indicate that it leads to false positive results because of the fluorophore on the substrate. They showed increased fluorescence readings without truly increasing SirT1 activity. Kaeberlein *et al.* utilized radioactivity deacetylase assays to evaluate the properties of the potential sirtuin activator resveratrol. For this purpose, a p53 peptide or an H4 peptide was used as a substrate, either containing or lacking the fluorophore. In both assays, resveratrol induced an enhancement of deacetylation only for substrates containing the fluorophore. Furthermore, it was shown that the presence of the fluorophore on the acetyl-peptide substrate decreases the binding affinity of SirT1 for this peptide. This indicates that resveratrol may stimulate deacetylation of substrates containing the fluorophore by increasing their binding affinity for SirT1 (Kaeberlein et al. 2005).

To directly monitor SirT1 deacetylase activity without any interference or radioactivity, Beher *et al.* utilized a further deacetylase assay. It is an analytical method using high performance liquid chromatography (HPLC) to directly quantify products from the deacetylation reaction of SirT1 by their different retention times on the HPLC column (Hoffmann et al. 1999; Liu et al. 2008). In this study, it was shown that the 'Fluor de Lys-SirT1' substrate (RHKK(Ac)) without the fluorophore could not function as a SirT1 substrate. In this case, it seems that the fluorophore increases the binding affinity of SirT1 for the 'Fluor de Lys-SirT1' peptide, but it was proposed that this peptide is not an appropriate SirT1 substrate. Consistent with the results of (Kaeberlein et al. 2005), it has been shown that resveratrol does not activate SirT1 when a substrate without a fluorophore is used (Beher et al. 2009).

1.6 Sirtuin modulators

Based on the variety of substrates of each sirtuin and associated functions in diverse pathways and tissues, sirtuins are enzymes that may have a significant influence on different human diseases. Therefore, small molecules that selectively influence the ability of sirtuins to deacetylate proteins may be useful therapeutic agents against a variety of human diseases.

1.6.1 Endogenous Modulators

To date, two specific endogenous modulators of SirT1 have been identified. It was shown that the **a**ctive **r**egulator **o**f **S**irT1 (AROS) interacts with and activates SirT1 (Kim et al. 2007b). AROS is a short nuclear protein of 142 amino acids that interacts with the N-terminus of SirT1 (114-217) both *in vitro* and *in vivo*. The AROS/SirT1 interaction promotes p53 deacetylation and suppresses p53 transcriptional activity, thus mediating cell survival in response to DNA damage. It is not clear whether AROS induces a conformational change in SirT1 or whether AROS binds other proteins that regulate SirT1 activity. Further experiments are needed to determine the mechanism of AROS-mediated SirT1 activation.
Another endogenous inhibitor of SirT1 is the human protein **d**eleted in **b**reast **c**ancer **1** (DBC1). It was previously identified as a region that is homozygously deleted in human breast cancer (Hamaguchi et al. 2002). Knockdown of DBC1 shows activation of SirT1 and a decrease of apoptosis by p53 through DNA-damaging agents (Kim et al. 2008; Zhao et al. 2008). DBC1 binds directly through a leucine-zipper-like motif to the catalytic core domain of SirT1. It was shown that DBC1 contains an inactive Nudix domain (Anantharaman and Aravind 2008), which is able to bind NAD^+-like molecules and the product of sirtuin deacetylation, *O*AADPr (Grubisha et al. 2006). Recently, Zannini *et al.* have shown that DBC1 is directly phosphorylated on Thr^{454} by ATM (ataxia telangiectasia mutated) and ATR (ataxia telangiectasia and Rad3 related) kinases. In response to DNA damage, ATM/ATR phosphorylate DBC1, and this enhances the DBC1-SirT1 interaction and thereby inhibits deacetylation of p53 and promotes apoptosis (Zannini et al. 2012).

1.6.2 Small-molecule activators of sirtuins

Because of the potential of sirtuins to influence a broad range of diseases including obesity, diabetes, cardiovascular, neuronal and aging-related diseases, the manipulation of sirtuin activity has obtained particular attention. CR is particularly beneficial in age-related disorders such as diabetes, cancer and cardiovascular disease, and it increases lifespan in animal models (Schwer and Verdin 2008). CR can also protect neurons against degeneration in animal models of Alzheimer's disease (AD), Parkinson's disease, Huntington's disease (HD) and stroke (Mattson et al. 2003). Several lines of evidence suggest that the mechanisms of CR are mediated by sirtuins in yeast, worms, flies and mammals (Kaeberlein et al. 1999; Lin et al. 2000; Tissenbaum and Guarente 2001; Wood et al. 2004; Boily et al. 2008). However, several

studies discovered that lifespan extension by CR is independent of sirtuins both in yeast and worms (Kaeberlein et al. 2004; Lamming et al. 2005; Tsuchiya et al. 2006; Greer et al. 2007). Nonetheless, it has been shown that the increase of sirtuin activities in mammals accelerates fat mobilization, glucose consumption and insulin sensibility. Therefore, there is growing interest in identifying molecules that activate sirtuin activity and mimic the effects of CR (Alcain and Villalba 2009a).

A leading candidate for activating sirtuins is resveratrol, a polyphenol found in red wine. It was the first candidate to be reported to mimic CR by stimulating sirtuins (Howitz et al. 2003; Wood et al. 2004). It was identified in the 'Fluor de Lys' assay, together with other compounds that share structural similarity, for instance the chalcone butein and the flavone quercetin, as an activator of sirtuins (Howitz et al. 2003) (**Figure 1.4**).

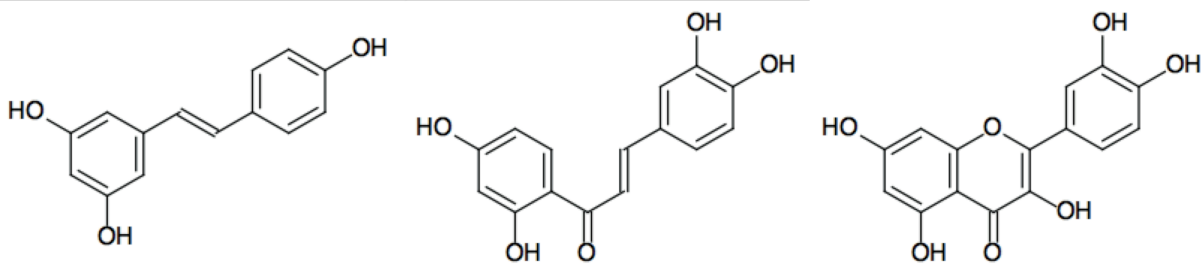

Figure 1.4: Chemical structure of sirtuin activators

In the 'Fluor de Lys' assay, these compounds activated human SirT1 activity 4 to 13 fold. However, due to the problem with this 'Fluor de Lys' assay (described in **1.5**), these activators might be experimental artifacts. Even so, it is thought that these compounds may activate sirtuin deacetylase activity *in vivo*. Resveratrol increases cell survival by stimulating SirT1-dependent p53 deacetylation. In yeast, it promotes rDNA stability and induces lifespan extension (Howitz et al. 2003). In *D. melanogaster,* a lifespan extension was observed when flies were fed an abundant diet containing fisetin or resveratrol (Wood et al. 2004). However, recently it has been shown that the effect of lifespan extension by resveratrol depends on both gender and dietary nutrient conditions in flies (Wang et al. 2011). In addition, Keaberlein *et al*. were unable to detect any significant increase of lifespan extension of several yeast strains in response to resveratrol (Kaeberlein et al. 2005). Nonetheless, it has been shown that resveratrol leads to increased survival and insulin sensitivity of mice that were fed a high-fat diet (Baur et al. 2006; Lagouge et al. 2006). Furthermore, resveratrol has also been reported to have a protective effect on vascular oxidative stress and inflammation, which can be induced by cigarette smoke. These protective effects were abolished by knockdown of SirT1, whereas

the overexpression of SirT1 mimicked the effect of resveratrol (Csiszar et al. 2008). However, the half-life of resveratrol in plasma is very short and it has a poor bioavailability (Asensi et al. 2002). The highest concentrations detected in rat tissues were found in liver and kidney and reached less than 1 % of the administered dose (El Mohsen et al. 2006). Therefore, Sirtris (a pharmaceutical company) has developed the SirT1 activator SRT501, a formulation of resveratrol that has an improved bioavailability of 11 % (Milne et al. 2007) and is being used in clinical trials.

Researchers from Sirtris have identified further SirT1 activators by using the 'Fluor the Lys' assay. These compounds (**Figure 1.5**) are structural unrelated to resveratrol and 1000 - fold more potent than resveratrol (Milne et al. 2007). However, similar to resveratrol, there are also some controversies concerning their potential to activate SirT1 (Pacholec et al. 2010). Even so, they have been proposed for the treatment and/or prevention of a wide variety of diseases including diabetes, cancer, inflammation and many more. SRT1720, the most potent activator, has a bioavailability of 50 % and improves blood glucose level and insulin sensitivity by increased mitochondrial activity in diet-induced obese and genetically obese mice. SRT1460 and SRT2183 show similar effects, but to a lesser extent (Milne et al. 2007). They are already being used in clinical trials, but no further results have yet been published (Sirtris pharmaceuticals US2007037827; 2007).

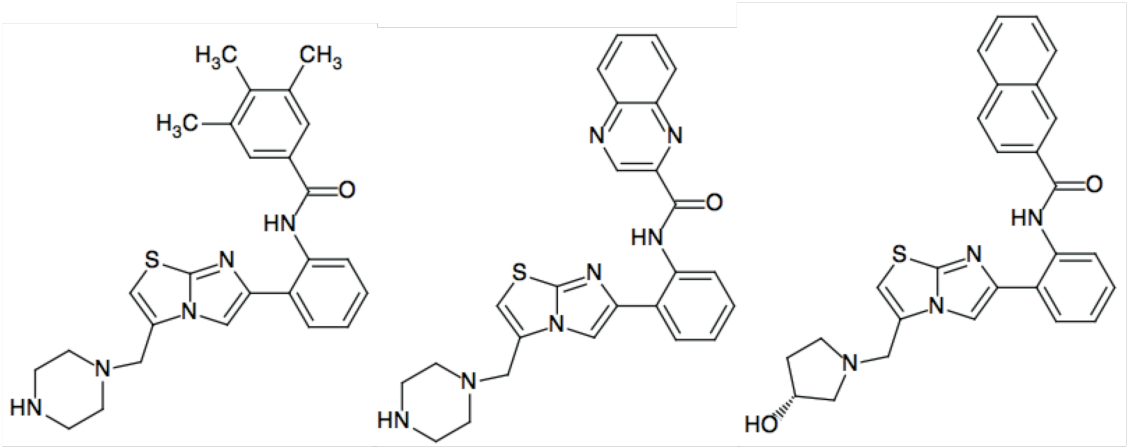

Figure 1.5: Chemical structures of SirT1 activators

1.6.3 Small-molecule inhibitors of sirtuins

Cancer cell lines, as well as tissue samples obtained from cancer patients, revealed higher endogenous levels of SirT1 expression compared to normal cells. As mentioned above, SirT1 deacetylates and inhibits the tumour suppressor p53, resulting in reduced apoptosis in

response to DNA damaging agents. This raises the possibility that inhibiting SirT1 activity might suppress cancer cell proliferation, and that sirtuin inhibitors may be useful agents for cancer therapy.

Splitomicin and its derivates

Splitomicin was the first small-molecule sirtuin inhibitor to be identified. It was isolated in a high-throughput yeast phenotypic screen for inhibitors of Sir2 (Bedalov et al. 2001). It selectively inhibits yeast Sir2 and is an inefficient inhibitor for human sirtuins. In an *in vitro* histone deacetylase assay with a [^{3}H]-acetylated histone H4 peptide, splitomicin inhibits yeast Sir2 with an IC_{50} value of 60 µM (Bedalov et al. 2001). However, it undergoes rapid hydrolysis at neutral pH, thus limiting its use in cell culture conditions. Several structure-activity relationship studies have been performed and proposed that the hydrolytically instable aromatic lactone is required for the inhibition of Sir2 (Hirao et al. 2003; Posakony et al. 2004). Based on these results, Pagans *et al.* identified the stable splitomicin derivate **HR73** (**Figure 1.6**), which inhibits human SirT1 activity *in vitro* with an IC_{50} value lower than 5 µM. They could also show that HR73 *in vivo* suppresses Tat-dependent HIV1 (human immunodeficiency virus 1) transcription in a dose-dependent manner. Furthermore, it induces hyperacetylation of the tumour suppressor p53, a target of SirT1, at a concentration of 1 µM (Pagans et al. 2005).

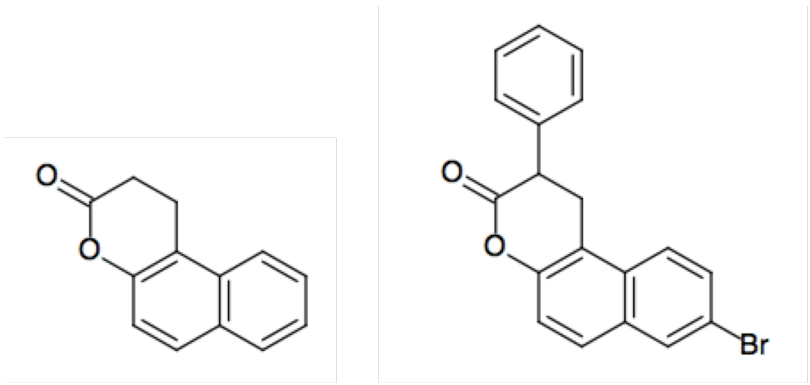

Splitomicin HR73

Figure 1.6: Structure of splitomicin and its analogue HR73

The group of M. Jung (University of Freiburg) developed a series of analogues of **β-phenylsplitomicins** and found that the orientation of the β-phenyl group was important for the inhibition of SirT2. The most potent inhibitors of this series (5c and 8c; **Figure 1.7**) inhibit SirT2 with an IC_{50} value of 1.5 µM using a fluorescent lysine derivate (ZMAL) as a

substrate. Selected inhibitors of this series show antiproliferative properties and tubulin hyperacetylation in MCF7 breast cancer cells (Neugebauer et al. 2008).

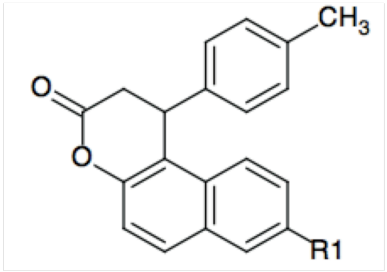

5c: R1 = Br
8c: R1 = Me

Figure 1.7: Structure of splitomicin derivates
Both compounds 5c (β-phenyl-8-bromosplitomicin) and 8c (β-phenyl-8-methylsplitomicin) are analogues of splitomicin and selectively inhibit human SirT2 with an IC_{50} value of 1.5 µM (Neugebauer et al. 2008).

Sirtinol and its derivates

Besides splitomicin, sirtinol was also an early sirtuin inhibitor that was identified in a high throughput yeast phenotypic screen (Grozinger et al. 2001). Sirtinol inhibits yeast Sir2 *in vitro* (IC_{50} = 70 µM) as well as human SirT2 (IC_{50} = 40 µM), and therefore is potentially more potent against human SirT2. However, *in vivo* it affects only yeast Sir2 in a *URA3* reporter gene assay. 25 µM of sirtinol inhibits transcriptional silencing at all three loci (*HM*, telomeric and rDNA) in yeast. In contrast, the sirtinol treatment of HeLa cells does not show an increased acetylation of α-tubulin or H3 and H4 acetylation, as is the case after TSA treatment. Further structure-activity studies were performed and suggest that the 2-hydroxyl-1-naphtol moiety is sufficient for the inhibition of sirtuins (Grozinger et al. 2001). Mai *et al.* synthesized two further analogues of sirtinol, ***meta*- and *para*-sirtinol** (**Figure 1.8**), which are 2- to 10-fold more potent than sirtinol against SirT1 and SirT2. In the yeast *in vivo* assay, the inhibitory effect is equal to sirtinol (Mai et al. 2005).

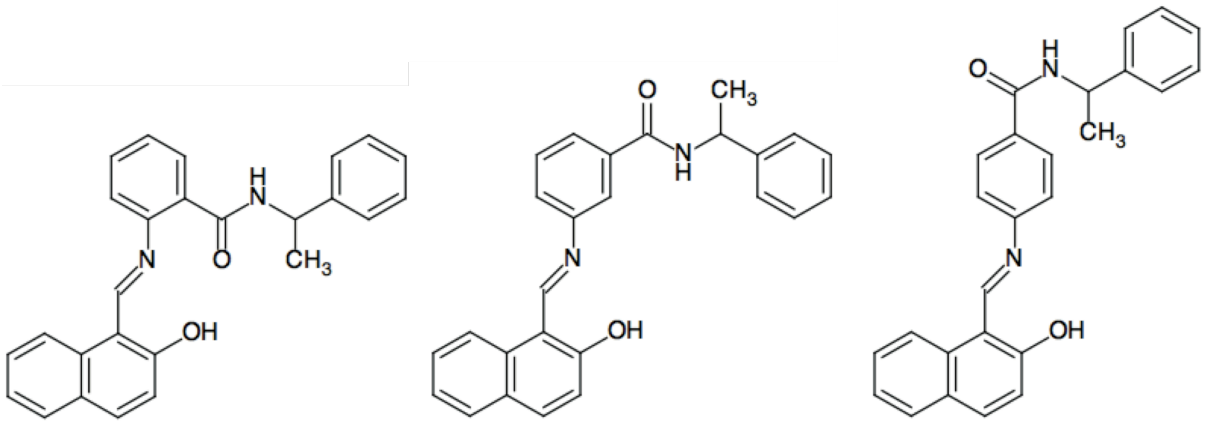

Sirtinol *meta*-Sirtinol *para*-Sirtinol

Figure 1.8: Structure of sirtinol and its derivates

Furthermore, sirtinol induces senescence-like growth arrest in human breast cancer MCF7 and lung cancer H1299 cells, which is accompanied by impaired activation of mitogen-activated protein kinase (MAPK) pathways (Ota et al. 2006). Treatment of the human prostate cancer cell line PC3 with sirtinol inhibits cell growth and increases sensitivity to two well-known anticancer drugs, cisplatin and camptothecin (Kojima et al. 2008). However, the molecular mechanism of theses effects is still unclear. These results suggest that inhibitors such as sirtinol might have high anticancer potential. A further sirtinol derivate, **salermide,** with a modified structure was synthesized to generate a stronger sirtuin inhibitor. The hydrophobic π–π interactions between amino acids F^{119} and H^{187} of SirT2 and the naphtol residue are maintained. Further, the change of the amide moiety created an additional polar interaction between the oxygen of the amide and the amino acid Q^{167} in the C-pocket of SirT2 (Q^{345} correspondingly of SirT1) (**Figure 1.9**). The inhibitory effect was measured with the 'Fluor de Lys' assay, and it was shown that 100 µM of salermide inhibits 80 % of SirT1 activity, whereas the same concentration of sirtinol reduces SirT1 activity by < 5 %. However, salermide is more efficient at inhibiting SirT2; at 25 µM it inhibits 80 % of SirT2 activity (Lara et al. 2009).

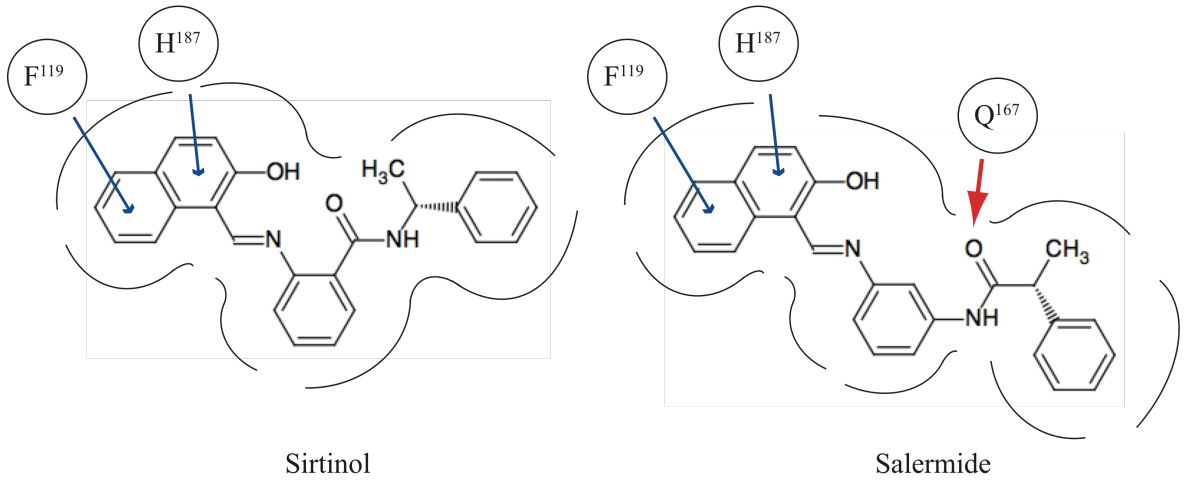

Sirtinol Salermide

Figure 1.9: Schemes of proposed interactions for sirtinol and salermide with SirT2
The blue arrows display the hydrophobic π–π interactions between amino acid F^{119} and H^{187} of SirT2 and the naphtol residue of both sirtinol and salermide. The red arrow shows the newly created polar interaction between the carbonyl group of salermide and amino acid Q^{167} of SirT2 (Lara et al. 2009).

A range of *in vivo* experiments showed that salermide is well tolerated by mice at concentrations up to 100 µM and induces apoptosis in a wide range of cancer cell lines, but not in normal cells (Lara et al. 2009). Although salermide is a more potent SirT2 inhibitor, a putative SirT2-mediated apoptotic pathway was ruled out, because no alteration of the acetylation level of SirT2 targets, H4K16 or α-tubulin could be observed. Consistent with this, only knockdown of SirT1, but not SirT2, induces apoptosis in cancer cells. Finally, it was shown that the apoptotic effect of salermide is p53-independent. Salermide reactivates

proapoptotic genes such as PUMA, TNF and CASP8 that are epigenetically repressed exclusively in cancer cells by SirT1-mediated H4K16 deacetylation (Lara et al. 2009).

Cambinol

The group of Antonio Bedalov identified and characterized the compound cambinol (Heltweg et al. 2006), which shares a β-naphtol pharmacophore with sirtinol and splitomicin (**Figure 1.10**). Cambinol inhibits human SirT1 and SirT2 deacetylase activity *in vitro* with IC_{50} values of 56 and 59 μM using a [^{3}H]-acetylated histone H4 peptide as substrate. It also inhibits human SirT5 but to a lesser extent. *In vivo* experiments have shown that cambinol-induced inhibition of SirT1 sensitized cells to chemotherapeutic agents, such as etoposide and paclitaxel. Furthermore, it induces hyperacetylation of known sirtuin targets implicated in stress responses like p53, Ku70 and FOXO3a in combination with DNA damaging agents. An increase of acetylated α-tubulin could only be observed after treatment with cambinol in combination with TSA, which indicates a shared role of HDACs, especially HDAC6, and SirT2, in tubulin acetylation (Heltweg et al. 2006).

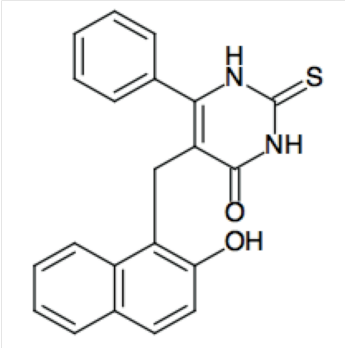

Cambinol

Figure 1.10: Structure of cambinol

Competition studies with NAD^+ and peptide substrates show that cambinol competes with the peptide substrate-binding site and not with the NAD^+-binding site, similar to splitomicin. This could be an explanation for the selectivity among Sir2 family members and low toxicity *in vivo* (Heltweg et al. 2006).

Suramin

A further potent sirtuin inhibitor is suramin (**Figure 1.11**), a symmetric polyanionic naphthylurea that was developed by Bayer AG in 1916. Originally, it was used for the treatment of *trypanosomiasis*, sleeping sickness, and *onchocerciasis*, also known as river

blindness. It inhibits sirtuins with IC_{50} values of 297 nM for SirT1, 1.15 µM for SirT2 and 22 µM for SirT5 (Schuetz et al. 2007; Trapp et al. 2007).

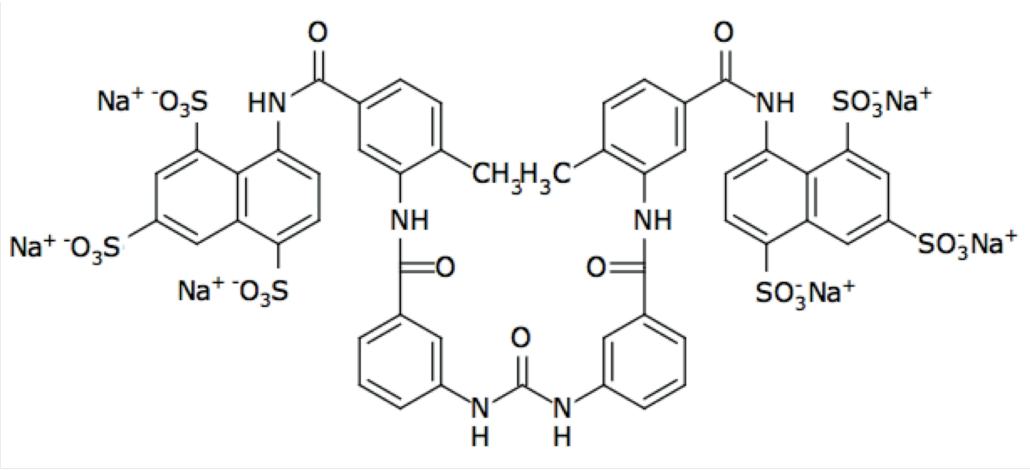

Suramin

Figure 1.11: Structure of suramin

It was reported that suramin has antitumor effects, and it also is a potent reverse transcriptase inhibitor (Perabo and Muller 2005). However, it is unsuitable for therapeutic treatment because of its neurotoxicity and other systemic side effects (Peltier and Russell 2002). Due to the highly polar sulfonic acids, its cellular uptake is generally quite limited. A low concentration of 2 % albumin in the medium inhibits suramin uptake by more than 90 % (Gagliardi et al. 1998). Structural studies with suramin and SirT5 showed that suramin targets the NAD^+-binding pocket of SirT5. It thus seems to be nonselective for similar binding pockets (Schuetz et al. 2007). Indeed, suramin inhibits various other NAD^+/$NADP^+$-dependent enzymes such as lactate dehydrogenase from *Dirofilaria immitis* and *Onchocerca* (Walter 1979; Walter and Schulz-Key 1980).

Tenovin-1 and -6

Lain *et al.* found two SirT1 inhibitors through a cell-based screen of 30.000 drug-like compounds with the ability to activate a p53-driven reporter gene. These two agents, tenovin-1 and the more water-soluble tenovin-6 (**Figure 1.12**), decrease tumour growth *in vitro* in the one-digit micromolar range and delayed tumour growth *in vivo* as single agents (Lain et al. 2008).

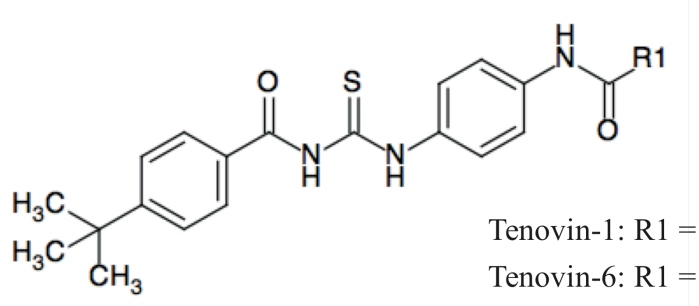

Figure 1.12: Structure of tenovin

It has been shown that tenovin-6 inhibits the growth of *S. cerevisiae* cultures with an IC_{50} of 30 µM and is more toxic to yeast than tenovin-1. Results of the yeast genetic screen showed that a strain heterozygous for a partial deletion of *SIR2* is hypersensitive to tenovin-6. In the biochemical 'Fluor de Lys' assay, tenovin-6 decreases human SirT1 activity with an IC_{50} of 21 µM and human SirT2 activity with an IC_{50} of 10 µM. It shows relatively poor inhibition of human SirT3 with an IC_{50} of 67 µM. *In vivo,* tenovin-1 and tenovin-6 increase levels of acetylated p53, H4K16 and α-tubulin (Lain et al. 2008).

Indoles

The most potent sirtuin inhibitors are a series of indoles that were found in the 'Fluor de Lys' assay against human SirT1. They are selective for SirT1 and inhibit it with IC_{50} values in the nanomolar range. The most potent inhibitor of this series is **Ex527** (**Figure 1.13**), which has an IC_{50} value of 0.098 µM for SirT1, 19.6 µM for SirT2 and 48.7 µM for SirT3 (Napper et al. 2005).

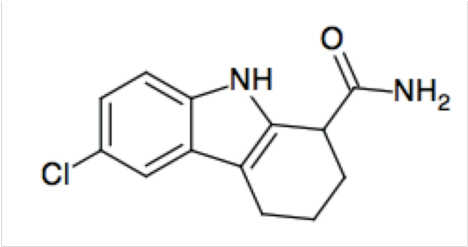

Ex527

Figure 1.13: Structure of the indole, Ex527

Peck *et al*. have shown that Ex527 triggers cell cycle arrest but not cell death, as is the case for salermide and sirtinol. However, it is not able to increase the acetylation level of p53 and α–tubulin. Computational modelling and docking studies showed that Ex527 only forms strong interactions with SirT1, but not with SirT2. This is in contrast to salermide and sirtinol, which interact with both SirT1 and SirT2 and are able to induce acetylation of p53 and cell

death. Therefore, the authors proposed that the inhibition of both SirT1 and SirT2 is required for increased p53 acetylation and inducing cell death (Peck et al. 2010).

1.7 Sirtuins and disease

As mentioned above, several lines of investigation indicate that sirtuins are involved in the development of age-related diseases such as diabetes, cancer, neurodegenerative diseases and many more. The intriguing thing about sirtuins, especially of SirT1, is that both inhibiting and activating of its activity may be useful in therapies for a broad range of different diseases. SirT1 plays a dual role in cell survival and in cell death, depending on tissue and environmental cues and can be modulated in different directions by a variety of different stimuli. This paragraph concentrates on three examples of disorder, metabolic disease, cancer and neurodegenerative diseases. In the case of metabolic diseases such as diabetes or obesity, sirtuin activators are of interest, whereas sirtuin inhibitors may be useful agents for certain cancer therapies.

Aging and metabolism

Several studies have shown that a diet of reduced calories, also known as calorie restriction (CR), promotes lifespan extension by up to 50 % in many organisms, including yeast, worms, flies and mice (Sinclair 2005). In mammals, CR triggers physiological changes that improve glucose homeostasis. It decreases insulin and glucose levels and improves insulin sensitivity. It is thought to be relevant to aging, because decreasing insulin signaling is implicating in longevity regulation in studies of model organisms (Guarente and Kenyon 2000). During aging, signs of metabolic imbalance, such as insulin resistance, are observed with increasing frequency. Such abnormal metabolic processes often become manifest as obesity and diabetes (Haigis and Sinclair 2010). As mentioned above, several studies have shown that yeast Sir2 and mammalian SirT1 may mediate the effects of CR, and although called to question, they were thought to be the missing link between genetic and environmental determinants of longevity (Guarente and Picard 2005). SirT1 interacts and deacetylates PGC-1α, a potent inducer of mitochondrial biogenesis as well as of the uptake and utilization of substrates for energy production in a number of cell types. Through deacetylation by SirT1, PGC-1α becomes active and promotes the induction of gluconeogenic genes and the suppression of glycolytic genes (Rodgers et al. 2005). In skeletal muscle, deacetylated and active PGC-1α promotes transcription of mitochondrial fatty acid oxidation genes, and SirT1 is required for

the switch to fatty acid oxidation under low nutrition conditions (Canto and Auwerx 2008; Canto and Auwerx 2009). SirT1 overexpressing transgenic mice gain weight, similar to wild type mice, but display protection from hepatic steatosis when fed a high-fat diet (Pfluger et al. 2008). However, the connection between SirT1 and CR mediated longevity is still a matter of debate and therefore more *in vivo* studies are needed to understand these complex mechanisms. Based on the theory that increased SirT1 activity mimics the effects of CR, sirtuin activators could be useful agents for therapies against age-related diseases such as diabetes or obesity.

Cancer

In view of one well-known substrate of SirT1, the tumour suppressor p53, most of the evidence is in favour of SirT1 being an oncogene. Through deacetylation of lysine 382 on p53, SirT1 reduces p53 activation and prevents apoptosis and senescence in response to stress and DNA damage (Luo et al. 2001; Vaziri et al. 2001). As mentioned above, several cancer cell types including colon, skin, breast, prostate and lung cancers show higher expression of SirT1 compared to the corresponding normal tissue (Fraga and Esteller 2007; Stunkel et al. 2007). Cancer cells with increased SirT1 levels have lower levels of acetylated p53, and they are more resistant to p53-dependent cell-cycle arrest and apoptosis (Luo et al. 2001; Vaziri et al. 2001). Consistent with this, cells derived from *SIRT1* knockout mice or transfected with siRNA against SirT1 show increase levels of acetylated p53 and increase sensitivity to stress (Cheng et al. 2003; Ford et al. 2005; Lain et al. 2008). Furthermore, Ford *et al.* have shown that specific inhibition of SirT1 by siRNA can increase tumour cell death with no toxic effect on normal cells. However, in a subsequent study, it was shown that p53 is not essential for tumour cell death by SirT1, but this does not rule out participation by p53 (Ford et al. 2005). These results show that sirtuin inhibitors might be useful agents against cancer types that overexpress SirT1.

However, the involvement of SirT1 in cancer biology is not simple. There also exist cancer cell types that show reduced levels of SirT1 compared to normal tissues, for example prostate and bladder carcinoma, glioblastoma and ovarian cancer (Wang et al. 2008). Several studies indicate that SirT1 can also act as a tumour suppressor. Firstly, SirT1 knockdown does not always affect cell viability or cell growth and is not always sufficient to induce activation of endogenous p53 (Ford et al. 2005; Solomon et al. 2006; Huang et al. 2008). Secondly, cell culture studies showed that SirT1 can also stimulate TNFα-induced cell death (Yeung et al. 2004). In support of a tumour-suppressor function, SirT1 was shown to be involved in repairing broken DNA and maintaining genome stability (Oberdoerffer et al. 2008; Wang et

al. 2008). In the case of SirT1's function as a tumour suppressor, small molecule activators may be useful therapeutic agents.

Neurodegenerative diseases

Several studies support the idea that sirtuins also have a therapeutic potential in neurodegenerative diseases such as stroke, Alzheimer's disease (AD), Parkinson's disease (PD) and Huntington's disease.

One hallmark of AD neuropathology is the abnormal deposition of the amyloid beta (Aβ) peptides in discrete area of the brain. Recent studies suggest that humans who maintain a low-calorie diet have a reduced risk of developing AD (Hendrie et al. 2001; Luchsinger et al. 2002; Mattson 2003). Furthermore, in various animal models, it has been shown that CR prevents amyloid neuropathology as seen in AD (Patel et al. 2005; Wang et al. 2005). Based on the evidence that sirtuins mediate the effect of CR, sirtuin activators may have beneficial effects in AD neuropathology. Consistent with this theory, SirT1 was shown to protect against neurodegeneration by deacetylation of p53 and PGC-1α in an AD mouse model (Kim et al. 2007a). Furthermore, it has been shown that SirT1 protects against Aβ-induced neurotoxicity by inhibiting NF-κB signalling (Chen et al. 2005).

After AD, PD is the second most common neurodegenerative disorder, which is characterized by the dysfunction and degeneration of dopaminergic neurons in the *substantia nigra* located in the midbrain. It alters the balance of neurotransmitters and results in the progressive loss of movement control (Gelb et al. 1999). The pathological hallmark of PD is the accumulation of protein aggregates called Lewy bodies (LB), which consist mainly of the protein α-synuclein (Spillantini et al. 1997). It was shown that SirT2 regulates α-synuclein inclusion number, size and cytotoxicity. Therefore, SirT2 inhibition prevents α-synuclein toxicity and salvages the degeneration of dopaminergic neurons in models of PD (Outeiro et al. 2007). However, it has also been shown that resveratrol protects SirT1-dependent neuroblastoma cells (SK-N-BE) against α-synuclein toxicity (Albani et al. 2009). The exact mechanism is still unknown, but these examples indicate that both sirtuin inhibitors and activators may be useful agents in neurodegenerative disorders, and that further investigation of the role of sirtuins in neuropathology is required.

1.8 Aim of this thesis

Based on the fact that sirtuins can be found at different locations in the cell and have a variety of different substrates, they are involved in many biological processes. For this reason, they play important roles in several human diseases, including cancer, age-related diseases, type II diabetes and neurodegenerative diseases (Longo and Kennedy 2006; Milne and Denu 2008; Haigis and Sinclair 2010). Furthermore, SirT1 plays a dual role in cell survival and in cell death and it can be modulated in different directions by a variety of different stimuli. Several lines of investigation indicate that small molecules that inhibit or activate sirtuin activity are promising candidates for the therapy of a number of age-related diseases as well as cancer. Most of the known sirtuin modulators have high IC_{50} values, interact with multiple targets or have low bioavailability, therefore the identification of novel sirtuin modulators, especially of SirT1, is a promising field. For this reason, the aim of this thesis was the identification of novel sirtuin inhibitors and activators. For this approach we established a fluorescence-based MAL (Methylaminocoumarinacetyllysin) deacetylation assay that is suitable for a high-throughput screen (Hoffmann et al. 1999; Heltweg and Jung 2003). Subsequently, two libraries (BIOMOL, ChemBioNet) were screened in order to identify new inhibitors as well as activators of SirT1. Furthermore, the results of the screens were validated with the help of another deacetylase activity assay that is based on an acetylated p53-derived peptide without fluorophore. Moreover, the specificity of the identified modulators was characterized by the usage of other sirtuin family members in the MAL deacetylation assay. Furthermore, we measured the inhibitory effect of the identified compounds on SirT1 constructs that were truncated in the N-terminal region in order to determine potential interaction sites between the inhibitor and SirT1. In a second set of experiments, the *in vivo* influence of the inhibitors and their anticancer potential were analyzed. Furthermore, we determined whether the inhibitors might affect acetylation of known *in vivo* targets of sirtuins, such as p53 and α-tubulin.

2. Material & Methods

2.1 Media and growth conditions

E. coli strains used for plasmid amplification were cultured according to standard procedures (Sambrook 1989) at 37 °C in Luria-Bertani medium (LB: 5 g/l yeast extract, 10 g/l tryptone, 5 g/l NaCl) supplemented with either 100 µg/ml ampicillin or 50 µg/ml kanamycin. In the case of the Rosetta *E. coli* strain 34 µg/ml chloramphenicol was additionally added.
S. cerevisiae were cultured at 30 °C in standard complete medium (YPD: 10 g/l yeast extract, 20 g/l peptone, 2 g/l glucose) or standard minimal medium (YM: 6,7 g/l yeast nitrogen base w/o amino acids) as described previously (Sherman, 1991). YM medium was supplemented with 2 % glucose and as required with 20 µg/ml for adenine, uracil, tryptophan, methionine and histidine or 30 µg/ml for leucine and lysine. YM + 5-FOA (5-fluoro-orotic acid; US Biological) medium contained 5-FOA at 1 mg/ml, 20 µg/ml uracil and 2 % glucose.
Human cancer cell lines were cultured in RPMI 1640 medium (Biochrom) containing 10 % or 0.5 % fetal calf serum (FCS), 1 % penicillin/streptomycin and 2 mM L-glutamine. Cells were maintained at 37 °C in a humidified atmosphere containing 5 % CO_2. Cells were passaged at 70-80 % confluence by trypsinization.

2.2 *E. coli* strains

All *E. coli* strains used in this study were from the laboratory strain collection.

Tabelle 2.1: *E. coli* strains used in this study

Strain	Genotype
DH5α	F^- φ80d*lac*ZΔM15 Δ(*lac*ZYA-*arg*F)U169 *rec*A1 *end*A1 *hsd*R17(r_k^-, m_k^+) *pho*A *sup*E44 *thi*-1 *gyr*A96 *rel*A1 λ^- (Invitrogen)
Rosetta (DE3)	F^- *omp*T *hsd*SB (r_B^- m_B^-) *gal dcm* pRARE (Cam^R) (Merck)

2.3 Saccharomyces cerevisiae strains

Yeast strains used in this study are listed in **Table 2.2** Unless indicated otherwise, strains were constructed during this study or were from the laboratory strain collection. Yeast was grown and manipulated according to standard procedures (Sherman, 1991). Marker selection

was performed on selective YM plates. Plates containing 5-FOA were used to select against *URA3*.

Tabelle 2.2: *S. cerevisiae* strains used in this study

Strain	Genotype
AEY264	*MAT***a** *his4*
AEY325	ROY1 *mat*αΔp *hml*αΔp *HMR*ssα *trp1-1 ade2 leu2-3,112 ura3, his*$^-$
AEY4017	*MAT*α *ade2-1 ura3-1 his3-11,15 leu2-3, 112 trp1-1 can1-100* (=W303-1B) *adh4::URA3-*UAS_{Gal}*-*$(C_{1-3}A)_n$ sir2Δ*::KanMX*
AEY4335	AEY4017 + pAE1369
AEY4336	AEY4017 + pAE1365
AEY4337	AEY4017 + pAE1366
AEY4338	AEY4017 + pAE1370
AEY4339	AEY4017 + pAE1367
AEY4340	AEY4017 + pAE1368

2.4 Human cancer cell lines

Cell lines used in this study were obtained from M. Schuler (University Hospital Essen).

A549 cell line was initiated in 1972 by D.J. Giard et al. through explant culture of lung carcinomatous tissue from a 58 year old Caucasian male (www.atcc.org).

NCI-H460 cell line was derived by A.F. Gazdar and associates in 1982 from the pleural fluid of a patient with large cell cancer of the lung. The cells express detectable p53 mRNA levels comparable to normal lung tissues and exhibit no gross structural DNA abnormalities (www.atcc.org).

NCI-H1299 cell line was derived by A.F. Gazdar, H.K. Oie, J.D. Minna and associates from a lymph node metastasis. The cells have a homozygous partial deletion of the p53 gene and lack expression of p53 protein (www.atcc.org).

2.5 Molecular cloning

Plasmid generation was performed according to standard cloning techniques (Sambrook et al. 1989). Kits for plasmid isolation and gel elution were purchased from Qiagen and Macherey-Nagel. Restriction enzymes and respective buffers were used from NEB, pGEMT vector systems kit from Promega and T4 DNA Ligase from Roche.

In yeast, gene fusions were created by PCR-mediated plasmid gap repair (P-MPGR). For this

purpose, the corresponding DNA fragments were amplified by PCR and introduced into a linearized plasmid by homologous recombination in yeast.

For amplification of truncated SIRT1 constructs for heterologous expression, the SIRT1 full-length plasmid (pAE1287) was used as template. One specific reverse primer with overhang containing a BamHI restriction site and different specific forward primers with overhang containing an NdeI restriction site were used to amplify SIRT1. These truncations were cloned into the pET15b vector. For the exchange of single amino acids within the SIRT1 catalytic domain to create inactive mutants, the PCR sewing technique was used. In the first step, short complementary overhangs were generated that contain the desired mutations and served as polymerase start site in a second PCR reaction.

Tabelle 2.3: Plasmids used in this study

Plasmid[a]	Description	Source
pAE231	pRS315-Sir2	
pAE232	pRS315-Sir3	
pAE1287	pET30z-SIRT1	
pAE1365	pRS414-Sir3-Sir2 (243-562)	Marc R. Gartenberg
pAE1366	pRS414-Sir3-Hos3 (2-549)	Marc R. Gartenberg
pAE1367	pRS414-LexA-Sir2 (78-252)-Hos3 (2-549)-Sir2 (522-562)	Marc R. Gartenberg
pAE1368	pRS414-LexA-Sir2 (78-252)-Hos3 (2-549 AA)-Sir2 (522-562)	Marc R. Gartenberg
pAE1369	pRS414-Sir3-Sir2 (2-562)	Marc R. Gartenberg
pAE1370	pRS414-LexA-Sir2 (78-562)	Marc R. Gartenberg
pAE1423	pET30z-SIRT1 (Rosetta)	
pAE1394	pET24a(+)-Sir2-His6x (Rosetta)	
pAE1690	pET15b-SIRT1_A (156-664)	
pAE1692	pET15b-SIRT1_B (172-664)	
pAE1694	pET15b-SIRT1_C (219-664)	
pAE1696	pET15b-SIRT1_D (225-664)	
pAE1698	pET15b-SIRT1_E (230-664)	
pAE1700	pET15b-SIRT1_F (235-664)	
pAE1702	pET15b-SIRT1_G (240-664)	
pAE1704	pET30z-SIRT1_N (N346A)	
pAE1706	pET30z-SIRT1_H (H363A)	

[a] Unless indicated otherwise, plasmids were constructed during the course of this study or were from the laboratory plasmid collection.

Oligonucleotides used for plasmid constructions are listed in **Table 2.4**. Oligonucleotides were designed using Ape software and synthesized by Metabion.

Tabelle 2.4: Oligonucleotides used for cloning and mutagenesis

Oligonucleotides	Sequence (in 5' to 3' direction)[a]
SIRT1 fw	CAGCcatatgATGGCGGACGAGGCG
SIRT1 rv	TATAggatccTTAGTCATCTTCAGAGTCTGAATATACCTC
SIRT1_A fw	CAGCcatatgATGGGTTTTCATTCCTGTGAAAGTGATGAGGAG
SIRT1_B fw	CAGCcatatgATGAGCTCTAGTGACTGGACTCCAAGGCCACGG
SIRT1_C fw	CAGCcatatgATGACACTGTGGCAGATTGTTATTAATATCCTT
SIRT1_D fw	CAGCcatatgATGATTAATATCCTTTCAGAACCACCAAAAAGG
SIRT1_E fw	CAGCcatatgATGGAACCACCAAAAAGGAAAAAAAGAAAAGAT
SIRT1_F fw	CAGCcatatgATGAAAAAAAGAAAAGATATTAATACAATTGAAGATGCT
SIRT1_G fw	CAGCcatatgATGATTAATACAATTGAAGATGCTGTGAAATTACT
N346A rv	CCTGTTCCAGCGTGTCTATG**GC**CTGGGTATAGTTGCGAAGTAGTT
H363A rv	GATGCTGTTGCAAAGGAACCA**GC**ACACTGAATTATCCTTTGGATTCCC

[a] Sites for restriction endonucleases are shown in lower case letters, bold letters indicate nucleotide changes as compared to wild-type SirT1.

2.6 Silencing assays in *Saccharomyces cerevisiae*

HM silencing was measured by determining the mating ability of a strain with a mating-type tester strain in a patch-mating assay. For this assay, the candidate strains were streaked in 1 cm^2 patches on YPD plates and grown over night at 30 °C. Thereafter, they were replicated on YM plates with a lawn of 2 OD_{600} of a mating-type tester strain *MAT***a** *his4* (AEY264) and incubated for two days at 30 °C. The amount of grown diploid cells served as a measurement of the mating efficiency and thus *HMR* silencing. To test the influence of compounds on *HM* silencing, the mating-type tester and ROYI (AEY325) strain were grown to 0.9 OD_{600}, mixed and plated together on a YM plate to a final OD_{600} of 0.5 of each strain. Subsequently, filters containing different amounts of compound solution (in DMSO) were placed on this YM plate. Cells were incubated for two days at 30 °C. The yield of diploid cells was taken as indicator for *HM* silencing.

Telomeric silencing assays were performed using a telomeric *URA3* reporter (Gottschling et al. 1990). *URA3* silencing was tested by spotting serial dilutions of cells on YM plates with or without uracil and YM plates with 5-FOA. After incubation of two days at 30 °C, the growth of the cells was monitored.

2.7 Protein purification of recombinant SirT1

Polyhistidine-tagged recombinant proteins can be purified with the help of immobilized metal affinity chromatography (IMAC (Hochuli 1988)), known as His-tag purification. This purification is based on the affinity of the 6xHis-Tag for Ni^{2+}-ions, which are immobilized onto a chelating surface. It allows efficient purifications under native and denaturating conditions.

Rosetta *E. coli* strains carrying the expression vector were freshly grown in LB medium supplemented with either 100 µg/ml ampicilin or 50 µg/ml kanamycin and 34 µg/ml chloramphenicol and used to inoculate a larger culture. Depending on the protein, 500 ml up to 2 l LB medium supplemented with either 100 µg/ml ampicilin or 50 µg/ml kanamycin and 34 µg/ml chloramphenicol were inoculated to a final OD_{600} of 0.2. Cells were grown at 37 °C to an OD_{600} of 0.6-0.9, and protein expression was subsequently induced with 1 mM IPTG (Isopropyl-β-D-thiogalactopyranosid) for 4 h at 30 °C or 37 °C. Subsequently harvested at 6000 rpm, 4 °C for 10 min, mixed with small amounts of lysozyme and stored at -20 °C. Cell pellets were slowly thawed in the fridge and lysed in sonication buffer (30 mM potassium phosphate buffer (KPi) pH 7.0, 300 mM KCl, 10 % Glycerin (v/v), 0.1 mM DTT, complete Protease Inhibitor Cocktail; Roche) by repeated addition of small amounts of lysozyme. This lysate was stirred on ice up to 2 h and sonicated for 10 min using 10 sec intervals. Subsequently, the lysate was centrifuged at 4000 rpm for 30 min until it was almost clear. The lysate was incubated with 1,5 ml Ni-beads (Profinity IMAC Ni-charged resin; Bio-Rad), which were equilibrated with sonication buffer containing 20 mM imidazole, at 4 °C over night and then loaded onto a column. The protein-Ni-beads mixture was washed twice with sonication buffer containing 20-50 mM imidazole, and the protein was eluted from the beads with elution buffer (30 mM KPi pH 7.0, 300 mM KCl, 10 % Glycerin (v/v) 0.1 mM DTT) containing increasing imidazole concentrations (90-250 mM). Elution fractions containing the protein of interest (as measured by SDS-PAGE) were collected and dialyzed at 4 °C in dialysis buffer I (30 mM KPi pH 7.0, 200 mM KCl, 20 % Glycerin (v/v), 0.1 mM EDTA, 1 mM DTT) for 3 h and in dialysis buffer II (30 mM KPi pH 7.0, 100 mM KCl, 50 % Glycerin (v/v), 0.1 mM EDTA, 1 mM DTT) over night. The final protein concentration was determined by Bradford protein assay (Bio-Rad) according to the manufacturer's instructions.

2.8 Protein extraction from human cells

Cells cultured in 6-well plates (300000 cells per well) were collected in 2-ml tubes by trypsinization and centrifugation at 1400 rpm for 10 min. The pellet was washed with cold PBS (*Phosphat buffered Saline*) and lysed in 100 µl lysis buffer (20 mM Hepes pH 7.9, 400 mM NaCl, 25 % Glycerin (v/v), 1 mM EDTA, 1 mM EGTA, 1 mM DTT, complete Protease Inhibitor Cocktail; Roche and 1 % NP-40) for at least 30 min on ice. Subsequently, the cell lysate was flash frozen in liquid nitrogen and thawed on ice. The samples were centrifuged at 13000 rpm, 4 °C for 20 min and the supernatant containing proteins was transferred into a fresh 1.5-ml tube. The final protein concentration was determined by Bradford protein assay (Bio-Rad) before the samples were stored at -80 °C until further use.

2.9 Acid extraction of histones from human cells

For histone extraction, cells cultured in a 100 mm dish ($2*10^6$ cells per dish) were collected in 2-ml tubes by trypsinization and centrifugation at 1400 rpm for 10 min. The pellet was washed with 2 ml cold PBS and centrifuged again. The supernatant was discard and the pellet was re-suspended in 1 ml hypotonic lysis buffer (10 mM Tris-HCl pH 8.0, 1 mM KCl, 1.5 mM $MgCl_2$, 1 mM DTT, complete Protease Inhibitor Cocktail (Roche) and 1 mM PMSF (Phenylmethylsulfonylfluorid)) and incubated for at least 1 h on a rotator at 4 °C. The intact nuclei were collected by centrifugation at 13000 rpm, 4 °C for 20 min. The supernatant was discard again and the nuclei were re-suspended in 400 µl 0.2 M H_2SO_4 and incubated on the rotator at 4 °C over night. The samples were centrifuged at 13000 rpm, 4 °C for 20 min to remove nuclear debris. The supernatant containing histones was transferred to a fresh 1.5-ml tube, mixed gently with 132 µl TCA (*Trichloroacetic acid*) and incubated on ice for at least 1 h. Histones were collected by centrifugation at 13000 rpm, 4 °C for 20 min and the supernatant was carefully removed. The histone pellet was washed twice with ice-cold acetone without dissolving the pellet. The histone pellet was then air-dried at room temperature and dissolved in 50 µl H_2O. The histone concentration was determined by Bradford protein assay (Bio-Rad) before the samples were stored at -80 °C until further use.

2.10 SDS-PAGE and Western Blotting

Proteins were separated by SDS-PAGE in Tris-glycine buffer according to standard procedure (Laemmli 1970). Gels were stained with Coomassie blue (Bio-Rad) according to the manufacturer's instructions. Protein transfer to nitrocellulose membranes (Bio-Rad, GE Healthcare, Whatman) was accomplished by blotting with the Bio-Rad Tank Transfer System with 5.5 mA x h/cm^2 in transfer buffer (48 mM Tris-base, 39 mM glycine, 0.037 % SDS, 20 % methanol). The membrane was subsequently blocked for at least 1-2 h at room temperature in 5 % BSA, TBST (50 mM Tris-HCl pH 7.5, 150 mM NaCl, 0.1 % Tween-20, 5 % BSA powder) or in 3 % BA (ECL *Advance* blocking agent, GE Healthcare), TBS / 0.05 % Tween-20, depending on antibody used. Primary antibody was incubated over night at 4 °C and secondary antibody for 1 h at room temperature, both in 5 % BSA or 3 % BA (concentrations see Table below). Thereafter and between the antibodies the membrane was washed up to 5 times, in total no longer than 1 h in TBST. Western blot signals were detected using Amersham ECL^{TM} Western Blotting Analysis System (GE Healthcare) and Amersham Hyperfilm^{TM} ECL chemiluminiscence films (GE Healthcare).

Tabelle 2.5: Antibodies used in this study

Antibody	Company (Catalog)	Application notes
α-poly-Histidin	Sigma	1:3000 in 5 % BSA
α-Ac(K382)-p53	Millipore (04-1146)	1:1000 in 3 % BA
α-p53	BD Pharmingen (554294)	1:1000 in 3 % BA
α-Ac(K40)-Tubulin	Santa Cruz (sc-23950)	1:1000 in 3 % BA
α-Tubulin	Abcam (ab15246)	1:1000 in 3 % BA
α-rabbit-HRP	Sigma (A0545)	1:5000 in same solution as primary antibody
α-mouse-HRP	Sigma (A9044)	1:1000 in same solution as primary antibody

2.11 Fluorescence based deacetylase assay

The fluorescence-based assay used here is a nonradioactive assay to measure deacetylase activity of proteins and is suitable for high throughput screening (Hoffmann et al. 1999; Wegener et al. 2003). It is based on a substrate that contains an ε-acetylated lysine residue followed by a 7-amino-4-methylcoumarin moiety at their carboxy terminus (MAL = **M**ethylaminocoumarin**a**cetyl**l**ysin; Bachem). The assay is a two-step reaction as shown in **Figure 2.1**. In the first reaction, the substrate MAL is deacetylated to ML (**M**ethylamino-cumarin**l**ysin) by sirtuin. In the second reaction, ML is recognized as substrate by trypsin,

which cleaves only the deacetylated substrate ML. This generates the fluorophore AMC (7-amino-4-methylcoumarin) that can be detected by a fluorometic reader. AMC fluoresces at a excitation wavelength of 390 nm and an emission wavelength of 460 nm. The amount of fluorescence produced is proportional to the amount of deacetylated substrate.

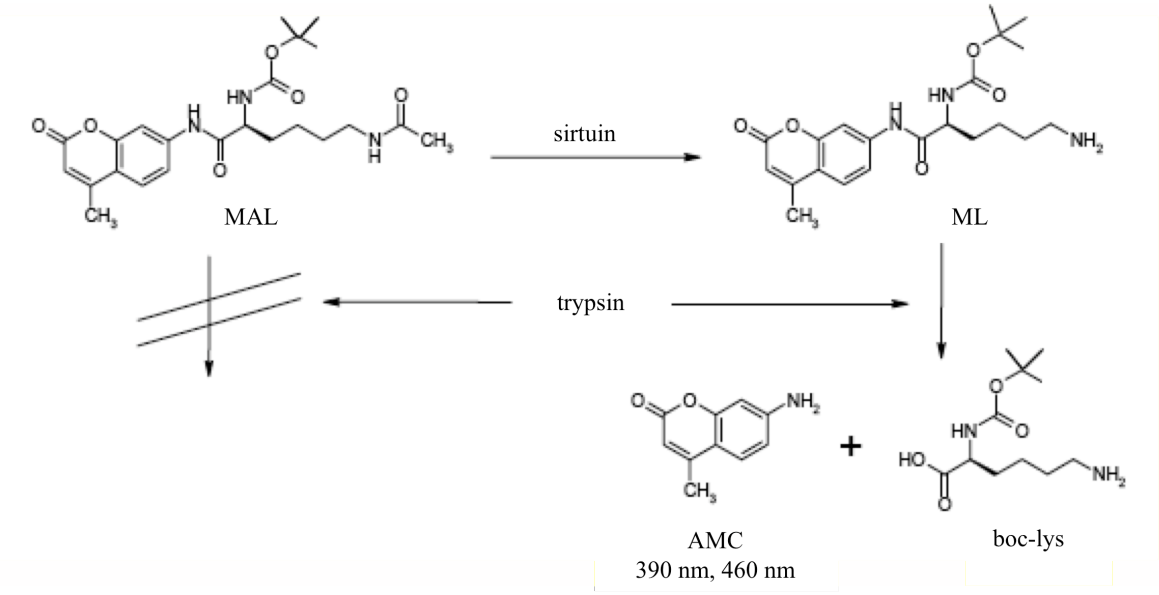

Figure 2.1: Fluorescence-Assay to measure deacetylase activity of sirtuins
In the first reaction the ε–acetylated lysine substrate MAL is deacetylated to ML by sirtuin. In the second reaction only the deacetylated substrate ML is cleaved by trypsin. This generates the fluorophore AMC, which can be detected by a fluorometic reader (390, 460 nm).

Purified recombinant human SirT1 was diluted in 1x SirT buffer (25 mM Tris-HCl pH 8, 1 mM $MgCl_2$, 2,7 mM KCl, 137 mM NaCl, freshly added 1 mg/ml BSA and 1 mM DTT). 10 µl of this dilution was placed per well in a 384-well Plate. Subsequently, 1 µl DMSO (positive and negative control reaction) or 1 µl compound (diluted in DMSO) was added in each well and incubated for 10 min at room temperature. The reaction was started with 10 µl substrate solution (100 µM MAL, 2 mM NAD^+ in 1x SirT buffer) followed by 4 h of incubation at 37 °C. After this incubation time, 20 µl trypsin solution (0,5 mg/ml in 1x SIRT buffer) was added and incubated for 1 h at 37 °C. The fluorescence was measured at an excitation wavelength of 360 nm and an emission wavelength of 465 nm with the fluorescence reader (GENiosPro, Tecan). With all measurements, positive and negative control reactions were performed simultaneously. Negative control reactions contain only the substrate solution, DMSO and trypsin solution, but no enzyme to determine the background fluorescence and subtract it from the positive control and the other measured values.

The control reaction to test for autofluorescence of each compound contains only the acetylated substrate (MAL) and the respective compound, but no enzyme. The control

reaction to test for trypsin inhibition contains the deacetylated substrate (ML; Bachem) and the trypsin solution and the compounds as applicable.

2.12 High Performance Liquid Chromatography (HPLC)-based deacetylase assay

The HPLC-based deacetylase assay was used to measured deacetylase activity of SirT1 without using a fluorescence-labelled substrate (Liu et al. 2008). Purified recombinant human SirT1 diluted in 1x SirT buffer was incubated with 100 µM acetylated p53 peptide (Ac-p53, HLKSKKGQSTSRHKK(Ac)LMFK, Biosyntan), 1 mM NAD^+ and 1 µl DMSO (positive control) or 1 µl compound (diluted in DMSO) for 30 min at 37 °C. Samples were analysed by HPLC (Jasco) using a Jupiter RP-C18 (5 micron, 250 mm x 4.60 mm; Phenomenex) column. A total injection volume of 40 µl of assay reaction was loaded on the column. The separation of Ac-p53 and deacetylated p53 peptide was achieved by a linear gradient of 1 % to 35 % acetonitrile in water containing 0.1 % TFA (Trifluoroacetic acid) over 30 min. The peptides were detected and quantified using a UV detector at a wavelength of 214 nm.

2.13 Flow cytometry

For cell cycle analysis of human cell culture, cells were cultured in 6-well plates (50000 cells per well) and incubated with compounds of interest for 24 h or 48 h at 37 °C. Subsequently, the supernatant and the cells were collected in 5-ml polypropylene tubes (BD). After centrifugation at 1400 rpm for 10 min, the supernatant was discarded and the cell pellet was dissolved in 300 µl propidium iodide staining solution (50 µg/ml propidium iodide, 0.1 % sodium citrate, 0.1 % Triton X-100). The specimens were incubated in the dark at 4 °C for at least 30 min and analysed with the flow cytometer (Calibur, BD).

2.14 Cell Proliferation and Viability Assay (MTT assay)

This assay is a sensitive, *in vitro* assay for the measurement of cell proliferation and reduction of cell viability, when metabolic events lead to apoptosis or necrosis.
Cells were cultured in a flat-bottom, 96-well tissue plate (2000-3000 cells per well) and incubated with compounds of interest at 37 °C. After a define incubation time, cells were

treated with 10 µl/well of a tetrazolium compound MTT (3-[4,5-dimethylthiazol-2-yl]-2,5-diphenyltetrazolium bromide), which is reduced by metabolically active cells to insoluble purple formazan dye crystals, for 4 h at 37 °C. Through the addition of 100 µl/well solubilisation solution (0.01 M HCl, 10 % SDS) and incubation over night at 37 °C, the crystals were solubilised, and the absorbance was read using a spectrophotometer (550-600 nm). The rate of MTT reduction is proportional to the rate of cell proliferation or cell viability.

3. Results

3.1 Identification of novel sirtuin modulators

3.1.1 Establishment of MAL deacetylation assay

To date, several inhibitors and putative activators of sirtuins, especially of SirT1, are known (reviewed in (Alcain and Villalba 2009a; Alcain and Villalba 2009b)). However, most of them have a low bioavailability, a high IC_{50} value and interact with multiple targets. For this reason, we sought to identify new inhibitors and activators of sirtuins, with a focus on SirT1, in a high throughput screen. In the past, the deacetylation activity of sirtuins was measured in assays based on protein marked with radioactivity labeled acetyl-lysine residues, which however are not suitable for high-throughput screening. Subsequently, the fluorescence-based assay 'Fluor de Lys' was developed that functions without the use of radioactivity and is convenient for high-throughput screening (Heltweg et al. 2003; Wegener et al. 2003). As mentioned above, this assay is controversial, because of the fluorophore on the substrate that influences the activity of sirtuins. Nonetheless, we sought to establish this assay in our lab and use it to screen different compound libraries, because it is easy to perform, suitable for high-throughput and cost-effective. However, we used a modified assay, because the 'Fluor de Lys' assay was only available as kit (BIOMOL) and cost-intensive. We used, instead of a p53-derived peptide, an acetylated lysine coupled with a fluorophore (MAL; (Hoffmann et al. 1999)) that is commercially available. To set up the assay, different assay conditions such as substrate (MAL), NAD^+ and sirtuin concentrations were assessed. Furthermore, different time course experiments were performed in order to determine the adequate incubation time of the deacetylation reaction as well as the subsequent trypsin cleavage reaction (described in **2.11**). In view of the fact that we planned to perform high-throughput screens, the MAL deacetylation assay was adapted for 384-well low volume plates. In order to determine the appropriate 384-well plate, several plates (Corning, Eppendorf) with different properties such as low binding affinity and low background noise were tested. Subsequently, the complete reaction volume was reduced from 50 µM to 20 µM, whereas the substance concentrations were constant.

As a source of SirT1, polyhistidin-tagged recombinant human SirT1 protein was expressed and purified from *E. coli*. The protein was eluted from the Ni^{2+}-agarose beads with increasing imidazole concentrations and the elution fractions were subjected for SDS-PAGE gel electrophoresis. The fractions were analyzed by Western blotting against SirT1-6xHis with an

α-poly-His antibody, and the proteins were stained with Coomassie blue to determine which fractions contained most of the protein of interest. The corresponding fractions were pooled and dialyzed as described in **2.7**. As shown in **Figure 3.1**, next to the SirT1 protein band, additional bands could be observed in the Coomassie blue stained SDS-PAGE gel, resulting probably from other contaminating proteins that were co-eluted from the column. The expected molecular weight of SirT1 was 81.7 kDa (Frye 2000), however it ran constantly below the 130 kDa band of the molecular weight marker.

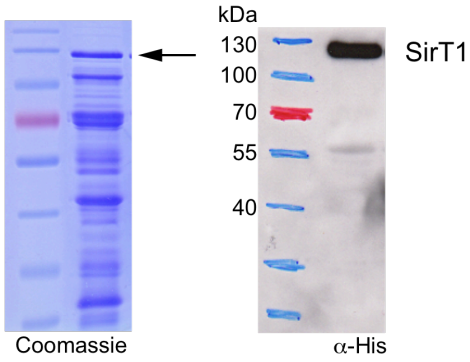

Figure 3.1: Purification of recombinant human SirT1
Coomassie-stained SDS-PAGE gel of purified fraction of recombinant human SirT1, the respective band is highlighted by the arrow. SirT1-containing fraction was identified by Western blotting with α-poly-His antibody.

The activity of the purified SirT1 was subsequently tested in the MAL deacetylation assay. For this purpose, a serial dilution of the purified SirT1 was performed, and 10 µl of each dilution was placed in wells of the 384-well plate. Subsequently, 1 µl of DMSO or a compound of interest was added and pre-incubated for 10 min at room temperature. The deacetylation reaction was initiated with the addition of 10 µl 2x concentrated substrate solution containing MAL (200 µM) and NAD^+ (2 mM). After an incubation time of 4 h at 37 °C, the reactions were stopped with the addition of 20 µl trypsin solution (0.5 mg/ml) and a further incubation of 1 h at 37 °C. Finally, the fluorescence was measured using a fluorescence reader (GENiosPro, TECAN) with the excitation wavelength set to 360 nm and the emission set to 465 nm.

In the following experiments, a negative control reaction where the sirtuin is absent as well as a control reaction containing DMSO was performed simultaneously with test for inhibition or activation. The negative control was subtracted from each measurement value, and the DMSO control was set to 100 %. As shown in **Figure 3.2**, the purified SirT1 protein (approximately 0.5 µM) was active, and it could be stimulated by resveratrol, the putative activator of SirT1 and inhibited by suramin, the well-known inhibitor of SirT1. This indicated that the purified enzyme was indeed active and constituted SirT1.

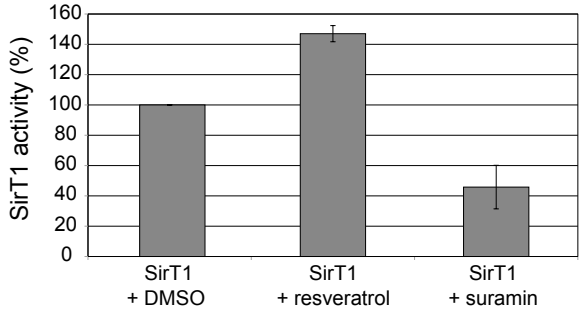

Figure 3.2: Deacetylase activity of purified recombinant human SirT1
The deacetylase activity of SirT1 purified from *E. coli* was measured by the MAL deacetylation assay and can be enhanced by the addition of 25 µM of resveratrol, a known activator of SirT1. Conversely 12.5 µM of suramin, a known inhibitor of SirT1, impairs the activity of SirT1. The control reaction containing DMSO was set to 100 %. Values correspond to the average enzyme activity of three independent experiments ± standard deviation.

To verify that the deacetylation activity that was measured in the MAL deacetylation assay, really depended on the purified SirT1 protein, we constructed two inactive SirT1 constructs. The activity of yeast Sir2 depends on amino acids N^{345} and H^{364}, which are highly conserved residues in the catalytic core domain of sirtuins (Imai et al. 2000). Correspondingly, we generated alanine mutations of N^{346} (SirT1-N346A) and H^{363} (SirT1-H363A) of SirT1 (pAE1706 and pAE1707) by site-directed mutagenesis. Similar to SirT1, both mutants were expressed and purified from *E. coli* using His-tag purification. The amount of protein was determined by a Bradford assay and Coomassie stained SDS-PAGE gel, and the SirT1 corresponding fractions were also analyzed by Western blotting with α-poly-His antibody (**Figure 3.3A**).

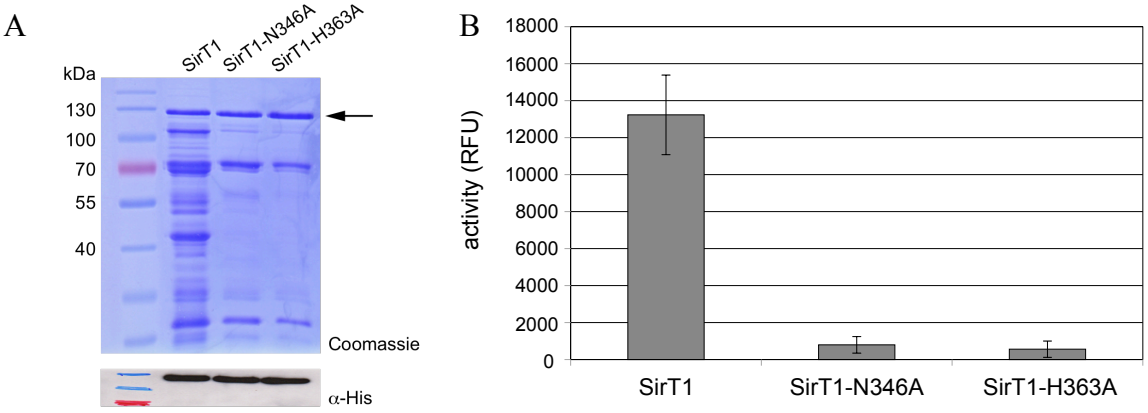

Figure 3.3: SirT1 catalytic mutants showed no deacetylation activity
(A) The amount of protein was determined by Coomassie stained SDS-PAGE gel, the respective band is highlighted by the arrow. The expression of SirT1 protein in the respective fractions was analyzed by Western blotting with α-poly-His antibody. (B) Deacetylase activity of inactive SirT1 mutants (SirT1-N346A and SirT1-H363A) was measured by the MAL deacetylation assay and compared with active SirT1 purification. From all SirT1 constructs the same amount of protein was put into the MAL deacetylation assay and their activity was measured. The values correspond to the average enzyme activity of a three-fold determination ± standard deviation of one experiment.

Subsequently, the activity of SirT1-N346A and SirT1-H363A was analyzed with the MAL deacetylation assay in comparison to a purification of the wild-type SirT1 protein. As can be seen in **Figure 3.3B**, both alanine mutants showed no deacetylase activity in comparison to wild type SirT1. This suggested that the observed deacetylase activity in the MAL deacetylation assay was indeed the activity of SirT1 rather than a co-purifying protein.

3.1.2 High throughput screening of compound libraries

BIOMOL library

After the establishment of the MAL deacetylation assay, a small library of approximately 500 natural compounds (purchased from BIOMOL) was screened for SirT1-deacetylating activities. All compounds were diluted in DMSO (1 mg/ml), and approximately 125 µM of each compound was added to the 384-well plate for the SirT1 deacetylation assay. This screen resulted in 13 potential activators and 15 potential inhibitors of SirT1, whereby compounds with an inhibition of more than 50 % (i.e. decreased fluorescence as compared to the control reaction) or an activation of more than 200 % of SirT1 activity (i.e. increased fluorescence compared to the control reaction) were considered.

It was possible that some of the potential activators showed autofluorescence and thus increased fluorescence readings without truly increasing MAL deacetylation. To examine the fluorescence measurements, each compound was taken in a MAL reaction without the addition of SirT1. Indeed, 3 of these 13 activators showed increased fluorescence (Camptothecin, Harmaline HCl, Harmalol HCl), although no enzyme was added, indicating autofluorescence. These compounds therefore were not purchased.

In the case of inhibitors, it was possible that they inhibited the trypsin reaction rather than MAL deacetylation, which would also lead to decreased fluorescence readings. To examine this, we obtained the deacetylated substrate (ML) and incubated it with trypsin in the presence of the inhibitor. If the inhibitors do not inhibit the trypsin reaction, then trypsin cleavage of ML showed and to a measurable increases fluorescence. This was the case for all 15 inhibitors indicating that they did not inhibit trypsin cleavage.

In a next step, the remaining 10 activators and 15 inhibitors were validated in the MAL deacetylation assay. Different concentrations of each compound were measured for MAL deacetylation in at least three independent experiments. After the validation, only 3 activators and 4 inhibitors could be verified, because the other compounds showed no activation or inhibition in dose-dependent manner. Interestingly, three compounds, quercetin, luteolin and kaempferol, are already known as SirT1 activators (Howitz et al. 2003). One of the four

inhibitors was rottlerin, a known protein kinase C (PKC) inhibitor, that might be unspecific and therefore was not further investigated. The other three inhibitors, shikonin, dihydrotanshinone and cryptotanshinone (**Figure 3.4**) have a low IC_{50} value in the micro-molar range, and they are not known as sirtuin inhibitors so far.

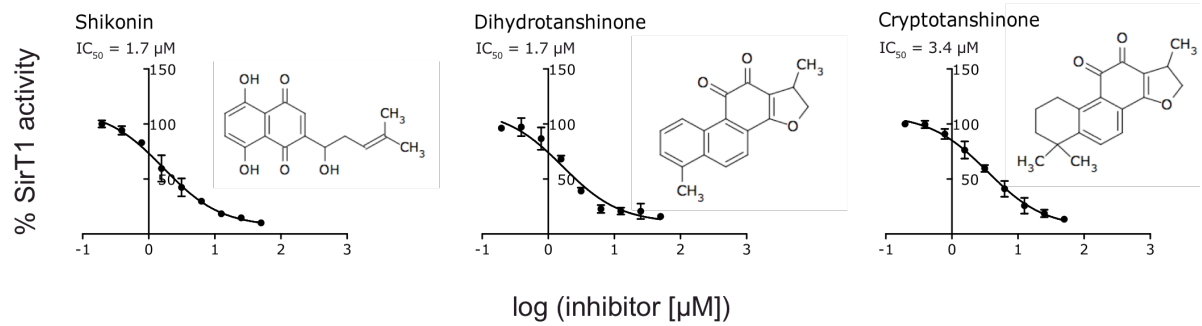

Figure 3.4: Identification of potential SirT1 inhibitors from the BIOMOL library
SirT1 deacetylation activity was strongly inhibited by shikonin, dihydrotanshinone and cryptotanshinone. SirT1-dependent MAL deacetylation was measured by the MAL deacetylation assay. The control reaction containing DMSO was set to 100 %. IC_{50} values and curve fitting were performed using GraphPad. Values correspond to the average enzyme activity of three independent experiments ± standard deviation.

ChemBioNet library

Next, we screened the ChemBioNet library, which is located at the FMP (Screening Unit of the Leibniz-Institute for Molecular Pharmacology Berlin) and consists of approximately 18.000 compounds, for SirT1 activators and inhibitors. For this screen, several measurements were required in advance to optimize the MAL deacetylation assay, including the improvement of the deacetylation rate. Therefore, a series of measurements were performed, for instance different concentrations of buffer components (Tween, BSA and DTT) as well as MAL and enzyme concentrations were tested. Finally, higher concentrations of DTT (dithiothreitol; 1mM) and SirT1 enzyme (approximately 1 µM) improved the deacetylation of MAL. Furthermore, the procedure of the assay had to be tested with the automatic pipetting system, each solution was added to the plate with a different pipetting system to prevent contaminations.

The first screen of this library achieved 352 potential results, both inhibitors and activators that were further validated as for the compounds of the BIOMOL library. The analysis of the screen was performed using a computer analysis program of the Screening Unit in collaboration with computer analysts of the FMP. A z-factor that quantified the suitability of an assay for use in a high-throughput screen was determined and thereof potential activators and inhibitors were determined. For the validation of the first screen, different concentrations (ranging from 0.2 to 50 µM) of each of theses 352 potential modulators were measured again

using the MAL deacetylation assay. To test for autofluorescence of each compound, the fluorescence was measured directly after compound addition and before the substrate was added. The test for trypsin inhibition was performed after validation in a separate measurement with the deacetylated substrate ML. This second screen also resulted many candidates. With help of a chemist of the FMP (Dr. Edgar Specker) a few candidates were eliminated based on their properties such as reactivity and specificity. Finally, 15 inhibitors and 13 activators were obtained, and most of them, 14 inhibitors and 12 activators were subsequently reordered from ChemDiv, Asinex or Enamine for further analysis.

During my further thesis, we have concentrated on the inhibitors that we identified in both screens. Because of the known problems with activators in the MAL deacetylation assay, the sirtuin inhibitors seemed to be promising candidates worth pursuing, whereas the activators may be affected by the fluorophore on the MAL substrate. The activators were independently pursued by Louisa Hill during her master thesis (overview in 3.4), and some of her results have been followed up on in this thesis.

The inhibitory effect of the 14 compounds was confirmed using the MAL deacetylation assay to generate IC_{50} values and inhibition curves of each compound (**Figure 3.5**). For the purpose of this thesis, the compounds were sorted by increasing IC_{50} values and labeled A to M. The influence on SirT1 activity of different concentrations ranging from 0.49 to 250 µM of each compound was measured by MAL deacetylation assay in three independent experiments. The IC_{50} values and the curve fitting were performed with help of the computer program GraphPad Prism. Suramin is a well-known inhibitor of SirT1 (Trapp et al. 2007) and was used as control here. In our MAL deacetylation assay, it had an IC_{50} value of 4.7 µM, which is somewhat higher than in other publications described (0.6 µM (Sanders et al. 2009) or 297 nm (Trapp et al. 2007)), but this could be through the use of different assay conditions and other substrates. Except of one compound (N), the inhibitory effect of the inhibitors that we had reordered could be confirmed. All of them showed a dose-dependent inhibition of SirT1 deacetylase activity, the IC_{50} values vary from 2.4 µM (compound A) to 173.2 µM (compound M). These results indicated that we had identified a total of 16 potential SirT1 inhibitors from the BIOMOL and the ChemBioNet library.

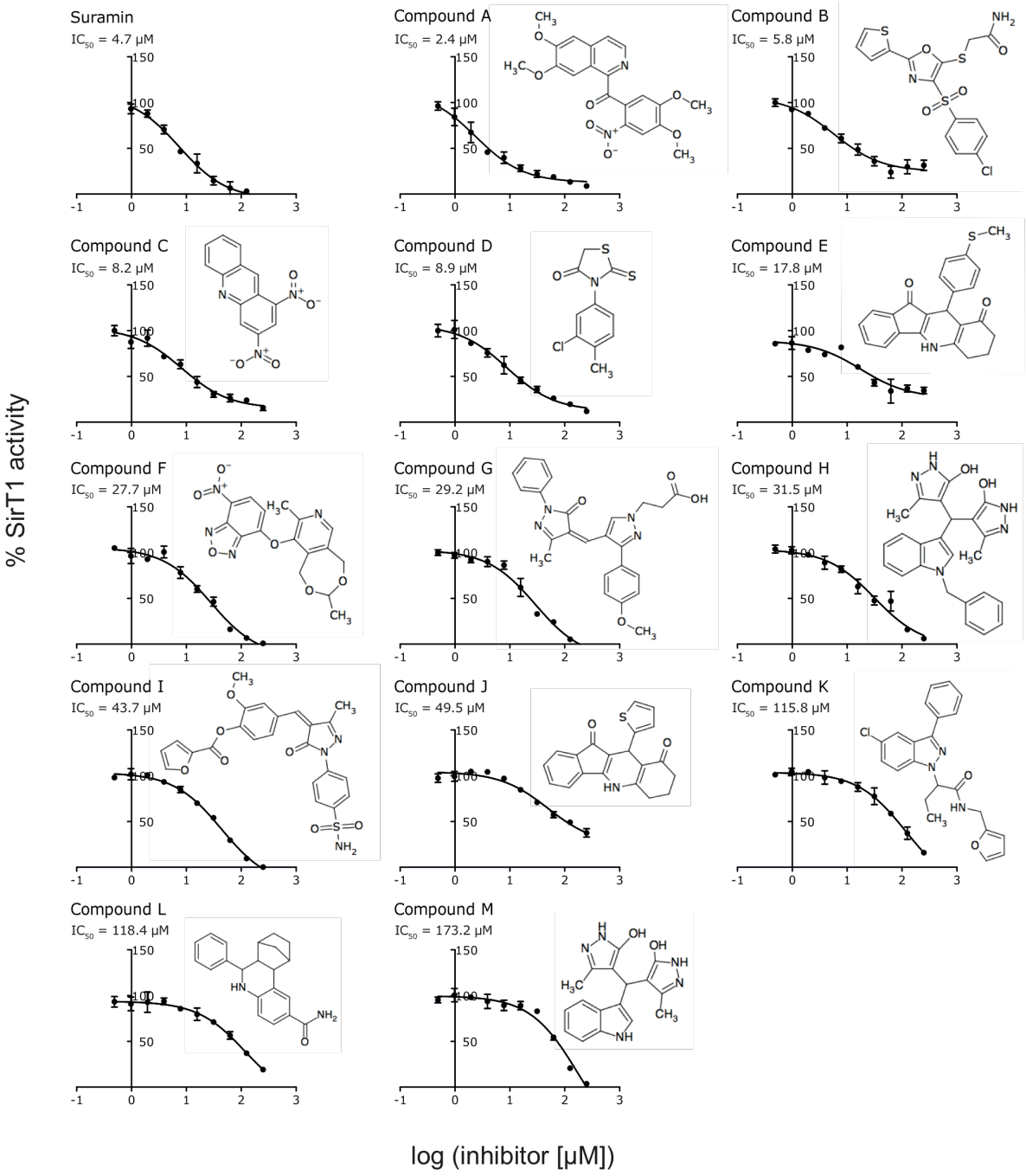

Figure 3.5: Identification of potential SirT1 inhibitors from the ChemBioNet library
The effect of the inhibitors on SirT1-dependent MAL deacetylation was measured by the MAL deacetylation assay. Compound labeling and order are corresponding to their IC_{50} values. The control reaction containing DMSO was set to 100 %. IC_{50} values and curve fitting were performed using GraphPad. Values correspond to the average enzyme activity of three independent experiments ± standard deviation. To the right of the IC_{50} curves the chemical structure of each compound is shown. The chemical structure of suramin is not shown here due to the lack of space (see 1.6.3 Figure 1.11).

3.1.3 Establishment of an HPLC-based p53 deacetylation assay

As mentioned above the MAL deacetylation assay is controversial, because the fluorophore that is coupled to the substrate influences the activity of SirT1. Although the activators probably more affected by the fluorophore than the inhibitors, we sought to establish a

deacetylase assay in our lab that is independent of the presence of the fluorophore. The assay is described in (Liu et al. 2008), and for this we used a p53-derived peptide (aa 368 – 386 of p53) that carries an acetylated lysine (K^{382}) and lacks any fluorophore as substrate. The sirtuin-dependent deacetylation of this peptide was measured by HPLC (high performance liquid chromatography) -based separation of the acetylated and the deacetylated peptide. Because of their different retention time on the column, it was possible to separate the peptides (**Figure 3.6**). The peptides were eluted from the HPLC column using an increasing acetonitrile gradient (1 % to 35 %) over 30 min. The percentage of deacetylation was calculated by dividing the area under the peak of the deacetylated peptide by the sum of the areas under the peak of both peptides.

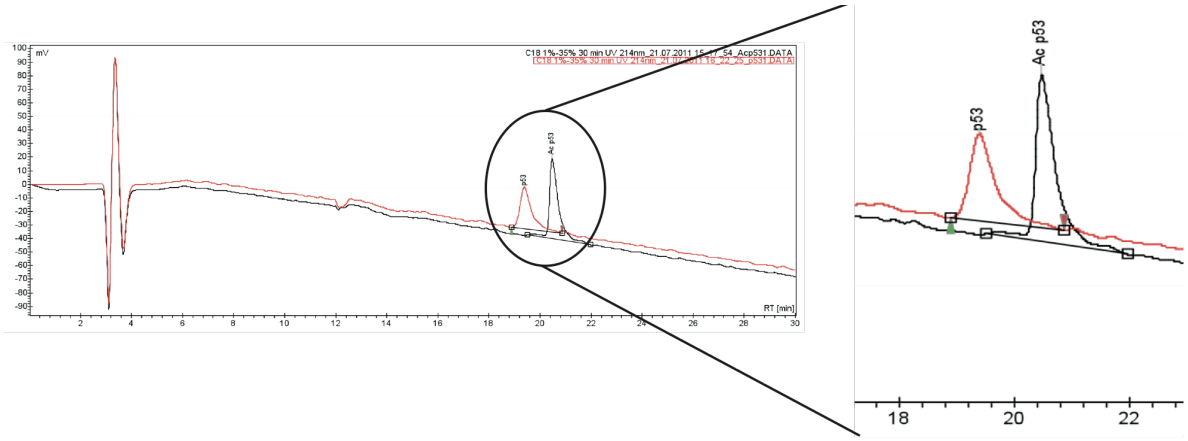

Figure 3.6: Separation of p53 (aa 368-386) and Ac-p53 (aa 368-386) by HPLC
The separation of Ac-p53 and p53 peptides is shown as an overlay of two samples that were both eluted from the HPLC column by a linear gradient of 1 % to 35 % acetonitrile in 0.1 % trifluoroacetic acid over 30 min. The peptides were detected and quantified using a UV detector at a wavelength of 214 nm.

The reaction conditions for the HPLC-based p53 deacetylation reaction were nearly the same as in the MAL deacetylation assay, except that the reaction time was only 30 min instead of 4 h. The p53 peptide is a substrate of preference for SirT1, and therefore it was deacetylated more quickly than the MAL substrate. The reaction time was calculated such that 50 % of the substrate was deacetylated by SirT1. As previously published (Beher et al. 2009; Pacholec et al. 2010), resveratrol did not enhance the activity of SirT1 in this p53 deacetylation assay. However, suramin was able to inhibit SirT1 activity in this HPLC-based p53 deacetylation assay, but to a lesser extent than in the MAL deacetylation assay (**Figure 3.7**).

3.1.4 Effect of inhibitors on SirT1-dependent p53 deacetylation

Subsequently, the inhibitory effect of each compound on SirT1 activity was measured by the HPLC-based p53 deacetylation assay. All in all, several of the inhibitors also showed some degree of inhibition of SirT1 in the p53 deacetylation assay (**Figure 3.7**), although a higher compound concentration was needed in comparison to the MAL deacetylation assay. The IC_{50} values that were achieved in the MAL deacetylation assay (**Figure 3.7**, right side) are much lower in comparison to the inhibitor concentrations that were needed to inhibit 50 % of the SirT1 activity in the p53 deacetylation assay.

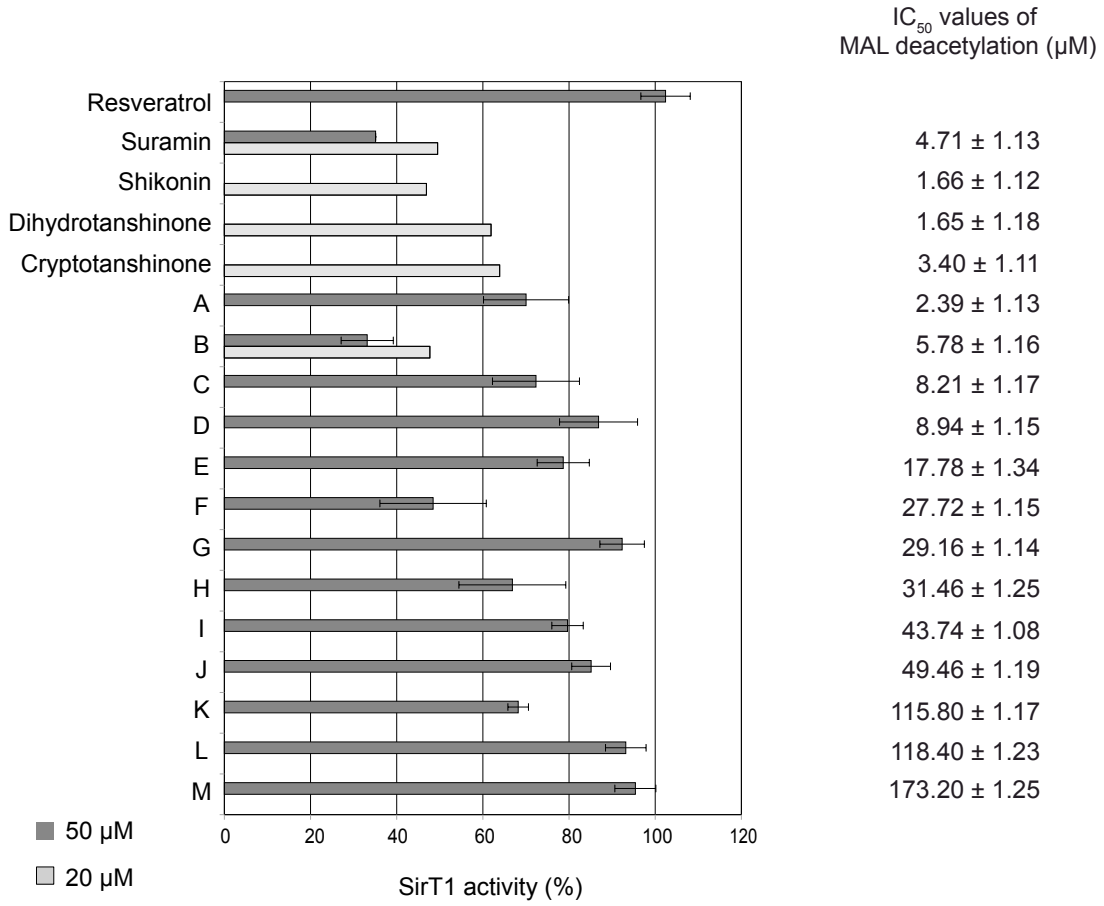

Figure 3.7: Influence of inhibitors on SirT1-dependent p53 deacetylation
The inhibitory effect of 20 µM and/or 50 µM of each compound on SirT1 was analyzed by HPLC-based p53 deacetylation assay and displayed as % of SirT1 activity. DMSO was used as control and set on 100 %. Values correspond to the average enzyme activity of three independent experiments ± standard deviation, except of the values of suramin, shikonin, dihydrotanshinone, cryptotanshinone and compound B (20 µM), which correspond to one experiment. The IC_{50} values of each inhibitor that were achieved in the MAL deacetylation assay are displayed on the right side for comparison.

Suramin, which was used as control, showed only 50 % inhibition of SirT1 at 20 µM in comparison to its IC_{50} value of 4.7 µM in the MAL deacetylation assay. The inhibitors shikonin, dihydrotanshinone, cryptotanshinone and compound **B** showed the strongest inhibition to approximately 50-60 % of SirT1 activity at a concentration of 20 µM. Compound **F** inhibited approximately 50 % of SirT1-dependent p53 deacetylation, whereas

the compounds **A**, **C**, **H** and **K** failed to inhibit 50 % SirT1 activity at a concentration of 50 µM. The inhibitors **D**, **E**, **G**, **I**, **J**, **L** and **M** showed hardly inhibition of SirT1-dependent p53 deacetylation. However, it has been reported that SirT1 has poor affinity for the substrate MAL (Heltweg et al. 2003). Most likely, for this reason, a lower concentration of inhibitor is necessary to inhibit the deacetylation of MAL in comparison to p53 deacetylation, which is the preferred substrate (Pan et al. 2012). In support of this theory, it is been reported that the fluorophore on the substrate decreases the binding affinity of SirT1 for this substrate (Kaeberlein et al. 2005). This suggests that the results of the p53 deacetylation assay are more potent than the IC_{50} values of the MAL deacetylation assay.

3.2 *In vitro* characterization of potential SirT1 inhibitors

3.2.1 Generation of N-terminal truncations of SirT1

Several studies have shown that the N- and C-terminal regions have an influence on the deacetylase activity of sirtuins. They play important roles in acetyl-lysine and NAD^+ binding (Zhao et al. 2003a), subnuclear distribution (Cockell et al. 2000) and interaction with cellular binding partners (Cuperus et al. 2000; Tennen et al. 2010). Furthermore, the ability of resveratrol or other STACs to activate SirT1 is dependent on the presence of the N-terminus (Milne et al. 2007). Based on theses results, we asked whether this was also the case for the sirtuin inhibitors identified here. To determine whether they also interacted with the N-terminus of SirT1, a series of SirT1 truncations in analogy to (Milne et al. 2007) were generated. Five (SirT1_A, B, D, E and F) of seven constructs that are truncated at the N-terminus (**Figure 3.8A**) could be successfully expressed and purified from *E. coli*. The purified fractions were subjected to SDS-PAGE gel electrophoresis and stained with Coomassie blue to determine the amounts of purified protein of each construct (**Figure 3.8B**). The protein purification of construct SirT1_G was not efficient enough to observe sufficient amounts of proteins in the Coomassie blue stained SDS-PAGE gel. The SirT1 truncations were analyzed by Western blotting with α-poly-His antibody. As shown in **Figure 3.8B**, the constructs ran slightly above the expected size (SirT1_A 57.3 kDa, SirT1_B 55.5 kDa, SirT1_C 50.0 kDa, SirT1_D 49.5 kDa, SirT1_E 49.0 kDa and SirT1_F 48.4 kDa), which was determined using ExPASy (http://web.expasy.org/protparam/). Subsequently, the deacetylase activity of the purified SirT1 truncations was determined by the MAL deacetylation assay (**Figure 3.9**). Five SirT1 truncations (SirT1_A, SirT1_B, SirT1_D, SirT1_E and SirT1_F) showed deacetylase activity in the MAL deacetylation assay, though to varying degrees.

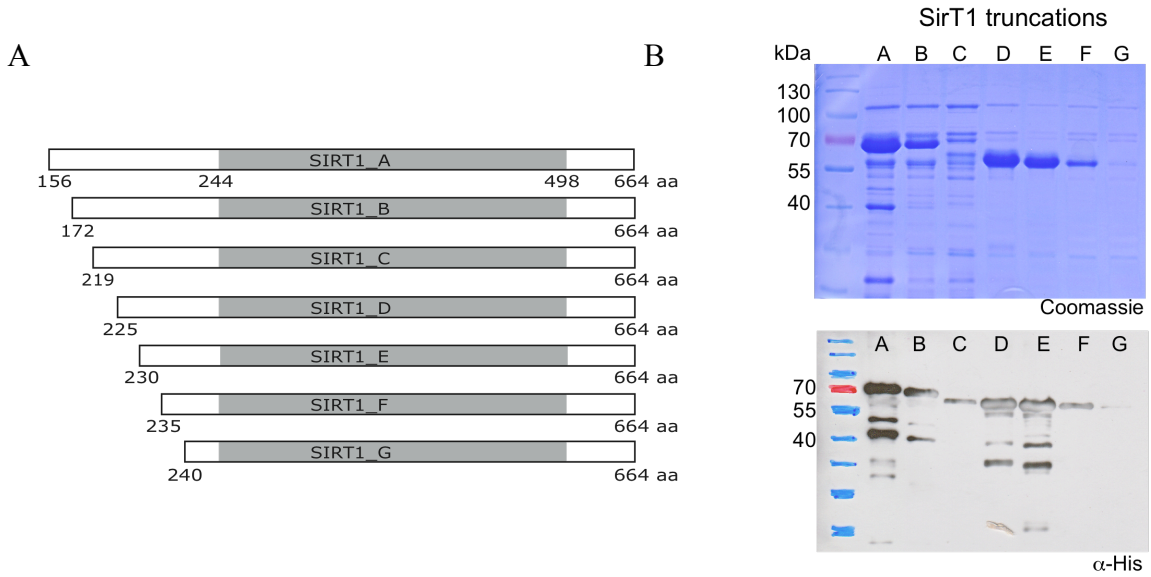

Figure 3.8: Generation of truncated SirT1 constructs
Different constructs of SirT1 with varying length of the N-terminal domain (A) were generated to characterize potential binding sites of SirT1 inhibitors and activators. The catalytic core domain (gray) is located between amino acid 244 and 498. Five of these constructs were successfully purified from *E. coli* by His-tag purification. (B) Coomassie-stained SDS-PAGE gel of purified truncations of SirT1. SirT1-containing fractions were identified by Western blotting with α-poly-His antibody.

Although construct SirT1_C showed a signal in the Western blot against α-His antibody, the amount of purified protein of the constructs SirT1_C as well as SirT1_G were insufficient to observe a deacetylase activity in the MAL deacetylation assay.

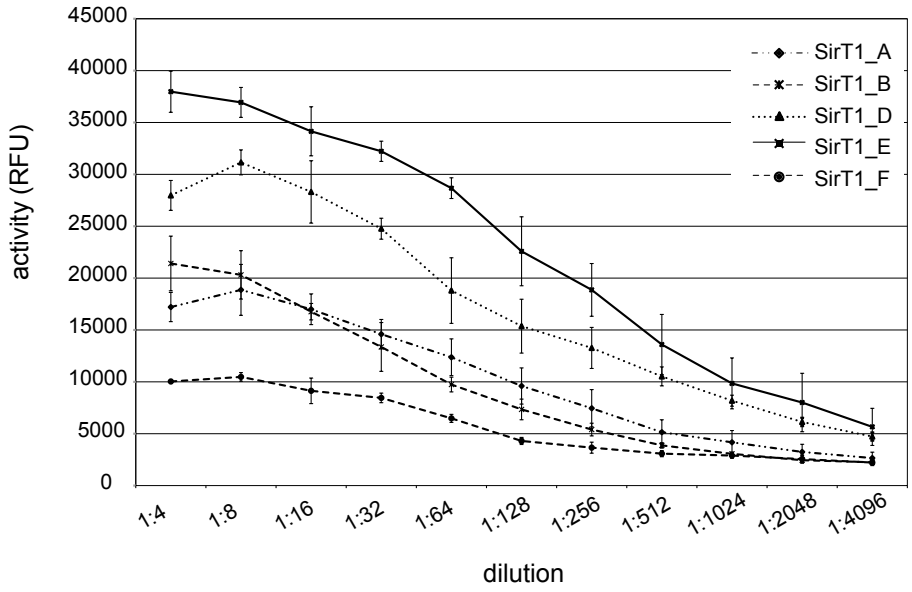

Figure 3.9: Deacetylase activity of SirT1 truncations
The deacetylase activity of truncated SirT1 constructs was measured by the fluorescence-based assay. Of each construct a serial dilution was performed. The values correspond to the average enzyme activity of a three-fold determination ± standard deviation of one experiment.

To test whether these varying degrees of deacetylase activity depend on the different amounts of purified protein, the same amount of protein was determined by Bradford and Coomassie

blue stained SDS-PAGE and put in the MAL deacetylation assay, whereby the activity of full-length SirT1 was set to 100 % (**Figure 3.10**). The constructs SirT1_A and SirT1_B had more or less the same deacetylase activity as full-length SirT1, whereas the constructs SirT1_D and especially SirT1_E showed a higher deacetylase activity as the full-length SirT1. The activity of the shortest construct SirT1_F was strongly reduced in comparison to the full-length SirT1, suggesting that the N-terminal region of SirT1 has an influence on the deacetylase activity of SirT1. For further experiments, the final dilution of each construct was chosen such that an activity of approximately 10.000 RFU (relative fluorescence unit) was achieved. Thus, the truncations were diluted as follows: SirT1_A and SirT1_B 1:100, SirT1_D 1:250, SirT1_E 1:400 and SirT1_F 1:40.

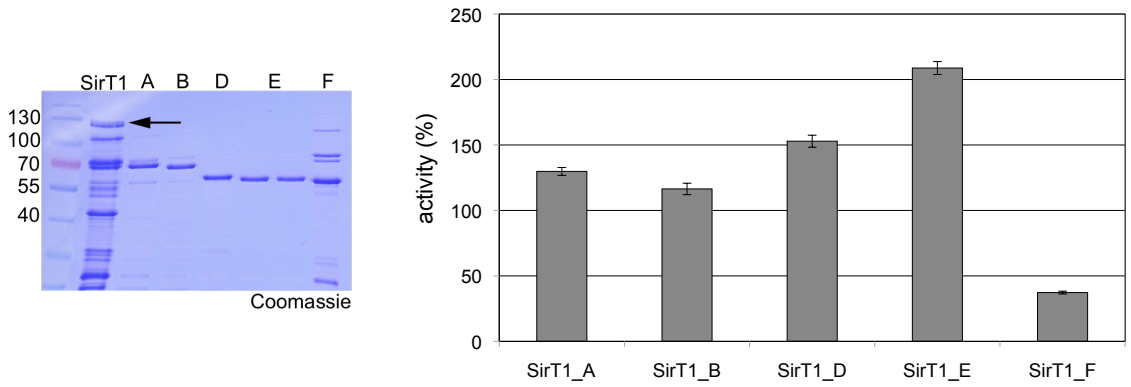

Figure 3.10: SirT1 truncations had different deacetylase activity
The amount of protein was determined by Coomassie blue stained SDS-PAGE gel, the respective full-length SirT1 protein band is highlighted by the arrow. For the construct SirT1_E two samples were loaded on the gel. The deacetylase activity of each construct was measured in the MAL deacetylation assay. The activity of full-length SirT1 was set to 100 %. The values correspond to the average enzyme activity of a four-fold determination ± standard deviation of one experiment.

Furthermore, the influence of resveratrol and suramin on the SirT1 truncations was measured by the MAL deacetylation assay (**Figure 3.11**). Resveratrol at a concentration of 50 µM stimulated the deacetylation activity of the truncations SirT1_A and SirT1_B, which both have an extended N-terminal region. The shorter constructs SirT1_D, SirT1_E and SirT1_F were not activated by resveratrol. These results are in agreement with published data, where it has been shown that the N-terminal region is required for the enhancement of SirT1 activity by resveratrol (Milne et al. 2007). In contrast, suramin was able to inhibit all SirT1 truncations to approximately 50 % or more. This indicates that the N-terminus is not required for the inhibition by suramin, suggesting that suramin itself does not interact with the N-terminal region of SirT1.

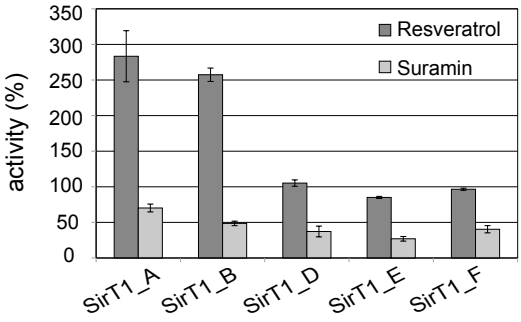

Figure 3.11: Influence of resveratrol and suramin on SirT1 truncations
The influence of resveratrol (50 µM) and suramin (6.25 µM) on SirT1 truncations was measured by fluorescence-based assay. The control reactions of each construct containing DMSO and were set to 100 %. Values correspond to the average enzyme activity of three independent experiments ± standard deviation.

3.2.2 Deacetylase activity of further sirtuin family members in the MAL deacetylation assay

For further characterization of the inhibitors identified in this work, the Sir2 protein from *S. cerevisiae* (ySir2) was also expressed and purified from *E. coli* using His-tag purification, and its activity was measured by the MAL deacetylation assay (**Figure 3.12**). ySir2 showed deacetylase activity and could be inhibited to approximately 50 % by 125 µM splitomicin, which is a well-known inhibitor of ySir2 (Bedalov et al. 2001). However, Bedalov *et al.* determined an IC_{50} value of 60 µM for ySir2 using an acetylated H4 peptide, whereas in our MAL deacetylation assay a higher concentration of splitomicin was needed to inhibit 50 % of ySir2 activity.

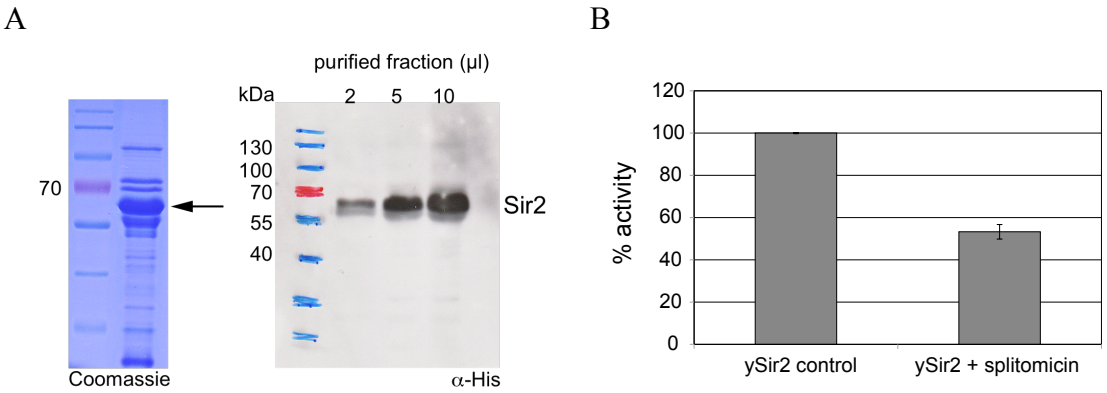

Figure 3.12: Purification and deacetylase activity of ySir2
The Sir2 protein from *S. cerevisiae* (ySir2) was expressed in *E. coli* and purified by His-tag purification. (A) Coomassie stained SDS-PAGE gel with 10 µl of the purified fraction. The identification of the ySir2 protein was performed by Western blotting with α-poly-His antibody. (B) The deacetylase activity of ySir2 purified from *E. coli* was measured by the MAL deacetylation assay and could be inhibited by 125 µM of splitomicin, a known inhibitor of ySir2. The control reaction containing DMSO was set to 100 %. Values correspond to the average enzyme activity of three independent experiments ± standard deviation.

We also obtained purified samples of further members of the sirtuin family (SirT2 to SirT7; BIOZOL) except SirT4, which has no obvious deacetylase activity (Haigis et al. 2006). Their

deacetylase activity was measured by the MAL deacetylation assay and compared with that of purified SirT1 (**Figure 3.13**).

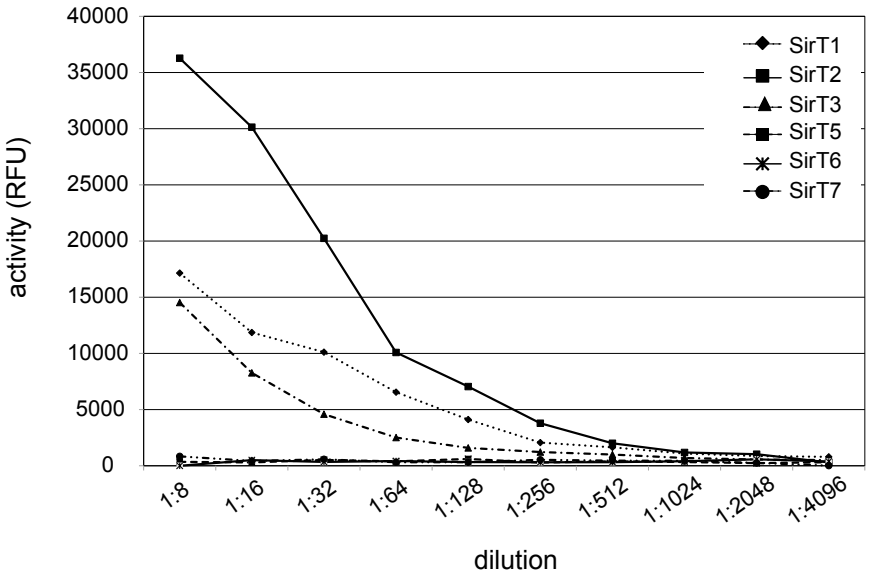

Figure 3.13: Deacetylase activity of human sirtuins in the MAL deacetylation assay
The deacetylase activity of further sirtuin family members was measured by the MAL deacetylation assay. Of each construct a serial dilution was performed. The values correspond to the enzyme activity of one experiment.

Next to SirT1, only SirT2 and SirT3 were able to deacetylate MAL in the fluorescence-based assay. However, it is not surprising that MAL is unsuitable as a substrate for the other sirtuins. So far, the only known substrates of SirT6 and SirT7 are histones (Michishita et al. 2008; Barber et al. 2012) and maybe they need a more complex protein than a simple lysine to recognize it as substrate. SirT5 has only weak deacetylase activity (Du et al. 2011), which may be insufficient for the MAL deacetylation assay. Similar to the SirT1 truncations, for further experiments SirT2 and SirT3 were diluted such that an activity of approximately 10.000 RFU was achieved (SirT2 1:100 and SirT3 1:30).

3.2.3 Influence of inhibitors on further sirtuin family members

The influence of the 16 potential SirT1 inhibitors that were identified in this work was measured with the SirT1 truncations, SirT2, SirT3 and ySir2 (**Figure 3.14**) in order to gain insight into their specificity and to get further information about their interaction sites with small molecule compounds that influence their activity. 50 µM of each inhibitor was used in the MAL deacetylation assay.

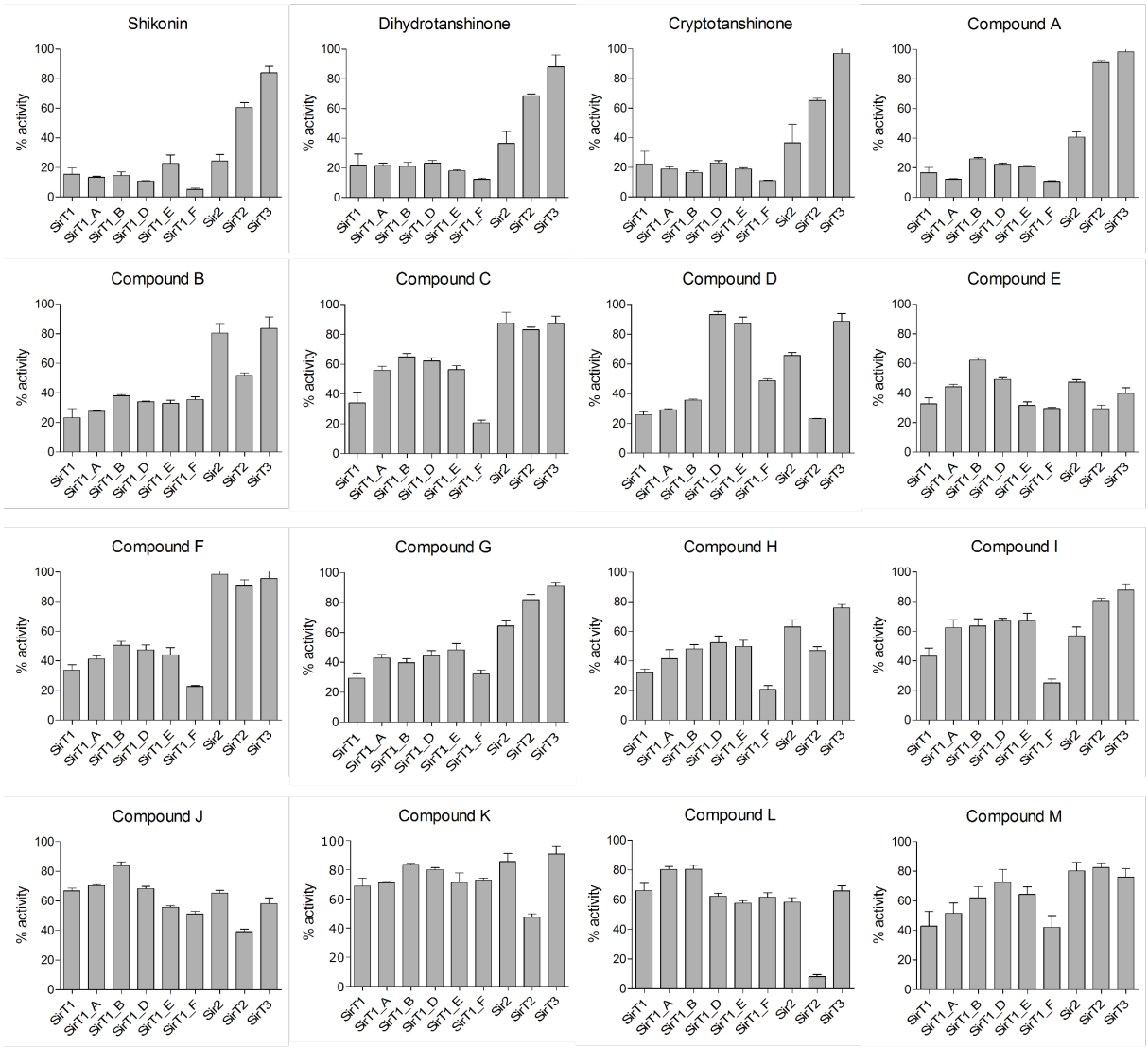

Figure 3.14: Influence of inhibitors on further sirtuin members
The effect of the inhibitors on each sirtuin was analyzed by the MAL deacetylation assay and displayed as % of activity in the control reaction. The control reaction contained DMSO and was set to 100 %. 50 µM of each inhibitor (diluted in DMSO) was used. Values correspond to the average enzyme activity of three to six independent experiments ± standard deviation.

The compounds shikonin, dihydrotanshinone, cryptotanshinone, **A** and **B** were SirT1-specific inhibitors, because they showed the strongest inhibition of SirT1 and their truncations that were inhibited to approximately 20 % - 30 %. Except for **B**, they also showed strong inhibition of ySir2, which may not be surprising, because SirT1 is the closest homolog of ySir2. These results also indicate that shikonin, dihydrotanshinone, cryptotanshinone as well as **A** and **B** may not interact with the N-terminus of SirT1, because the truncations were inhibited as strongly as full length SirT1 in the MAL deacetylation assay. The compounds **C**, **F**, **G**, **H**, **I** and **M** showed the strongest inhibition of full length SirT1 and the shortest construct, SirT1_F (235-664). Perhaps theses compounds interact with and inhibit the SirT1 core domain, and these interactions become stronger after deletion of the N-terminal region. Furthermore, the strong inhibition of SirT1_F could also be due to the low deacetylase

activity of the short construct. In the case of compound **D**, it seems that it interacts with the first 225 amino acids of N-terminal region, because it inhibited only full length SirT1 as well as the constructs with an extended N-terminus, SirT1_A (156-664) and SirT1_B (172-664). The shorter constructs SirT1_D (225-664) and SirT1_E (230-664) were not affected by the inhibitor **D**. Furthermore, compound **D** also showed a strong inhibition of SirT2 that has an extended N-terminus in comparison to SirT3, whose active form lacks a N-terminal region. However, **D** inhibited ySir2 to a lesser extent than SirT1, although ySir2 also has an extended N-terminus, but it is known that the N-terminal region of sirtuins is not conserved. This suggests that compound **D** interacts with a specific site of the N-terminus of SirT1 and SirT2. Compound **E** and **J** appear to be unspecific sirtuin inhibitors, because they inhibited more or less all SirT1 truncations, ySir2 as well as SirT2 and SirT3. Compound **K** and especially **L** showed the strongest inhibition of SirT2. **L** inhibited SirT2 activity to approximately 10 % at a concentration of 50 µM. This suggests that compound **L** could be a potent SirT2 inhibitor. For this reason SirT2-dependent MAL deacetylation was measured with different concentrations of **L** and an IC_{50} curve was performed (**Figure 3.15**). Remarkably, compound **L** showed approximately a six-fold stronger inhibition of SirT2 (IC_{50} = 18.5 µM) than of SirT1 (IC_{50} = 118,4 µM; **Figure 3.5**).

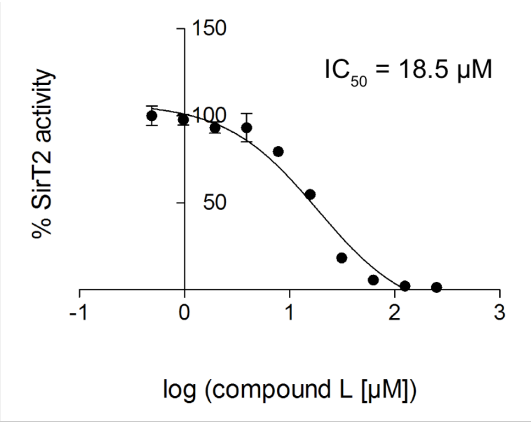

Figure 3.15: Compound L is a potent SirT2 inhibitor
SirT2-dependent MAL deacetylation was measured by fluorescence-based assay. The control reaction containing DMSO was set to 100 %. IC_{50} values and curve fitting were performed using GraphPad. Values correspond to the average enzyme activity of three independent experiments ± standard deviation.

The influence of compound **L** on SirT2 activity was also measured by the HPLC-based p53 deacetylation assay. Notably, the inhibition of p53 deacetylation by **L** is comparable with the inhibition of MAL deacetylation in the fluorescence-based assay (**Figure 3.16**). At 20 µM compound **L** inhibited SirT2 activity by more than 50 %, and this value was comparable with the IC_{50} value of 18.5 µM in the MAL deacetylation assay. These results support the idea that compound **L** is a potent SirT2 inhibitor.

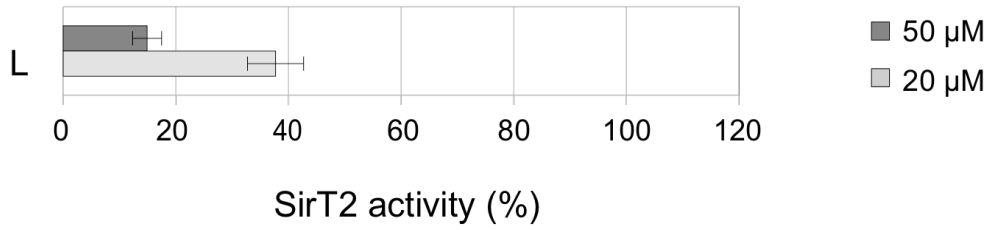

Figure 3.16: Inhibitory effect of compound L in the p53 deacetylation assay
The inhibitory effect of 20 µM and 50 µM of compound L on SirT2 activity was measured by HPLC-based p53 deacetylation assay and displayed as % of SirT2 activity. DMSO was used as control and set to 100 %. Values correspond to the average enzyme activity of three independent experiments ± standard deviation.

3.2.4 Sirtuin inhibition by derivates of compounds H and L

Since we so far had identified potential sirtuin inhibitors, we were interested to develop them further for *in vivo* use. Based on the *in vitro* as well as *in vivo* results that will be described later, compound **H** and **L** appeared to be of particular interest. Based on their chemical structure, it can be hypothesized that they are cell permeable and do not display unspecific reactivity (Prof. Dr. M. Kaiser, UDE, personal comment) Based on this assessment, we obtained derivates of compound **H** and **L** in order to perform a structure-function analysis and to speculate about the part of their chemical structure that is required for their inhibitory effect. In case of compound **H**, we were able to obtain two derivates (**H-I** and **H-II**), that are structurally distinct from each other. These derivates shared different parts of the structure with compound H. In **Figure 3.17A**, the structure of **H** is divided into two parts by the dashed line. The structure above the dashed line is present in **H-I**, whereas the part below the line is a component of **H-II**. The inhibitory effect of these two derivates was measured in the MAL deacetylation assay (**Figure 3.17B**). Interestingly, while **H-I** showed a slight inhibition of SirT1 deacetylase activity (IC_{50} = 231.9 µM), **H-II** was unable to inhibit SirT1 at concentrations as high as 250 µM. This indicated that the structure part of compound **H** above the dashed line is necessary for the inhibitory effect on SirT1 in contrast to the structure part below the line. However, in view of the high IC_{50} value of **H-I**, the structure below the dashed line also contributed to acting, it might also contributed to the inhibitory effect, but to a lesser extent than the structure above the dashed line. Probably, the sum of all ring systems of **H** as well as **H-I** is necessary for the generation of π-π interactions with the SirT1 enzyme and to inhibit SirT1. Perhaps for this reason, compound **H** is a more potent inhibitor than **H-I**. However, to verify this theory more derivates of compound **H** with different substitutes would be necessary.

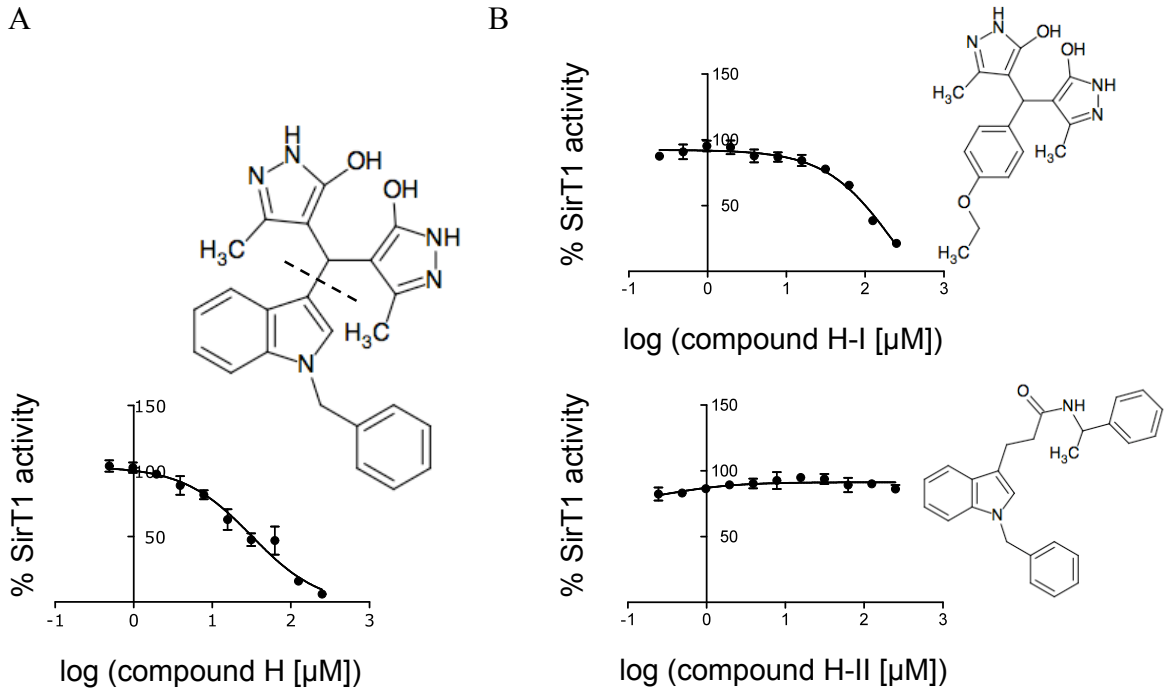

Figure 3.17: Inhibitory effect of H derivates on SirT1 dependent MAL deacetylation
(A) Chemical structure and IC_{50} curve of compound H. The dashed line within the structure indicates where the substituents were changed to generate new derivates. (B) The inhibitory effect of H-I and H-II on SirT1 was measured by fluorescence-based assay. The control reaction containing DMSO was set to 100 %. IC_{50} values and curve fitting were performed using GraphPad. Values correspond to the average enzyme activity of three independent experiments ± standard deviation. To the right of the IC_{50} curves the chemical structure of each compound is pictured.

We furthermore were able to obtain four derivates (**L-I** to **L-IV**) of compound **L** that were structurally similar to one another, but had different substituents attached at the carboxamidegroup. Since **L** showed the strongest inhibition with SirT2, the inhibitory effect on SirT2 was determined by the MAL deacetylation assay (**Figure 3.18**). Strikingly, **L-I** had an IC_{50} value of 3.8 µM and thus showed a stronger inhibition of SirT2 than compound **L** (IC_{50} = 18.5 µM). **L-II** with an IC_{50} value of 18.7 µM had a similar inhibitory effect as compound **L**. **L-III** and **L-IV** had a weak or no inhibitory effect on SirT2. These results indicate that the addition of an aromatic ring increases the binding affinity of compound **L** for SirT2.

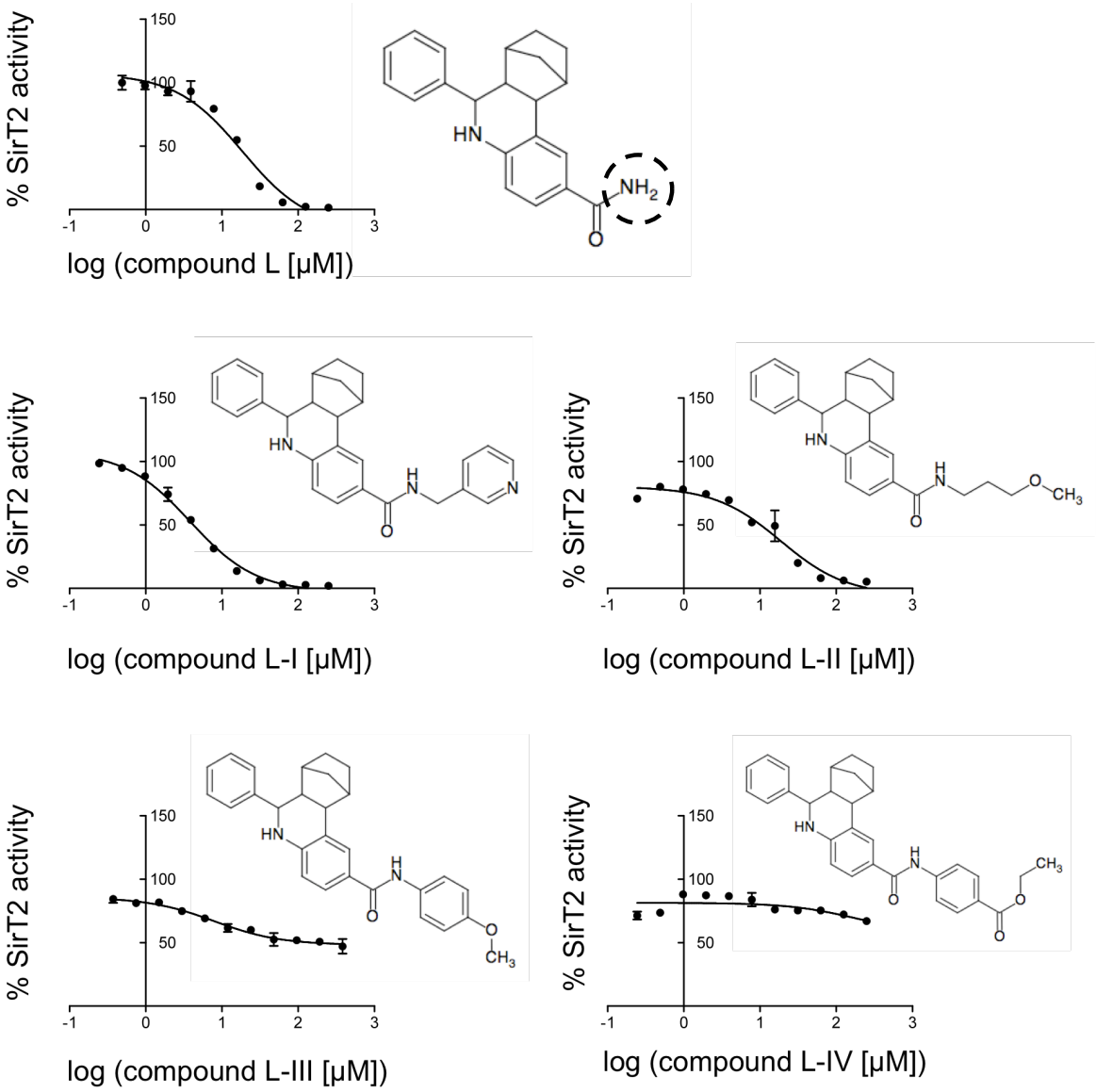

Figure 3.18: Inhibitory effect of L derivates on SirT2 dependent MAL deacetylation
The inhibitory effect of L derivates on SirT2 activity was measured by MAL deacetylation assay. The control reaction containing DMSO was set to 100 %. IC_{50} values and curve fitting were performed using GraphPad. Values correspond to the average enzyme activity of three independent experiments ± standard deviation. To the right of the IC_{50} curves the chemical structure of each compound is pictured. The IC_{50} curve and chemical structure of L are displayed for comparison. The dashed line around the carboxamidegroup highlight where the substituents were added.

The inhibitory effect of compound **L-I** on SirT2 was also measured using the HPLC-based assay with p53 as substrate. Compared to compound **L**, **L-I** showed a stronger inhibition of SirT2 activity in the p53 deacetylation assay (**Figure 3.19**). At a concentration of 20 µM **L-I** inhibited SirT2 deacetylase activity to approximately 20 % and to 10 % at 50 µM. This showed that compound **L-I** is a more potent SirT2 inhibitor than compound **L**. Similar to compound **H**, the aromatic pyridine ring could generate additional π-π interactions with the enzyme, and this may lead to a stronger binding affinity of compound **L-I** for SirT2.

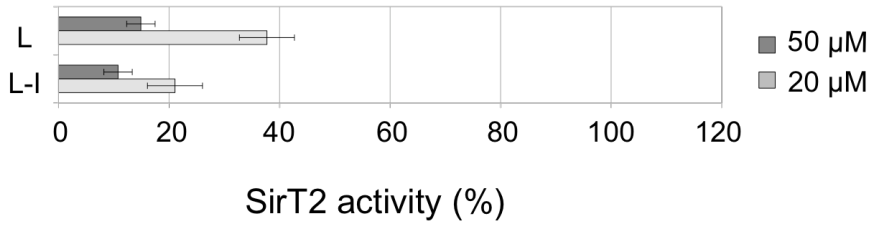

Figure 3.19: Compound L as well as L-I inhibited p53 deacetylation
The inhibitory effect of 20 µM and 50 µM of compound L and L-I on SirT2 was analyzed by HPLC assay and displayed as % of SirT2 activity. As control DMSO was used and set on 100 %. Values correspond to the average enzyme activity of three independent experiments ± standard deviation.

3.3 Characterization of sirtuin inhibitors *in vivo*

3.3.1 Increased apoptosis after inhibitor treatment

Sirtuins are known to play important roles in cell survival, apoptosis and cancer development due to their broad range of targets. Furthermore, SirT1 as well as SirT2 inhibitors such as cambinol, tenovin-6 and sirtinol have been shown to have high anticancer potential (Heltweg et al. 2006; Ota et al. 2006; Lain et al. 2008). For this reason, we wanted to analyze the *in vivo* influence and the anticancer potential of the inhibitors identified in this study. For this approach we used the human lung cancer cell line A549. This cell line was treated with different concentrations of each inhibitor. After treatment for 48 h, cell apoptosis was measured by determining the number of cells with a DNA content less than G1-phase cells (Sub-G1) by FACS analysis.

The treatment with the inhibitors shikonin, dihydrotanshinone as well as cryptotanshinone led to a strong increase of apoptosis at low concentrations of 1-2 µM, which corresponds to the IC_{50} value of 1.7 µM and 3.4 µM determined in the MAL deacetylation assay. However, these three inhibitors have a very reactive chemical structure and therefore they might interact with multiple cellular targets and not inhibited SirT1 specifically (Prof. Dr. M. Kaiser, UDE, personal comment). As shown in **Figure 3.20**, the inhibitors **C** and **H** showed a moderate increase of apoptosis to approximately 30 %, whereas compound **B** induced a slight increase to 10 % cell death and compound **F** lead a strong increase of apoptosis to 90 % at concentrations of 2-5 µM. Because of their ability to induce cell death of cancer cells the *in vivo* influence of the inhibitors **B**, **C**, **F** as well as **H** were further analyzed. Additionally, since compound **L** and **L-I** showed a strong inhibition of SirT2 *in vitro,* the *in vivo* influence of both compounds was also analyzed at higher concentrations, because compound **L** showed no effect on A549 cells at a concentration of 5 µM (**Figure 3.20**).

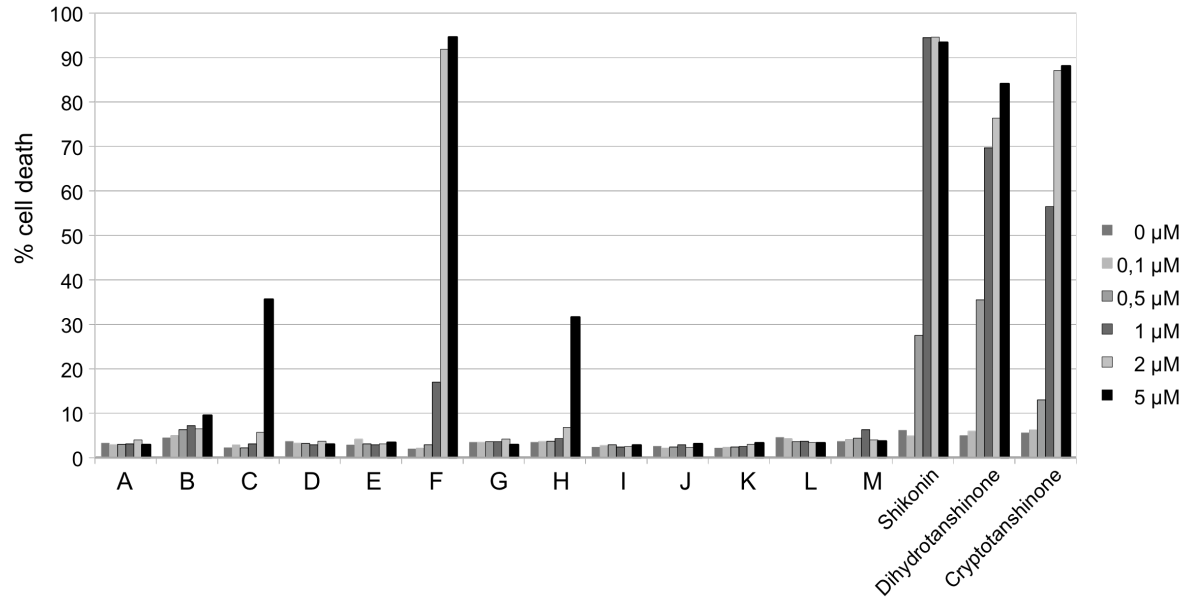

Figure 3.20: Cell death of A549 cells after inhibitor treatment
The lung cancer cell line A549 was treated with different concentrations of the inhibitors identified in this study. Apoptosis was measured by FACS analysis and displayed as % cell death. Values correspond to one experiment.

For further analysis the A549 cells were treated again with these six compounds **C**, **F**, **H** as well as **L** and **L-I**, but in combination with the chemotherapeutic agent etoposide (VP-16). Etoposide is a topoisomerase II inhibitor and causes DNA single-strand and double-strand breaks. Cancer cells are more affected by etoposide than normal cells, because they divide more rapidly (Hande 1998). This procedure causes DNA mismatches and promotes apoptosis of the cancer cells. It is known that apoptosis in response to stress, among others, is dependent on the tumor suppressor p53 (Levine 1997; Prives and Hall 1999) that can be inhibited by SirT1 deacetylation. Therefore, cell survival is promoted in response to DNA damage by inhibiting p53-dependent apoptosis (Luo et al. 2001). Several cancer forms including lung cancer cells show increased levels of SirT1 protein (Fraga and Esteller 2007; Stunkel et al. 2007) and this overxpression of SirT1 may be one reason for the resistance of cancer cells against chemotherapeutic agents, such as VP-16. In our further experiments, we found that only 7 % of untreated A549 cells died after treatment with VP-16, suggesting that they are resistant against VP-16. For further experiments, the A549 cells were treated with different concentrations of each inhibitor alone and in combination with VP-16 for 48 h. The hypothesis was that, if the compounds inhibit SirT1 in the cell, then p53 is active and we should observe an increase of apoptosis. Of the six inhibitors, three compounds **H, L** as well as **L-I** showed an additional increase of apoptosis after combined treatment with VP-16. The other inhibitors **C** and **F** showed no differences between the treatment with or without VP-16 at higher concentration of 5 µM, and compound **B** showed no further increase of apoptosis (**Figure 3.21**).

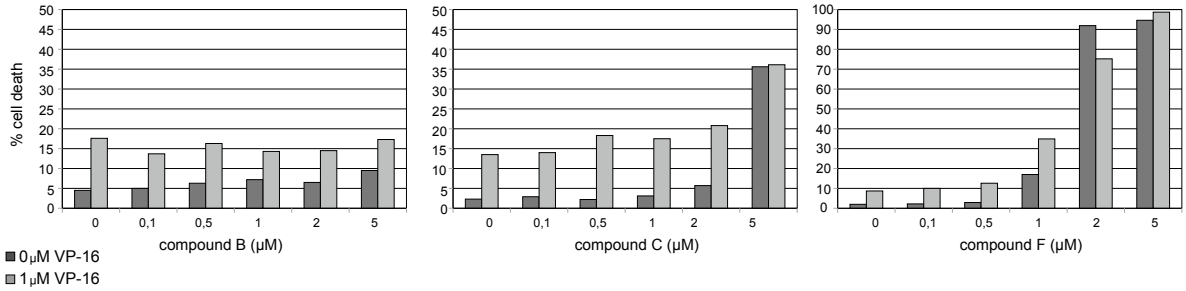

Figure 3.21: Influence of compound B, C and F on the cancer cell line A549
The A549 cell line was treated with different concentrations of the inhibitor B, C and F alone (dark gray bar) or in combination with 1 µM VP-16 (light gray bar). Apoptosis was measured by FACS analysis and displayed as % cell death. Values correspond to one experiment.

Compound **H** showed in combination with VP-16 a slight additional increase of apoptosis at low concentrations up to 5 µM in comparison to the treatment with **H** alone (**Figure 3.22A**). Because of this additional increase of apoptosis after combined treatment with VP-16, we sought to determine whether this effect may be p53-dependent. For this reason, we used the human lung cancer cells H1299, which have a partial deletion of the p53 gene and cannot express the p53 protein. Surprisingly, after treatment with compound **H** alone, apoptosis increased up to 45 % at 5 µM and up to 50 % at 10 µM, which represented a higher cell death rate than in the A549 cells. However, in combination with VP-16, apoptosis was decreased to approximately 20 %, a degree that was comparable to that in A549 cells (**Figure 3.22B**). Of course both cell lines have more differences than the expression of p53 protein, but this results indicated that, contrary to expectation, apoptosis mediated by compound **H** might not be p53-dependent.

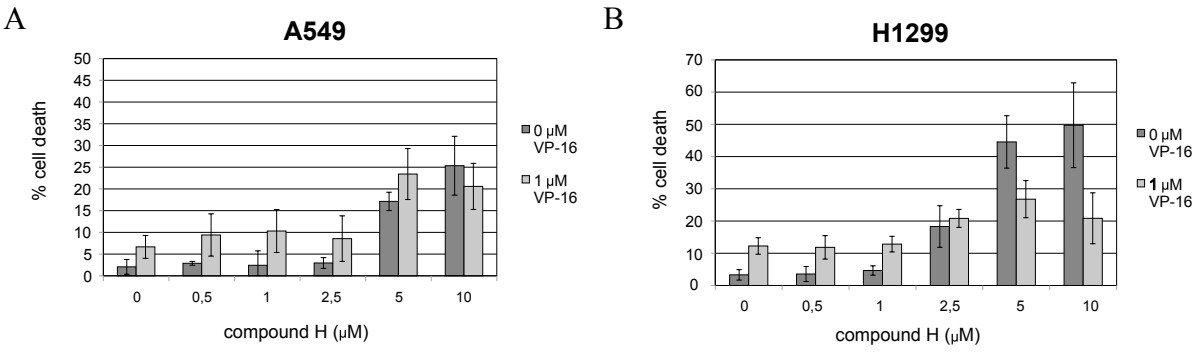

Figure 3.22: Compound H induced apoptosis of cancer cells
Lung cancer cell line A549 (A), which is p53 wild type, and H1299 (B), which is p53 negative, were treated with different concentrations of compound H alone (dark gray bar) or in combination with 1 µM VP-16 (light gray bar). SubG1 phase was measured by FACS analysis and displayed as % cell death. Values correspond to the average cell death of three independent experiments ± standard deviation.

In contrast to compound **H**, compound **L** as well as **L-I** induced a further increase of apoptosis when combined with VP-16 in comparison to the treatment with the compound alone (**Figure 3.23**). In both cases, apoptosis was increased from approximately 5 % with VP-

16 alone to approximately 20 % at the highest compound concentration of 20 µM. This effect was not very pronounced, but strikingly this effect could not be observed in H1299 cells. After treatment with the inhibitors alone, apoptosis increased to approximately 10 % at the highest concentration of 20 µM, which was comparable to the cell death in A549 cells. However, the combined treatment with VP-16 did not lead to a further increase of apoptosis. On the contrary, apoptosis of H1299 cells was decreased to approximately 5 % after treatment with 20 µM of compound **L-I** in combination with VP-16. Although **L-I** had a better IC_{50} value *in vitro* than **L**, its effect to induce apoptosis of A549 cells was comparable to the effect of **L**. In view of their chemical structure both may be metabolized in the cell in the same manner. This suggested that both inhibitors had s similar *in vivo* influence on the cells, which might be p53-dependent.

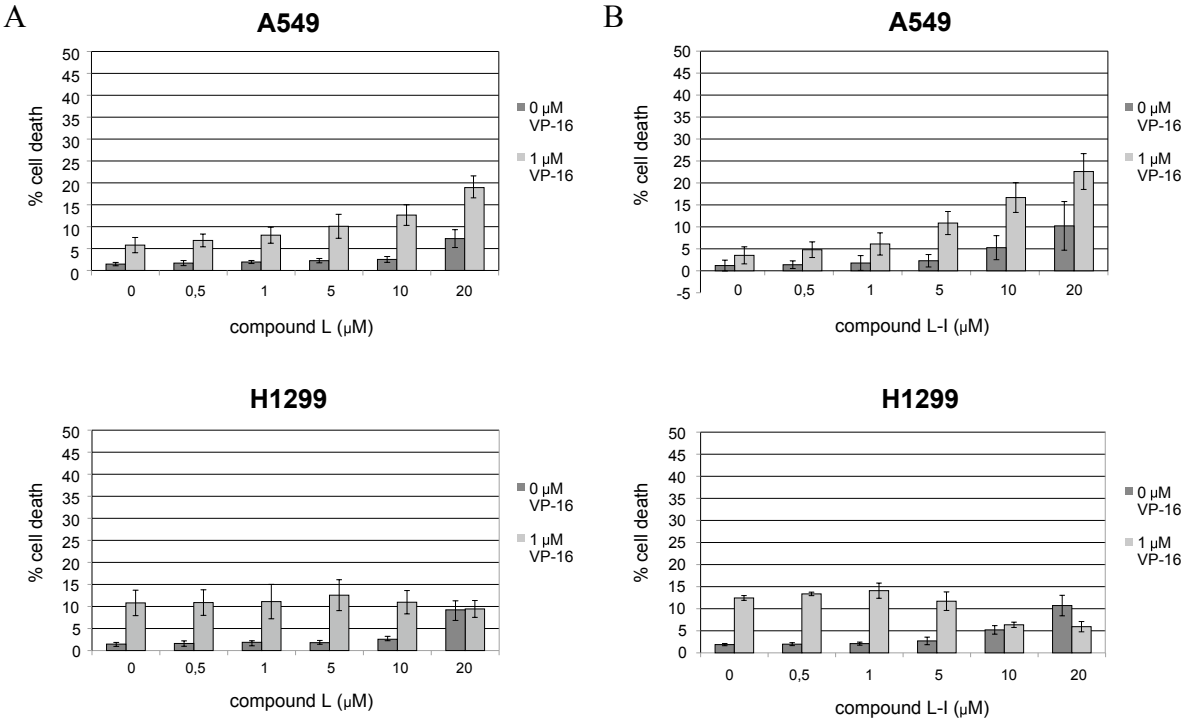

Figure 3.23: Influence of compound L on the cancer cell lines A549 and H1299
Lung cancer cell lines A549 and H1299 were treated with different concentrations of compound L (A) or L-I (B) alone (dark gray bar) or in combination with 1 µM VP-16 (light gray bar). SubG1 phase was measured by FACS analysis and displayed as % cell death. Values correspond to the average cell death of three independent experiments ± standard deviation.

3.3.2 Sirtuin inhibitors decreased cell viability and proliferation

To further characterize the anticancer potential of the three inhibitors **H**, **L** and **L-I** and to determine their ability to decrease cancer cell development, additional experiments such as proliferation and cell viability measurements were performed. For proliferation measurements, approximately 50.000 cells per dish were plated out and incubated at 37 °C

until the cells were adherent. Subsequently, the cell number of one dish that represents the time point before the treatment (0 h) was counted, whereas the other cells were treated with the inhibitor. After an incubation time of 48 h, the cell number was counted and the cell number of untreated cells containing DMSO was set to 100 % (**Figure 3.24**). Because of the high toxicity of compound **H** and to compare the results with **L** as well as **L-I**, a concentration of 10 µM was used instead of 20 µM as was the case for the FACS analysis (**Figure 3.23**). All three inhibitors decreased cell proliferation, whereby compound **L** showed the weakest effect. In A549 cells, compound **L** deceased cell proliferation by 40 %, but in H1299 only by 10 %. This suggested that the *in vivo* effect of compound **L** is not completely, but may be partly p53-dependent. Compound **L-I** had a stronger inhibitory effect on cell proliferation in both cell lines, where cell proliferation was decreased to approximately 20 % - 30 %. Compound **H** showed in both cell lines the same effect; it decreased cell proliferation to approximately 10 %. These results suggested that compound **H** as well as **L-I** were able to strongly reduce cancer cell proliferation independently of the p53 protein. In the future experiments, it should be determined whether this potential is limited to cancer cells.

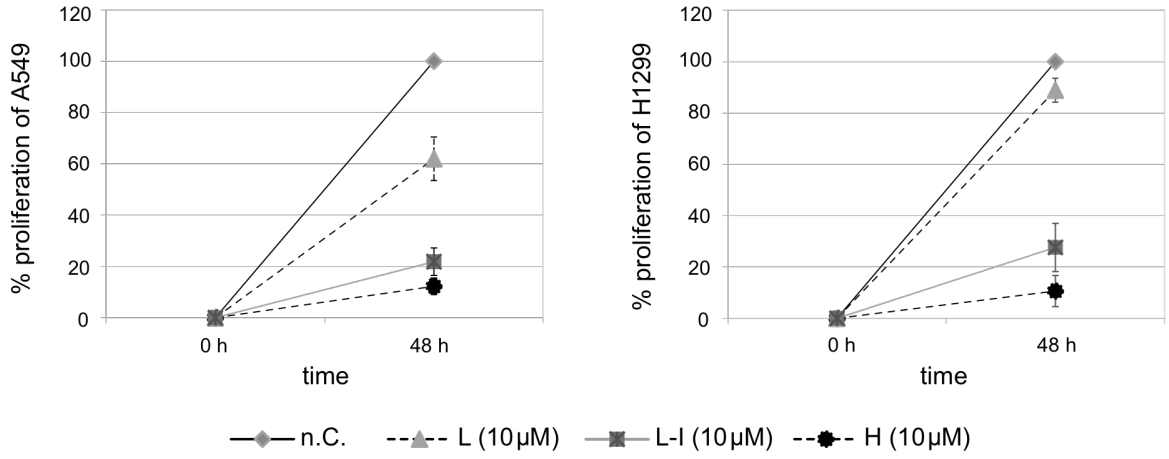

Figure 3.24: Cell proliferation was decreased after inhibitor treatment
Both cell lines A549 and H1299 were treated with 10 µM of compound H, L as well as L-I and after 48 h the cell number was counted. The cell number before the inhibitor treatment is displayed as 0 h. The negative control (n. C.) represents cells that were treated with DMSO and was set to 100 %. Values correspond to the average cell number of three independent experiments ± standard deviation.

For measurements of cell viability, we used the MTT (3-[4,5-dimethylthiazol-2-yl]-2,5-diphenyltetrazolium bromide) assay, which is a sensitive assay to measure reduction of cell viability, when metabolic events lead to apoptosis or necrosis. MTT is a yellow dye that is reduced to insoluble purple formazan dye crystals by metabolically active cells. Through the addition of solubilisation buffer (0.01 M HCl, 10 % SDS) the crystals were solubilised, and its absorbance was measured at 550-600 nm using a spectrophotometer. Both cell lines A549 and

H1299 were treated with different concentration (up to 10 µM) of the three inhibitors for 48 h and cell viability was determined by the MTT assay. As shown in **Figure 3.25**, all three inhibitors decreased cell viability to 50 % at the highest concentration of 10 µM. However, compound **L** and **L-I** did not induce as sharp a decrease of viability at lower concentrations as compound **H,** and the viability of H1299 cells was slightly higher than that of A549 cells after treatment with **L** or **L-I**.

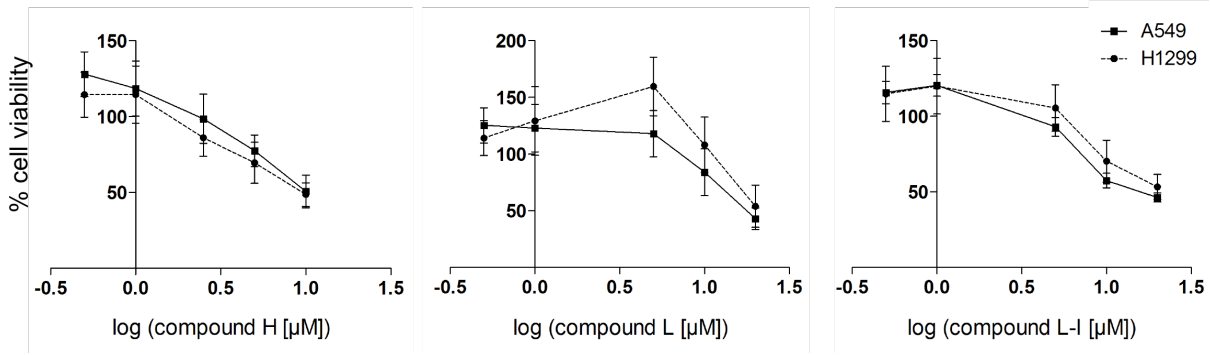

Figure 3.25: Cell viability was reduced after inhibitor treatment
The lung cancer cell lines A549 and H1299 were treated with different concentrations of compound H, L and L-I for 48 h. Afterwards, cell viability was measured by MTT assay. The control reaction containing DMSO was set to 100 %. Values correspond to the average cell viability of three independent experiments ± standard deviation.

These results suggested that all three inhibitors were able to decrease cell viability, supporting the results of the proliferation measurements, which showed that all inhibitors more or less reduced cell proliferation, though this was not completely dependent of the p53 protein. However, SirT1 as well as SirT2 have a broad range of targets that are responsible for cell cycle progression and that could be affected through the inhibitor treatment. It could also be that the inhibitors not directly inhibited SirT1 or SirT2 *in vivo*, but also other cell components that decrease the cell viability.

3.3.3 Induced apoptosis was partly dependent on p53

The results of apoptosis induced by compound **L** as well as **L-I** suggested that the *in vivo* effects of both inhibitors might be p53-dependent. In contrast, the results of the MTT assay showed that **L** as well as **L-I** could reduce cell viability to approximately 50 % in both cell lines and this therefore might not be p53-dependent. However, similar to SirT1, SirT2 affects a variety of different substrates that are involved in many biological processes, such as cell cycle progression and apoptosis. Through the inhibitor treatment, not only p53 may be affected, but the increase of apoptosis could be p53-dependent. And to assess this, we obtained H1299 (MS48) cells that were transfected with a p53 plasmid that carried a fusion of human p53 with a modified estrogen receptor ligand-binding domain (ER^{TM} = estrogen

receptor$^{Tamoxifen\ Mutant}$; Prof. M. Schuler, University Hospital Essen). The H1299 (MS48) cells expressed the p53-ER^{TM} gene, but p53 remained inactive until the synthetic steroid 4-hydroxytamoxifen was added and unmasked the p53-ER^{TM} fusion protein (Littlewood et al. 1995).

The expression of the p53-ER^{TM} protein in H1299 (MS48) cell was determined by Western blotting using an α-p53 antibody. As shown in **Figure 3.26**, we were able to detect the p53-ER^{TM} protein in the H1299 (MS48) cells in comparison to the wild-type H1299 cells. The p53-ER^{TM} protein migrated at a higher molecular weight than the 53 kDa of p53, because of the fusion with the estrogen receptor ligand-binding domain.

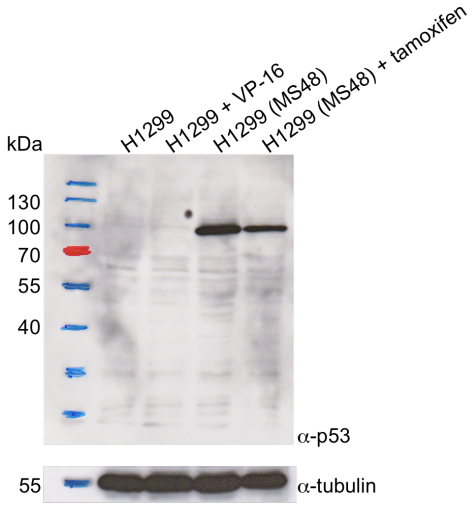

Figure 3.26: H1299 (MS48) cells expressed p53 protein
The expression of p53 protein was determined by Western blotting in whole cell extract with α-p53 antibody. The antibody α-tubulin was used as loading control.

The H1299 (MS48) cells were treated in the same manner as the H1299 and A549 cells with different concentrations of the inhibitors alone and in combination with VP-16, and apoptotic cells were measured by FACS analysis. To determine whether the presence of the p53-ER^{TM} fusion plasmid itself had an influence on the cells, we first performed the measurements without the tamoxifen treatment. As shown in (**Figure 3.27**), the H1299 (MS48) cells induce no additional apoptosis after combined treatment with compound **L** or **L-I** and VP-16, similar to the wild-type H1299 cells (**Figure 3.23A**). This suggested that the p53-ER^{TM} fusion plasmid per se had no influence on the inhibitory effect of the compounds.

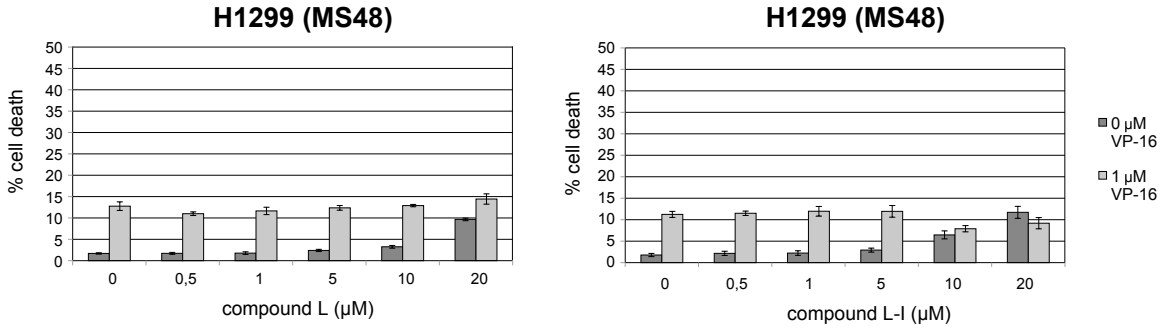

Figure 3.27: Influence of compound L and L-I on H1299 (MS48)
Lung cancer cells H1299 (MS48), which were transfected with a p53-ER^{TM} fusion plasmid, were treated with different concentrations of compound L or L-I alone (dark gray bar) or in combination with 1 µM VP-16 (light gray bar). SubG1 phase was measured by FACS analysis and displayed as % cell death. Values correspond to the average cell death of three independent experiments ± standard deviation.

In the next experiments, 100 nM tamoxifen (subsequently designated "+T" in the text) was added simultaneously with the inhibitors **L** or **L-I** and VP-16 to the cells, and cells were incubated for 48 h.

In the case of compound **L**, the treatment with 20 µM of the inhibitor alone led to an increase of apoptosis from approximately 7 % of untreated H1299 (MS48) +T cells to approximately 15 %. However, this is comparable to the H1299 (MS48) cells where p53 is not activated, suggesting that the induced apoptosis by **L** alone was not p53-dependent. The combined treatment of the H1299 (MS48) +T cells with compound **L** and VP-16 induced a slight additional increase of apoptosis from approximately 17 % of untreated cells to 22 % at the highest concentration of **L**, though this difference was not statistically significant. These results are also comparable to the H1299 (MS48) cells without p53 induction, and this further indicated that the additional induced apoptosis by compound **L** was not p53-dependent.

In the case of compound **L-I**, we observed that apoptosis increased from approximately 7 % of untreated H1299 (MS48) +T cells to 25 % of H1299 (MS48) +T cells that were treated with 20 µM of **L-I** alone. This effect was not observed in H1299 wild-type cells (**Figure 3.23B**), where **L-I** treatment induced 10 % cell death at 20 µM, suggesting that the p53 induction sensitizes cells to apoptosis by **L-I**. However, the combined treatment of H1299 (MS48) +T cells with **L-I** and VP-16 led to a measurable additional increase of apoptosis from approximately 20 % of untreated cells to 30 % at the highest concentration of **L-I**. In the A549 cells we observed an additional increase from approximately 4 % of untreated cells to 24 % at the highest concentration of **L-I** (**Figure 3.23B**), displaying a stronger effect of **L-I** in A549 cells than in the H1299 (MS48) +T cells. This indicated that the activation of p53 did not enhance L-I mediated apoptosis in VP-16-sensitized cells. Altogether, these results suggested that the inhibitor-mediated apoptosis by **L-I** might be partially p53-dependent. As

mentioned above, SirT2 inhibits a broad range of substrates, and the results indicated that more targets than p53 might be affected by the inhibitors **L**, **L-I** as well as **H** and may also be responsible for the *in vivo* effects.

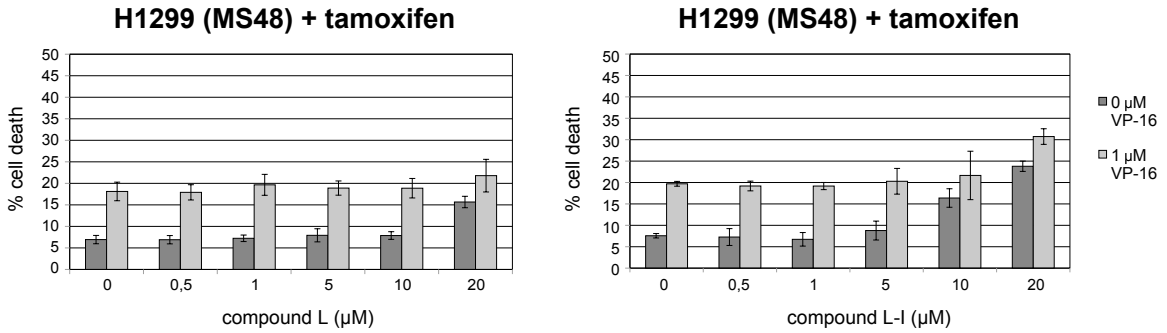

Figure 3.28: Influence of compound L and L-I on H1299 (MS48) after tamoxifen treatment
Lung cancer cells H1299 (MS48), which were transfected with a p53 plasmid, were treated with different concentrations of compound L or L-I alone (dark gray bar) or in combination with 1 µM VP-16 (light gray bar). Additionally, the cells were treated with tamoxifen to activate the p53 protein. SubG1 phase was measured by FACS analysis and displayed as % cell death. Values correspond to the average cell death of three independent experiments ± standard deviation.

3.3.4 Inhibitors did not change the acetylation level of sirtuin targets

To determine whether SirT1 or SirT2 were directly inhibited *in vivo* by the compounds **L**, **L-I** as well as **H** and to test which target of both enzymes were affected, we sought to analyze the acetylation level of p53, a target of both enzymes, as well as of α-tubulin, a substrate of SirT2. To determine the acetylation level of p53, the A549 cell line was treated with compound **H**, **L** or **L-I** alone and in combination with VP-16, similar to the experiments for the analysis of apoptosis. The p53 protein is often found in latent forms, and the levels of p53 protein are very low in unstressed cells, mainly due to degradation mechanisms (Luo et al. 2001). Therefore, we treated the cells with VP-16 in order to induce stress. Subsequently, whole cell protein was isolated and subjected to SDS-PAGE gel and Western blots. The acetylation level of p53 was determined by Western blotting with an α-Acp53 (K^{382}) antibody (**Figure 3.29**). As expected, treatment of cells with VP-16 led to an increase in total p53 levels as well as an increase in acetylated p53. This is in agreement with published data of (Luo et al. 2001), that after VP-16 treatment, cells were stressed and the p53 protein level was increased. The potent SirT1 inhibitor, Ex527 (Napper et al. 2005), was used as control, but it produced at most a marginal increase of the p53 acetylation signal (Lane 4) on VP-16-induced p53. The inhibitors **H**, **L** as well as **L-I** identified in this study were also not able to increase the acetylation level of p53 that was induced by VP-16 treatment. On the contrary, p53

induction per se as well as acetylation, especially after treatment with **H** and **L**, was reduced compared to VP-16 treatment alone, for reasons that are not clear.

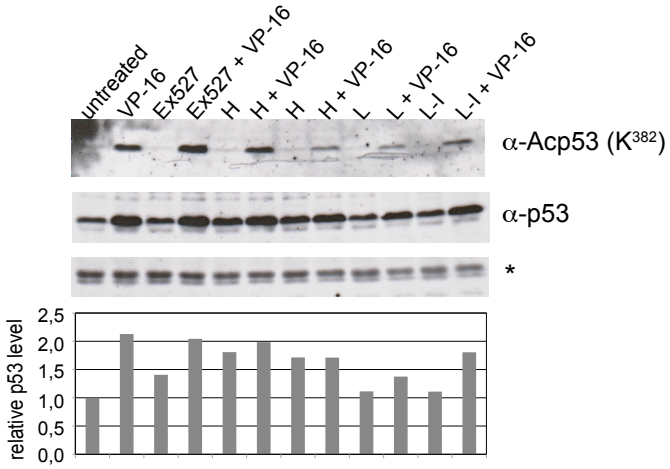

Figure 3.29: No additional increase of the p53 acetylation signal after inhibitor treatments
The A549 cells were treated 10 µM of each compound alone and in combination with 1 µM VP-16. The acetylation level of p53 protein was determined by Western blotting with α-Acp53 (K382) antibody. For the detection of cellular p53 level the α-p53 antibody was used. An unspecific band of the α-p53 antibody (*) was used as loading control. The p53 level was quantified using the program ImageJ, whereby the p53 level of untreated cells was set to 1.0.

The acetylation level of α-tubulin was determined by Western blotting with α-Ac-tubulin (K^{40}) antibody. As shown in **Figure 3.30**, no acetylation signal of α-tubulin could be observed after inhibitor treatment, except for the cells that were treated with trichostin A (TSA). TSA, a potent HDAC inhibitor, inhibits HDAC6 that is also known to deacetylate α-tubulin and this led to a strong increase of the α-tubulin acetylation signal. It is proposed that HDAC6 and SirT2 have a shared role in deacetylating α-tubulin (Heltweg et al. 2006), however an acetylation signal after treatment with **L** or **L-I** could not be observed.

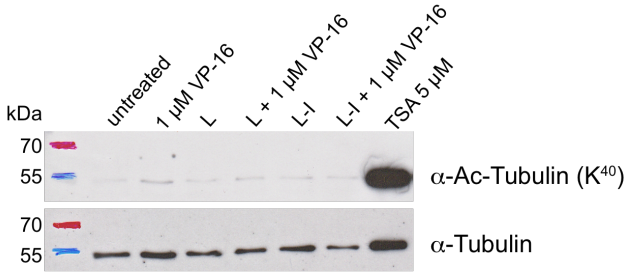

Figure 3.30: No acetylation signal of α-tubulin after treatment with L or L-I
The A549 cells were treated with 10 µM of L or L-I alone or in combination with 1 µM VP-16. The acetylation level of tubulin was determined by Western blotting with α-Ac-tubulin (K40) antibody. The level of whole tubulin was detected by α-tubulin antibody and used as loading control.

These results indicated that the *in vivo* influence of the inhibitors **H**, **L** as well as **L-I** is insufficient to observe an increase of the acetylation signal on p53 and α-tubulin, even though they are *in vitro* inhibitors of SirT1 and SirT2, respectively. This furthermore indicated that

their *in vivo* effect may result from inhibition of deacetylation of other target proteins, or from sirtuin-independent cellular effects.

3.3.5 ySir2 inhibitors did not inhibit silencing in yeast

Yeast Sir2 is required for silencing at the silent mating-type loci (*HMR* and *HML*), the telomeres and at rDNA in *S. cerevisiae.* Splitomicin is a potent ySir2 inhibitor with an IC_{50} value of 60 µM *in vitro* and is able to inhibit ySir2-dependent silencing at all three loci in yeast (Bedalov et al. 2001). Since the inhibitors identified in this study showed a similar degree of *in vitro* inhibition of ySir2 as splitomicin, we performed *HM* silencing assays to determine whether these compounds affected ySir2 *in vivo*. As described in **1.4.1**, haploid yeast cells contain one allele of *MAT* (**a** or α), which determines their mating-type, and two additional copies of the mating-type information (*HML* and *HMR*) that are silenced. Cells expressing α information can only mate with *MAT***a** cells, which produces *MAT***a**/α diploid cells. Here, we used a highly sensitive silencing assay to probe for Sir2 inhibition. For this purpose, a *mat***a**Δp strain carrying a modified *HMR* cassette was used (ROY1). This *HMR* allele (*HMR*-ssα) carries α instead of **a** information and is governed by a synthetic *HMR* silencer (ss) (Kamakaka and Rine 1998). Derepression of *HMR*, for instance by Sir2 inhibition, results in expression of α information, which in the *mat***a**Δp background leads to an α mating-type and thus to mating with a *MAT***a** tester strain. To test for Sir2 inhibition, logarithmically growing cells of both strains were plated on YM plate to a final OD_{600} of 0.5 of each strain. Subsequently, paper discs with 2 µl of DMSO or different concentrations of the inhibitor (all except for B, C, E, K and M) were placed onto the agar, and the plate was incubated at 30 °C for 2 days. Auxotrophic markers were selected such that diploid cells can grow on this medium. The yield of diploid cells was taken as indicator for *HMR* silencing, and 2 µl of splitomicin (10 mM) was used as positive control. Splitomicin inhibits ySir2 *in vivo* and thereby the ROY1 strain becomes an α–mater, which is able to mate with the mating-type tester strain *MAT***a**, as can be seen as the growth of diploids around the splitomicin filter disc. **Figure 3.31** shows an example for the results of all inhibitors that were tested. None of them showed an inhibition of the ySir2-mediated *HMR* silencing, suggesting that the inhibitors did not inhibit ySir2 *in vivo*.

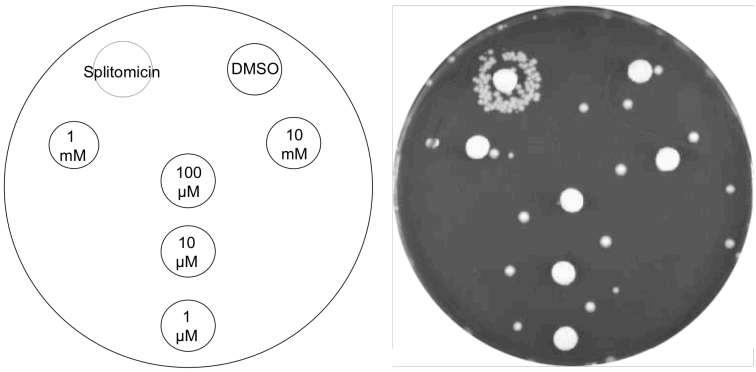

Figure 3.31: ySir2 inhibitors had no influence on *HMR* silencing
A *mat***a**Δp *HMR*-ssα (ROY1) as well as the mating-type tester *MAT***a** were plated on a YM plate (right site). Paper disc with 2 µl of different concentrations of ySir2 inhibitor were placed onto the agar as indicated by the scheme on the left site. 2 µl of DMSO as well as 2 µl of splitomicin (10 mM) were used as positive control.

3.4 Validation and characterization of potential sirtuin activators

The validation and characterization of the activators that were identified by the high throughput screen of the ChemBioNet library was performed by Louisa Hill during her master thesis (Hill 2012).

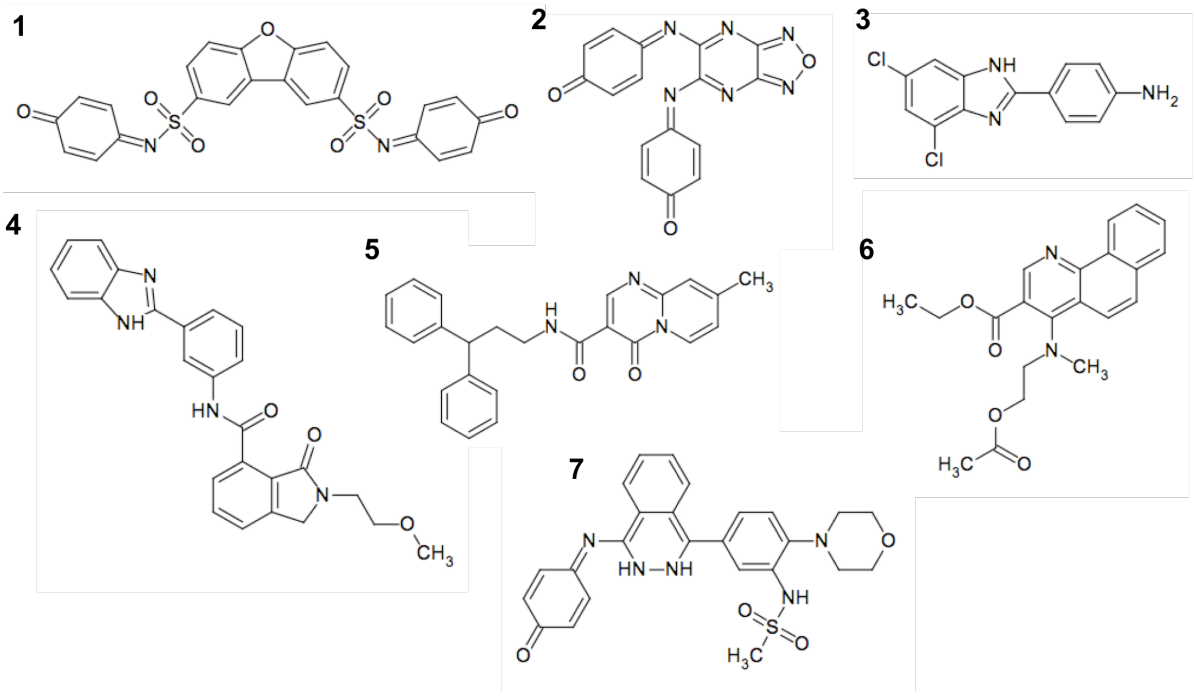

Figure 3.32: Chemical structures of potential SirT1 activators

The validation of the activators with the MAL deacetylation assay showed that of 12 activators, seven (**Figure 3.32**) induced a potent activation of SirT1 activity (**Figure 3.33**). The activators **1**, **2**, as well as **3** showed the strongest activation of SirT1, whereas the compounds **4** to **7** showed a moderate activation of SirT1.

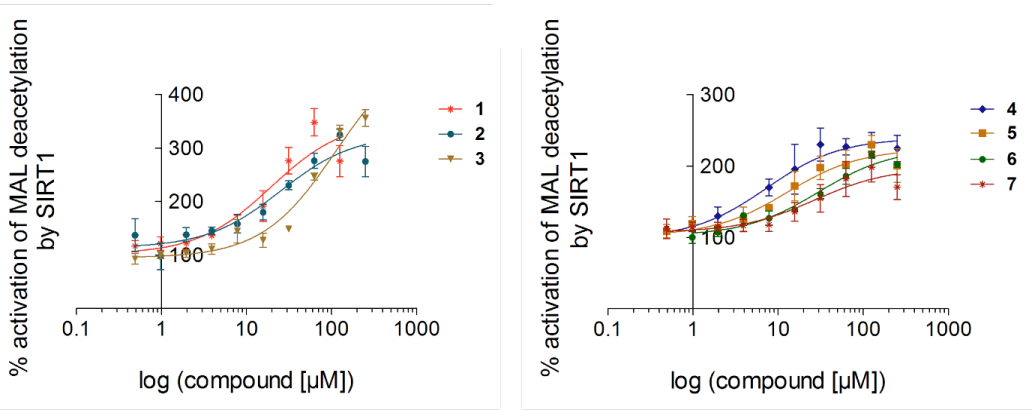

Figure 3.33: Identification of SirT1 activators
The influence of potential SirT1 activators (1-7) was determined by MAL deacetylation assay. The control reaction containing DMSO was set to 100 %. IC_{50} values and curve fitting were performed using GraphPad. Values correspond to average enzyme activity of a 3-fold measurement ± standard deviation. The MAL deacetylation assays were performed by Louisa Hill (Hill 2012).

Furthermore, the effect of these potential activators was measured by the HPLC-based p53 deacetylation assay, and this showed that none of them was able to enhance the activity of SirT1 (Hill 2012). As opposed to this, surprisingly, compound **1** (**Figure 3.32**) strongly inhibited SirT1 activity in the HPLC-based p53 deacetylation assay. This suggested that the influence of a small molecule on the SirT1 activity depends on the environment of the deacetylation substrate.

Furthermore, the effect of these potential activators was measured with the SirT1 truncations (see **3.2.1**) and with ySir2 in the MAL deacetylation assay.

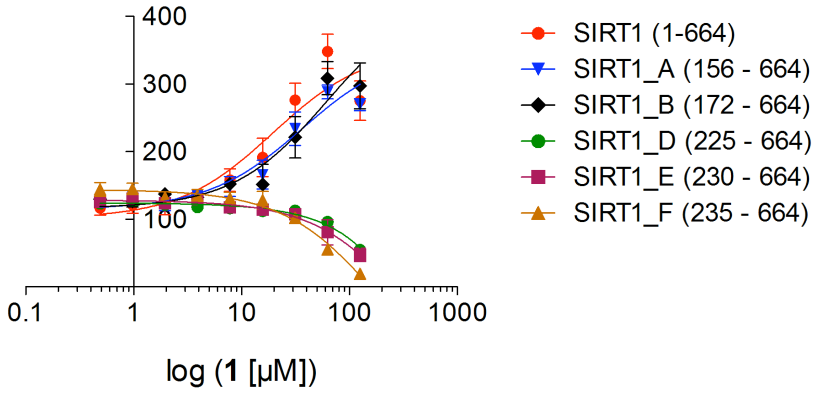

Figure 3.34: Influence of compound 1 on SirT1 truncations
The influence of compound 1 on SirT1 truncations was determined by MAL deacetylation assay. The control reaction containing DMSO was set to 100 %. IC_{50} values and curve fitting were performed using GraphPad. Values correspond to average enzyme activity of a 3-fold determination ± standard deviation. The MAL deacetylation assays were performed by Louisa Hill (Hill 2012).

Surprisingly, the shorter constructs SirT1_D, SirT1_E as well as SirT1_F were inhibited by compound **1** (**Figure 3.34**). These results indicated that the N-terminal region of SirT1 had an

influence of the enhancement of the SirT1 activity. Furthermore, compound **1** may be a more potent inhibitor when SirT enzymes with a shortening N-terminal region were used.

Based on these results from Louisa Hill, we measured the effect of compound **1** on the activity of ySir2 as well as of SirT2 in the MAL deacetylation assay, because both have a relatively short N-terminal region in comparison to SirT1. Notably, compound **1** inhibited both enzymes in the MAL-deacetylation assay (**Figure 3.35A**) with an IC_{50} value of 58.2 µM for ySir2 and 88.2 µM for SirT2. Additionally, SirT2 was also inhibited in the HPLC-based p53 deacetylation assay (**Figure 3.35B**), where a lower concentration was required to inhibit 50 % of SirT2 activity than the IC_{50} value of the MAL deacetylation assay.

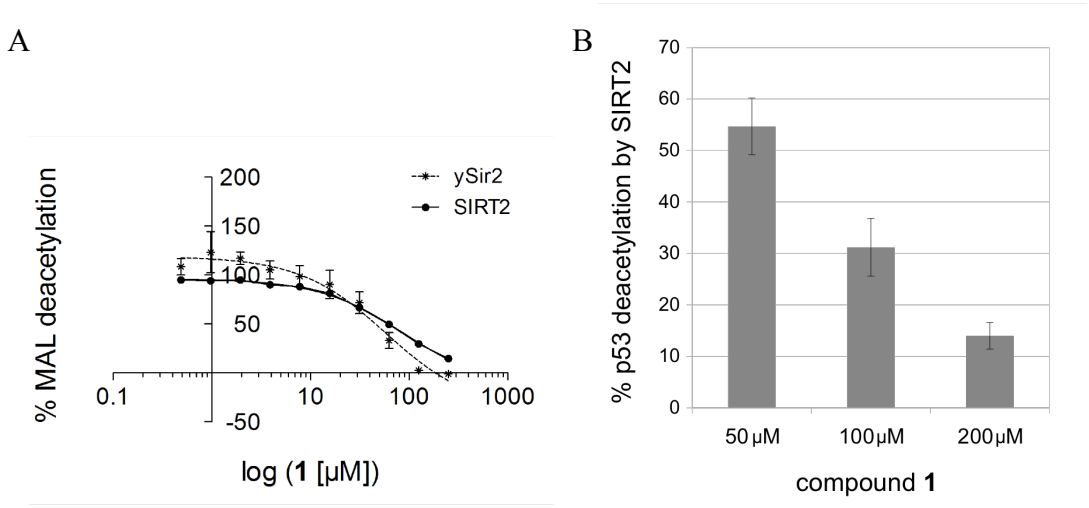

Figure 3.35: Inhibitory effect of compound 1 on SirT2 and yeast Sir2
(A) The inhibitory effect of compound 1 on SirT2 and yeast Sir2 activity was measured by fluorescence-based assay. IC_{50} curve fitting was performed using GraphPad. (B) The inhibitory effect of 50 µM, 100 µM and 200 µM of compound 1 on SirT2 was analyzed by HPLC-based assay and displayed as % of SirT2 activity. In both assays (A and B) the control reaction containing DMSO was set to 100 %. Values correspond to the average enzyme activity of three independent experiments ± standard deviation.

These results suggested that compound **1** might be a more potent inhibitor of SirT enzymes with a short N-terminal region independently of the deacetylation substrate.

The IC_{50} value of compound **1** (58 µM) for ySir2 was comparable with the IC_{50} value of splitomicin (60 µM; (Bedalov et al. 2001)). For this reason we performed *HM* silencing assay as described in 3.3.5. However no inhibition of ySir2-dependent *HM* silencing was observed. This indicated that compound **1** was not able to inhibit ySir2 *in vivo,* or its *in vivo* influence was insufficient to observe an effect.

4. Discussion

Sirtuin family members, homologs of the Silent Information Regulator Two (Sir2) protein from yeast, are best known as NAD^+-dependent deacetylases, and some family members possess ribosyltransferase, demalonylase and desuccinylase activities (Frye 1999; Landry et al. 2000; Du et al. 2011). They are conserved from bacteria to humans and target both histones and a broad range of non-histone proteins. The best and most extensively studied sirtuin is SirT1 that deacetylates a number of important transcription factors such as p53, FOXO family members, PGC1-α and many more. Therefore, SirT1 is involved in a variety of biological processes including cell survival, apoptosis, cancer development and stress resistance (reviewed in (McGuinness et al. 2011)). Based on these roles of sirtuins, small molecules that influence the activity of sirtuins are deemed promising candidates for therapies of a variety of different diseases. So far, a variety of modulators exist that inhibit or activate sirtuins, but most of them have a low bioavailability, interact with multiple targets or have a high IC_{50} value. Furthermore, many details of the sirtuin reaction mechanism and regulation are still unclear. The SirT5/suramin complex has provided important insights into the inhibitory mechanism of suramin (Schuetz et al. 2007), but this to date is the only sirtuin structure bound to an inhibitor, which limits our knowledge about sirtuins, especially considering that many other sirtuin inhibitors with greater selectivity have been identified (Yuan and Marmorstein 2012). Additionally, the effect of putative activators of sirtuins (Howitz et al. 2003; Milne et al. 2007) have been shown to be substrate and assay dependent (Borra et al. 2004; Kaeberlein et al. 2005; Beher et al. 2009; Pacholec et al. 2010). In this study, we have identified inhibitors of SirT1 as well as SirT2 that can be developed further for anticancer therapy.

4.1 Identification of SirT1 inhibitors

For the identification of novel small molecules that influence the deacetylase activity of sirtuins, in particular of SirT1, we established a high-throughput fluorescence-based deacetylation assay as described in (Heltweg et al. 2003). As a substrate, we used a acetylated lysine that is coupled with a fluorophore (MAL (Hoffmann et al. 1999)). The screen of a small natural compound library (purchased from BIOMOL) resulted in four inhibitors and three activators of SirT1. The inhibitors rottlerin, shikonin, dihydrotanshinone as well as cryptotanshinone showed IC_{50} values in the micro-molar range, and they have not been

identified as sirtuin inhibitors so far. However, rottlerin is a well-known protein kinase inhibitor C (PKC; (Gschwendt et al. 1994)). Since SirT1 requires NAD^+ as a cofactor, which shares structural features with ATP, the cofactor of kinases, it is therefore possible that rottlerin inhibits SirT1 via competitive inhibition in the NAD^+ binding pocket. This furthermore indicated that rottlerin may have further cellular targets and thus likely has pleiotropic effects in the cell. It therefore was not further investigated here.

Shikonin is isolated from the plant *Lithospermum* (purple gromwell) and is used in Chinese herbal medicine (Chen et al. 2003). It is known to inhibit cell growth and induces apoptosis that is mediated by activation of p53 (Wu et al. 2004a; Wu et al. 2004b). One therefore can speculate that shikonin inhibits SirT1, resulting in increased p53 acetylation, which becomes active in response to stress. However, the chemical structure of shikonin (Figure 3.4) contains a reactive para-quinone group (Prof. M. Kaiser, personal communication), and we therefore speculate that shikonin interacts with multiple targets and does not inhibit SirT1 specifically. Our *in vivo* experiments indicated that shikonin has a high cellular toxicity, since a concentration of 1 µM of shikonin induced nearly 100 % cell death.

The inhibitors dihydrotanshinone and cryptotanshinone are derived from the plant *Salvia miltiorrhiza* (red sage) and are also used in Chinese herbal medicine (Lee et al. 1999). Cryptotanshinone is a potent STAT3 (signal transducer and activator of transcription 3) inhibitor (Shin et al. 2009), whereas dihydrotanshinone inhibits cell proliferation and tumour growth of breast cancer (Tsai et al. 2007). Similar to shikonin, both contain a reactive quinone in their chemical structure (Figure 3.4) and therefore may be unspecific inhibitors, which might explain their high toxicity in the cell culture experiments.

The SirT1 activators quercetin, luteolin and kaempferol that were identified in the BIOMOL compound library are already known as sirtuin activators (Howitz et al. 2003). The fact that we were able to identify them in our screen confirmed the potential of identifying novel activators in the MAL deacetylase assay. Next, we performed a high-throughput screen of the ChemBioNet library. This screen resulted in several potential activators as well as inhibitors of SirT1. After subsequent validation steps, we arrived at 14 potential inhibitors and 12 activators. During this study, we concentrated on characterization of the inhibitors. The activating effect of the 12 putative SirT1 activators was characterized by Louisa Hill during her master thesis (overview in 3.5), and a number of follow-up experiments are presented in this thesis.

The inhibitory effect of 13 out of 14 inhibitors was confirmed by the MAL deacetylation assay. All of them showed a concentration-dependent inhibition of SirT1, and their IC_{50} values vary from 2.4 µM (compound A) to 173.2 µM (compound M). Several studies have

shown that the fluorophore attached on the substrate influences the activity of sirtuins in the fluorescence-based assays (Kaeberlein et al. 2005; Beher et al. 2009), though this has mainly been described for the putative activators of sirtuins. Here, we established a deacetylase activity assay that is independent of the presence of the fluorophore in order to verify the inhibitory effect of the compounds. For this assay we used an acetylated p53-derived peptide (aa 368 -386 of p53; K^{382}Ac) without fluorophore. Several of the inhibitors were able to inhibit SirT1-dependent p53 deacetylation, but their effect was less pronounced than in the MAL deacetylation assay. Suramin, the well-known SirT1 inhibitor that showed an IC_{50} value of 4.7 µM in the MAL deacetylation assay, inhibited SirT1-dependent p53 deacetylation to 50 % at 20 µM. Also the inhibitors shikonin, dihydrotanshinone as well as cryptotanshinone with an IC_{50} value of 1.6 µM and 3.4 µM in the MAL deacetylation assay, inhibited the p53 deacetylation to 50 % - 60 % at a concentration of 20 µM. The compounds A – D had IC_{50} values lower than 10 µM for MAL deacetylation, but except for compound B, they failed to inhibit p53 deacetylation to 50 % at a concentration of 50 µM. Compound B inhibited SirT1 activity to 50 % in this p53 deacetylation assay at 20 µM and that had an effect comparable to suramin. All the other inhibitors, except for compound F, failed to inhibit SirT1 activity to 50 % at a concentration of 50 µM. F showed inhibition of 50 % SirT1 activity at 50 µM, although it had an IC_{50} value of 27.7 µM in the MAL deacetylation assay. The poor inhibition of SirT1-dependent p53 deacetylation by the inhibitors in comparison to the MAL deacetylation could be due to the different substrates in the two assays. SirT1 has poor affinity for the substrate MAL, which is in contrast to the p53 peptide, which is the preferred substrate (Heltweg et al. 2003; Pan et al. 2012). For this reason, it is conceivable that a higher concentration of inhibitor is necessary to inhibit p53 deacetylation in comparison to the MAL deacetylation. Furthermore, Kaeberlein *et al.* showed that the fluorophore on the substrate decreases the binding affinity of SirT1 to this substrate (Kaeberlein et al. 2005), which is in agreement with our results.

Together, in comparison to the known inhibitor cambinol that induces a chemosensitization of cancer cells and has an IC_{50} value of 56 µM for SirT1, several inhibitors identified here are more potent SirT1 inhibitors. However, in view of the known inhibitors Ex527, tenovin-6 as well as HR73, a splitomicin derivate, which have IC_{50} values lower than 10 µM for SirT1, the compounds identified here are not the best SirT1 inhibitors.

4.2 The inhibitory activity of sirtuin inhibitors is influenced by the N-terminal region of sirtuins

A sequence alignment of sirtuins shows that they share a highly conserved catalytic core domain, but that their N- and C-terminal regions vary in length and sequence. These regions play important roles in acetyl-lysine and NAD^+ binding (Zhao et al. 2003a) and may perform protein-specific functions and possibly also confer substrate specificity (Sanders et al. 2010). Marmorstein *et al.* showed that the amino acids of the p53 peptide flanking the acetyl-lysine (K^{382}) mainly interact with the Sir2Tm (from bacteria *Thermotoga maritime*) enzyme, which includes hydrogen bonds with N^{165} and G^{163} as well as van der Waals interaction with F^{162} and V^{193}, and this has significant effect on the substrate binding affinity (Yuan and Marmorstein 2012). Here, we tested the MAL deacetylase activity of other sirtuin family members (SirT2 to SirT7) with the exception of SirT4 that has no obvious deacetylase activity (Haigis et al. 2006) and only SirT2 and SirT3 were able to deacetylate MAL. This may be in agreement with published data of (Yuan and Marmorstein 2012), because the MAL substrate has no amino acids that flank the acetyl-lysine and interact with the sirtuin enzymes, therefore the substrate binding affinity is very low and the substrate is not recognized by the other sirtuin members. In support of this, for SirT6 and SirT7 the only known substrates are histones (Michishita et al. 2008; Barber et al. 2012), and SirT5 has a weak deacetylase activity (Du et al. 2011).

Similar to (Milne et al. 2007), who show that the N-terminal region is required for SirT1 activation by resveratrol, we generated SirT1 constructs that are truncated in the N-terminus. In agreement with the published data of Milne *et al.*, we could show that resveratrol was able to activate the constructs with an extended N-terminus SirT1_A (156-664) and SirT1_B (172-664), but not the shorter constructs. Suramin inhibited all SirT1 truncations independently of the presence or the length of the N-terminal region, which indicates that suramin does not interact with the N-terminus. This is consistent with the observation of Schuetz *et al.* that the trisulfonyl naphthyl group of suramin binds to the NAD^+ binding pockets B and C, and that several of the benzene rings bind in the peptide binding site (Schuetz et al. 2007).

Our analysis showed that the N-terminal region of SirT1 has an influence of the inhibitory effect of compound D. The inhibitor D showed a strong inhibition of more than 50 % of the deacetylase activity only of full-length SirT1 as well as the longer SirT1 truncations SirT1_A (156-664) and SirT1_B (172-664) at a concentration of 50 µM. The shorter constructs SirT1_D (225-664) and SirT1_E (230-664) were not inhibited by compound D. These results indicate that D might interact with the first 225 amino acids of the N-terminal region of SirT1.

However, compound D also inhibited the activity of the shortest construct SirT1_F (235-664) to approximately 50 % at 50 µM, which was unexpected. However, this could be due to the reduced deacetylase activity of SirT1_F compared to the full-length SirT1 and the other SirT1 truncations, and therefore a lower inhibitor concentration might be sufficient to inhibit this construct. Furthermore, SirT2 was also inhibited by D to approximately 20 % at a concentration of 50 µM, similar to the inhibition of full length SirT1. This suggests that compound D might interact with a specific region in the N-terminal region of SirT1 and SirT2. In support of this theory, SirT3, whose active deacetylase form has no N-terminal region, was not inhibited by D. The ySir2 was also inhibited by compound D, but to a lesser extent than SirT1 and SirT2. In view of the fact that SirT1 is the closest homolog of ySir2, one could hypothesize that compound D inhibits ySir2 and SirT1 equally, but this was not the case. However, considering the sequence alignment of SirT1 versus SirT2 and ySir2 (**Figure 4.1**), SirT1 and SirT2 contain conserved residues in the N-terminal region that are not present in the N-terminus of ySir2. These residues are the amino acids P^{184}, G^{195} D^{204}, E^{208}, E^{214}, L^{220}, L^{228}, S^{229}, D^{239} and E^{244} of SirT1 (marked in bold in Figure 4.1), and perhaps one or more of theses residues are responsible for the interaction with compound D. To validate this hypothesis, the generation of alanine mutants of these specific residues could be useful. The enzyme with a mutation of the respective amino acid that is responsible for the interaction with compound D should not be inhibited by D any more.

```
           151                                                  200
SirT1      EIITNGFHSC ESDEEDRASH ASSSDWTPRP RIGPYTFVQQ HLMIGTDPRT
SirT2      .......... .......... .......... MAEPDPSHPL ETQAGKVQEA
Sir2       KFLDTYLPED LNSLYIYYLI KLLGFEVKDQ ALIGTINSIV HINSQERVQD
Consensus  .......... .......... .......... raePdpfhqq elqaGkdqra

           201                                                  250
SirT1      ILKDLLPET. IPPPELDDMT LWQIVINILS EPPKRKKRKD INTIEDAVKL
SirT2      QDSDSDSEGG AAGGEADMDF LRNLFSQTLS LGSQKERLLD ELTLEGVARY
Sir2       LGSAISVTNV EDPLAKKQTV RL.IKDLQRA INKVLCTRLR LSNFFTIDHF
Consensus  qdkDldpEg. aaggEaDddf Lr#ifi#iLS egpqrerrlD enTiEdaarl
```

Figure 4.1 Sequence alignments of SirT1 vs. SirT2 and ySir2
Alignment of the N-terminal region of SirT1 vs. SirT2 and ySir2 for comparison of specific residues (letters are marked in bold face). Catalytic core domain is located within amino acids 240 and 510 of SirT1. Alignments were generated using the webpage Multalin (http://multalin.toulouse.inra.fr/multalin/multalin.html).

The compounds C, F, G, H, I and M showed the strongest inhibition with the shortest construct SirT1_F that has 9 aa N-terminal to the core domain. However, as mentioned above, this could be due to the lower deacetylase activity of SirT1_F compared to the full-length SirT1. Considering the inhibition of full-length SirT1, SirT1_A, SirT1_B, SirT1_D and SirT1_E by these inhibitors, thus suggests that the N-terminal region has only a slight effect on the inhibition in comparison to compound D. The compounds C, F, G, H and I still

inhibited the shorter constructs by approximately 40 % - 50 % and compound M by approximately 30 % - 40 % at 50 µM. In support of this, compound H and M also inhibited ySir2, SirT2 as well as SirT3 by 20 % or more at 50 µM, suggesting that these both compounds also interact with the core domain that is conserved in all sirtuins. In contrast to this, compound C and F did not affect ySir2, SirT2 or SirT3, which suggested that next to the core domain and the N-terminal region, an additional factor has an influence on the inhibitory effect. This raised the question whether the C-terminal region of sirtuins, which varies among the sirtuin family members, also plays a role for the inhibitory effect of these compounds. The C-terminal region of SirT1 may potentiate the deacetylase activity by an intra-molecular mechanism, it interacts with the catalytic core domain to form a SirT1 holoenzyme (Pan et al. 2012). Perhaps, the inhibitors disrupt the interaction between the SirT1 core domain and the C-terminal region. This could also be an explanation for the inhibitory effect of the compounds shikonin, dihydrotanshinone, cryptotanshinone as well as compound A and B that showed a specific inhibition of SirT1 that is independent of the presence of the N-terminus. In agreement with this theory, the compounds showed no or a rather weak inhibition of SirT2 and SirT3. To investigate whether some of the inhibitors identified in this study interact with the C-terminal region of SirT1, the generation of SirT1 truncations at the C-terminus would be required.

4.3 Compound L is a potent inhibitor of SirT2

During the experiments with other sirtuin family members, we observed that compound L inhibited SirT2 to a greater extent than SirT1. We performed an IC_{50} curve and determined a 6-fold lower IC_{50} value for SirT2 (18.5 µM) in comparison to SirT1 (118.4 µM) in the MAL deacetylation assay. Additionally, compound L showed a stronger inhibition of SirT2-dependent p53 deacetylation as measured by the HPLC-based assay in comparison to SirT1. At a concentration of 50 µM, compound L inhibited SirT2 activity to approximately 20 %, whereas SirT1 activity was inhibited to 10 %. These results indicate that compound L is a potent SirT2 inhibitor independently of the substrate. These results show that compound L displays some degree of selectivity for SirT2 inhibition. The known inhibitor AC-93253 shows potent inhibition of SirT2 activity with an IC_{50} value of 6.0 µM, however it also inhibits SirT1 with an IC_{50} value of 43.5 µM (Zhang et al. 2009).

In an effort to determine which element of the chemical structure of compound L is important for its inhibitory effect, we obtained derivates of L and measured their inhibition of deacetylase activity by the MAL deacetylation assay. All derivates are structurally similar to

each other, but have different substituents attached at the carboxamidegroup. One of these derivates, compound L-I, showed a stronger inhibition of SirT2-dependent MAL deacetylation in comparison to L. The IC_{50} value was reduced to 3.8 µM. In the p53 deacetylation assay, L-I inhibited SirT2 activity to approximately 20 % at a concentration of 20 µM. These results suggest that the addition of the heterocyclic pyridine increases the binding affinity of compound L to SirT2, probably through additional π-π interactions. In contrast to this, the ether group of compound L-II had no obvious influence on the inhibitory effect. L-II inhibited SirT2 deacetylase activity to a similar extent as compound L. The compounds L-III and L-IV showed a weaker or no inhibition of SirT2-dependent MAL deacetylation. This suggests that the addition of an anisole group, as is the case for L-III, or a methyl benzoate group, as is the case for L-IV, decreased the binding affinity for SirT2. Both substituents are unpolar groups and probably led to a decrease in the interaction between the inhibitor and SirT2.

4.4 *In vivo* effect of Sirtuin inhibitors

Since our biochemical results indicated that we had identified sirtuin inhibitors, we sought to determine whether they inhibited sirtuins *in vivo* in order to assess the anticancer potential of these compounds. For this purpose, we treated the human lung cancer line A549 with different concentrations of the identified inhibitors A to M as well as shikonin, dihydrotanshione and cryptotanshinone and measured apoptotic cells by FACS analysis. The three inhibitors shikonin, dihydrotanshinone and cryptotanshinone showed a strong increase of cell death at low concentrations of 1-2 µM. This suggests a high toxicity of these compounds, which may be related to the reactive quinone in their chemical structure. Thus, these compounds probably interact with multiple targets in the cell and not only inhibit SirT1 *in vivo*.

Of the other compounds, B, C, F, H, L as well as L-I caused a moderate increase of apoptosis at higher concentrations, indicating that they had an effect on the cells. To gain more insight into the *in vivo* effect of these inhibitors, the A549 cells were treated with these six compounds in combination with the chemotherapeutic agent etoposide (VP-16). Etoposide forms a ternary complex with DNA and the topoisomerase II enzyme, prevents re-ligation of the DNA strands and therefore causes DNA strand breaks (Hande 1998). Cancer cells divide more rapidly than normal cells, and therefore cancer cells should be more affected by etoposide, and this promotes apoptosis of the cancer cells. However, most of the cancer forms are resistant against such chemotherapeutic agents. The tumor suppressor p53 is known to

exert anti-proliferative effects, including growth arrest, apoptosis and cell senescence in response to various types of stress (Levine 1997; Prives and Hall 1999). Luo *et al.* showed that SirT1 promotes cell survival in response to DNA damage by inhibiting p53-dependent apoptosis (Luo et al. 2001). Several cancer forms including lung cancer cells show increased levels of SirT1 protein (Fraga and Esteller 2007; Stunkel et al. 2007) and this might be the reason for the resistance of cancer cells against chemotherapeutic agents. This suggests that the combination with DNA damaging agents and SirT inhibitors may have synergistic effects in cancer therapy. In this study, we observed that A549 cells treated with VP-16 alone showed only a slight increase of cell death in comparison to untreated cells, consistent with the idea that they are resistant to such agents. After the treatment of A549 cells with the six inhibitors in combination with VP-16, the inhibitors H, L as well as L-I showed an additional increase of apoptosis, which is in line with published data of the expected effect of SirT1 inhibition (Hajji et al. 2010). In this paper, the human lung carcinoma cell line H157 was treated with 1 μM Ex527, a potent SirT1 inhibitor (Napper et al. 2005), in combination with VP-16 and this led to an increase of cell death by 20 % in comparison to the treatment with the SirT1 inhibitor alone. Furthermore, siRNA directed against SirT1 in H157 cells led to an increase of apoptosis by approximately 40 % after VP-16 treatment compared to the control siRNA (Hajji et al. 2010). SirT2 down-regulation using siRNA leads to a strong increase of apoptosis in cancer cells such as HeLa, but not in normal cells, which is caused by p53 accumulation (Li et al. 2011). Compound H showed a slight additional increase of apoptotic cells at low concentrations up to 5 μM in combination with VP-16. Compound L as well as L-I induced an additional increase of apoptosis by approximately 10 % at a concentration of 20 μM. Compared to the results of the inhibitor Ex527 (Hajji et al. 2010), our inhibitors showed a weaker effect, however Ex527 has a IC_{50} value of 0.098 μM for SirT1, so it is a more potent *in vitro* inhibitor than the compounds described here.

The inhibitors L as well as L-I were selective for SirT2 with IC_{50} values of 18.4 μM (L) and 3.8 μM (L-I), whereas compound H inhibited SirT1 with an IC_{50} value of 31.5 μM. Both enzymes SirT1 and SirT2 are known to deacetylate the tumor suppressor p53, the histone H4K16 and FOXO family members (reviewed in (McGuinness et al. 2011)). Additionally, SirT2 also deacetylates lysine 40 of α-tubulin, functioning together with another tubulin deacetylase, HDAC6 (North et al. 2003; Inoue et al. 2007). Therefore, both are connected with multiple cellular processes such as cell cycle progression and cell death. To determine whether the inhibitor-mediated induced cell death was p53-dependent, the lung cancer cell line H1299, which carries a partial deletion of the p53 gene and does not express p53, was used. As for A549 cells, H1299 cells were treated with different concentrations of the

inhibitors alone and in combination with VP-16, and apoptotic cells were quantified. The treatment with compound H alone led to a stronger increase of cell death in H1299 cells in comparison to the cell death in A549 cells. The combined treatment with VP-16 reduced the cell death in H1299 cells to a similar degree as in A549 cells. This suggests that cell death mediated by compound H was not solely dependent on p53. We showed that compound H strongly reduced cell proliferation as well as viability of cancer cell lines in a dose dependent manner, which suggest that H may be a potent antiproliferative agent. However, we have no indication as to whether it directly inhibited SirT1 *in vivo* and which SirT1 target was affected. We were unable to detect an increase of p53 acetylation after inhibitor treatment. Perhaps compound H did not directly inhibit SirT1 *in vivo,* or the effect was not sufficient to observe a change of the p53 acetylation level. Furthermore, compound H showed a moderate SirT1 inhibition with an IC_{50} value of 31.5 µM in the MAL deacetylation assay, therefore the concentration of 10 µM *in vivo* might be not sufficient to induce an effect. Peck *et al*. were unable to detect an increased p53 acetylation level of human breast carcinoma cell line MCF-7 that was treated with 50 µM Ex527 (Peck et al. 2010), although this compound is a more potent SirT1 inhibitor than compound H. In contrast, cambinol inhibits SirT1 and SirT2 with IC_{50} values of 56 µM and 59 µM and it is known to induce SirT1-dependent sensitization of the lung cancer cells H460 to etoposide as well as G2 cell cycle arrest, but not apoptosis. Furthermore, cambinol is able to increase the acetylation level of p53, Ku70 and FOXO3a after combined treatment with VP-16, but the cambinol-mediated chemosensitization is preserved in cells lacking each of these proteins, suggesting that none of these SirT1 targets are responsible for the cambinol-mediated sensitization to etoposide (Heltweg et al. 2006). In support of this, sirtinol induced senescence-like growth arrest in MCF-7 as well as p53-deficient H1299 cancer cells. Transfection of siRNA against SirT1 in H1299 as well as MCF-7 cells showed growth arrest that was comparable to sirtinol treatment, indicating a SirT1-dependent manner. Furthermore, neither the expression nor the acetylation of p53 was upregulated by sirtinol or siRNA directed against SirT1 in MCF-7 cells. The authors supposed that the senescence-like growth arrest by sirtinol was accompanied by impaired activation of mitogen-activated protein kinase (MAPK) pathways (Ota et al. 2006). These results suggest that the role of SirT1 during stress is complex and not always p53 dependent, the effects of its inhibition are still unclear and may be cell context-specific.

For compound L as well as L-I, we observed a decrease in viability of the cancer cell lines after treatment. However, the H1299 cells showed a slightly better viability than A549 cells after treatment with L or L-I. In case of compound L, we observed that the cell proliferation of A549 cells was reduced more strongly than for H1299 cells. Although both cell lines may

have more differences than only the p53 protein expression, this could be an indication that the effect of compounds L and L-I may be p53-dependent. In support of this theory, the H1299 cells showed no additional increase of cell death after combined treatment with L or L-I and VP-16, which was in contrast to A549 cells. To further investigate this, we obtained H1299 (MS48) cells that were transfected with a tamoxifen-regulated p53 expression vector (Prof. M. Schuler, University Hospital Essen) and as expected, cell death in this cell line was increased upon activation of p53 by tamoxifen, but only after treatment with 20 μM of inhibitor L-I alone and in combination with VP-16. As mentioned above, we observed that L-I also reduced the cell proliferation and cell viability of H1299 cells, which suggested that not solely p53 is responsible for the inhibitor-mediated effect. Furthermore, both inhibitors also induced apoptosis of H1299 cells to approximately 10 %. To test the direct inhibition of SirT2 by compound L or L-I *in vivo*, we performed western blot analysis, but we were unable to observe an increase of the acetylation level of p53 or α-tubulin. It is therefore unclear whether these inhibitors directly inhibited SirT2 *in vivo*, or whether they affect other cell components. Splitomicin derivates with IC_{50} values of approximately 1 μM for SirT2 are able to reduce cell proliferation of MCF-7 cells and to induce acetylation of α-tubulin. However, it is discussed that the acetylation of α-tubulin mostly controlled by HDAC6, because the level of tubulin hyperacetylation that can be reached by class I and II HDAC inhibitors (e. g. trichostin A) were never reached with any of the sirtuin inhibitors (Neugebauer et al. 2008). For this reason, it is possible that the effect of both inhibitors L and L-I is not sufficient to observe a change of the acetylation levels, as might be the case for compound H. Tenovin-6 inhibits SirT2 activity to the same extent as tenovin-1 with an IC_{50} value of 10 μM, and both are able to increase the acetylation level of α-tubulin (to a lower extent than HDAC inhibitors) as well as p53 in H1299 cells transfected with p53 gene (Lain et al. 2008). Although the inhibitor L-I identified in this study might be a more potent SirT2 inhibitor than Tenovin-1 or -6 *in vitro*, we did not observed an increase of the acetylation level of α-tubulin or p53. This suggested that the inhibitor L-I and L did not directly inhibit SirT2 *in vivo* or that they interact with multiple targets. Furthermore, we have no indication whether the inhibitors were able to enter the cell, although the dose-dependent decrease of cell viability or proliferation might be an indication that they were able to enter the cell. Nonetheless, several further experiments will be necessary to determine their cell permeability, and to determine their *in vivo* targets. Based on the results that potent SirT1 inhibitors such as Ex527 also failed to increase the acetylation level of p53 (Peck et al. 2010) or that the cambinol-mediated chemosensitization is independent of p53, Ku70 and FOXO3a (Heltweg et al. 2006), it is likely that unknown sirtuin targets exist that affect cancer cell survival.

4.5 A SirT1 activator is an inhibitor of SirT2 and ySir2

As mentioned earlier, the MAL deacetylation assay is controversial, because the fluorophore attached to the substrate influences the sirtuin activity. For this reason, the results of the putative activators of SirT1 identified in this study have to be interpreted with care. The validation and characterization of these compounds was performed by Louisa Hill during her master thesis (Hill 2012). She verified the activation of SirT1 by the compounds in the MAL deacetylation as well as in the HPLC-based p53 deacetylation assay. Similar to published data of resveratrol and other STACs (Kaeberlein et al. 2005; Beher et al. 2009), the putative activators failed to enhance the activity of SirT1 when the p53 substrate lacking a fluorophore was used. She also verified the activation by these compounds of the SirT1 truncations that were generated during this study. Only the longest constructs SirT1_A as well as SirT1_B could be activated by all compounds in the MAL deacetylation assay. The shorter constructs were not affected, and some compounds even inhibited their activity. One of these putative activators, compound 1 also inhibited the full-length SirT1 in the p53 deacetylation assay. This indicates that the effect of a modulator on sirtuin activity is strongly dependent on the molecular environment of the acetyl-lysine substrate residue.

Based on these results, we performed further analysis of compound 1 in order to characterize its properties. The influence of compound 1 on other sirtuin members like ySir2 and SirT2 was measured by the MAL deacetylation assay, and we observed that both were inhibited by compound 1 (IC_{50} for SirT2 88.2 µM and ySir2 58.0 µM). SirT2 activity was also strongly inhibited by compound 1 in the p53 deacetylation assay. At a concentration of 50 µM, compound 1 inhibited SirT2-dependent p53 deacetylation to approximately 50 %, which represents a greater inhibition of p53 deacetylation than MAL deacetylation. These results showed that we had identified a inhibitor of ySir2 and SirT2, even though the compound was originally identified as a potential SirT1 activator. To determine whether compound 1 affects SirT2 *in vivo*, we measured the acetylation level of α-tubulin after treatment, but we were unable to observe any differences. In view of the high IC_{50} value of SirT2, this result may not be surprising. Due to the concentration of the stock solution of compound 1 and the high volume of cell culture medium, the highest concentration that could be used was 10 µM and this was probably too low to efficiently affect SirT2 *in vivo*. Furthermore, it is unknown whether this compound was able to enter the cell and reach intracellular SirT2, because no effect on the cell could be observed. The IC_{50} value of ySir2 of 58.0 µM is comparable with the IC_{50} value of splitomicin for ySir2 (60 µM (Bedalov et al. 2001)). In view of the fact that splitomicin is able to inhibit ySir2-dependent silencing at telomeres, the silent mating-type

loci (*HMR* and *HML*), and at rDNA in *S. cerevisiae* (Bedalov et al. 2001), we tested the influence of compound 1 on *HMR* silencing in yeast. However, *HMR* silencing was not affected by compound 1. Possibly, this compound interacts with multiple targets *in vivo*, because of the reactive quinone derivates at each end of its chemical structure. For this reason it might not reach its actual target ySir2 or SirT2, or cell permeability. One possibility would be to identify derivatives of this compound with a less reactive structure that still display the inhibitory effect on sirtuins. To this end, it will be necessary to determine which structural elements are responsible for the inhibition, which could be performed with different derivates of compound 1 in the same manner as it was done in this study for compound L.

4.6 Summary and Outlook

In this study, we have identified several sirtuin inhibitors, compound H as a SirT1 inhibitor, and compound L as well as L-I as potent SirT2 inhibitors. We could show that all three have an antiproliferative potential, and in the case of compound L-I, we were able to show that the induced apoptosis might be partly p53-dependent. However we were not able to identify a sirtuin inhibitor that is more potent than all other known inhibitors.

In future experiments this will need to be validated in order to verify the direct *in vivo* SirT2 inhibition by compound L and L-I. Such experiments could be the analysis of the protein and mRNA expression of p53-downstream targets like p21 to determine whether these inhibitors activate p53 by SirT1 inhibition. However, several publications have shown that p53 is not always responsible for the sirtuin inhibitor-mediated effect; the actual target is mostly unknown (Heltweg et al. 2006; Peck et al. 2010). For this reason, target identification studies will be necessary. In view of the fact that SirT1 as well as SirT2 deacetylate a broad range of proteins, a genome-wide screen will be useful. Such screen could be a peptide array, where a number of different acetylated peptides are bound to a cellulose membrane and incubate with the sirtuin. Subsequently, the deacetylated peptides are detected by an antibody, which signal can be measured by a fluorescence-reader (Smith et al. 2011).

In collaboration with chemists, the three potent inhibitors H, L as well as L-I could be further derivatized in order to obtain an IC_{50} value in the nano-molar range and to optimize their inhibitory effect *in vivo.* For this purpose, it would be useful to obtain information about their solubility, permeability through the cell membrane and also their metabolization in the cell.

5. Abstract

Sirtuins (SirT1-7) are the human homologues of the NAD^+-dependent histone deacetylase Sir2 from *Saccharomyces cerevisiae* (ySir2). Since the overexpression of Sir2 in yeast increases lifespan, the study of mammalian sirtuins has gained widespread interest. Each sirtuin is characterized by a conserved 275 amino-acid catalytic core domain as well as by unique additional N-terminal and/or C-terminal sequences of variable length. Sirtuins hold promise as potential drug targets for the treatment of a variety of conditions, including cancer, metabolic diseases, diabetes and aging. Although, a number of sirtuin inhibitors as well as activators are known, the inhibitory mechanism of sirtuins is still unknown. In this study, we sought to identify novel inhibitors of SirT1, and we assessed their *in vivo* potential as chemotherapeutic agents. For this purpose, we established a fluorescence-based deacetylation assay using methyl-aminocoumarin-acetyllysine (MAL) as a substrate that is suitable for high-throughput screening. Two compound libraries (500 and 18.000 compounds, respectively) were screened for SirT1-modulating activities, and we identified 14 potential inhibitors and 12 potential activators of SirT1. Of the inhibitors, 9 showed inhibition of SirT1-dependent deacetylation of an acetylated p53 peptide. Interestingly, two of them also inhibited SirT2. Both SirT2 inhibitors were also able to inhibit the p53 deacetylation with IC_{50} values comparable to those determined in the MAL deacetylation assay. Moreover, we observed that the first 220 amino acids of the N-terminal region of SirT1 had an influence on the inhibitory effect of one inhibitor identified here. The potential activators failed to enhance the activity of SirT1 to deacetylate the p53 peptide. Surprisingly, one of them showed strong inhibition of SirT1 in this assay (Hill 2012) as well as inhibition of MAL deacetylation by ySir2 and SirT2. Subsequently, we determined the anticancer potential of the inhibitors identified in this study by different *in vivo* experiments with the lung cancer cell lines A549 and H1299. Three compounds that inhibited cell viability and proliferation of these cancer cells in a dose-dependent manner were pursued in more detail. These three inhibitors induced an additional increase of apoptosis after combined treatment with the chemotherapeutic agent etoposide. We observed that the additional increase of apoptosis mediated by one of theses inhibitors was p53-dependent. In summary, this study has led us to identify one SirT1 inhibitor as well as two SirT2 inhibitors that showed antiproliferation potential and can be developed further for cancer therapy.

6. Zusammenfassung

Sirtuine (SirT1-SirT7) sind die human Homologe der NAD^+-abhängigen Histondeacetylase Sir2 aus der Bäckerhefe *Saccharomyces cerevisiae*. Seit der Beobachtung, dass die Überexprimierung von Sir2 in Hefen einen lebensverlängernden Einfluss hat, ist das Interesse an der Erforschung der Sirtuine enorm gewachsen. Jedes Sirtuin besitzt eine konservierte katalytische Domäne von etwa 275 Aminosäuren, sowie N-terminale und/oder C-terminale Sequenzen, die sich in ihrer Länge unterscheiden. Sirtuine sind vielversprechende Ansatzpunkte für die Behandlung zahlreicher Krankheiten, wie zum Beispiel Krebs, Stoffwechselkrankheiten, Diabetes und Alterung. Obwohl bereits einige Sirtuin-Inhibitoren und -Aktivatoren bekannt sind, ist der Mechanismus der Inhibition ungeklärt. Das Ziel der vorliegenden Arbeit war es, neue Sirtuin-Inhibitoren zu identifizieren und deren *in vivo* Potential als Chemotherapeutika zu untersuchen. Dazu wurde ein fluoreszenz-basierter Assay etabliert, bei dem ein Methyl-Aminocoumarin-Acetyllysine (MAL) als Substrat verwendet wurde, der für High-throughput Screening geeignet ist. Für die Identifizierung von SirT1-Modulatoren wurden zwei Bibliotheken (500 und 18.000 Substanzen) gescreent, wobei 14 potentielle Inhibitoren, sowie 12 potentielle Aktivatoren identifiziert wurden. Von diesen Inhibitoren zeigten 9 auch Inhibition von SirT1-abhängiger Deacetylierung eines acetylierten p53-Peptids. Des weiteren konnten zwei dieser Substanzen auch SirT2 inhibieren. Beide SirT2 Inhibitoren waren auch in der Lage, die p53 Deacetylierung zu inhibieren. Weiterhin haben wir beobachtet, dass die ersten 220 Aminosäuren der N-terminalen Region von SirT1 einen Einfluss auf die Wirkung eines Inhibitors, der in dieser Arbeit identifiziert wurde, haben. Die potentiellen Aktivatoren zeigten keine Steigerung der SirT1 Aktivität bei der Deacetylierung des p53-Peptids. Erstaunlicherweise zeigte einer von ihnen starke Inhibition von SirT1 im p53 Deacetylierungs Assay (Hill 2012), sowie des ySir2 aus *S. cerevisiae* und von SirT2 mit MAL als Substrat. Im weiteren wurde das Potential der identifizierten Inhibitoren als Zytostatika mit unterschiedlichen *in vivo* Experimenten unter Verwendung der Lungenkrebszelllinien A549 und H1299 untersucht. Drei von ihnen, die der Lage waren, die Zellvitalität sowie die Zellteilung dosisabhängigen zu inhibieren wurden weiter untersucht. Interessanterweise verursachten sie einen zusätzlichen Anstieg der Apoptose nach kombinierter Behandlung mit dem Chemotherapeutikum Etoposide. Wir konnten zeigen, dass dieser Inhibitor-induzierte zusätzliche Anstieg der Apoptose zum Teil p53 abhängig war. Somit haben wir insgesamt einen SirT1-Inhibitor und zwei SirT2-Inhibitoren identifiziert, die

ein Antiproliferationspotential aufweisen und für Krebstherapien weiterentwickelt werden können.

7. Appendix

In *Saccharomyces cerevisiae* a complex of Sir2, Sir3 and Sir4 are responsible for the formation of heterochromatin-like structure, which repress gene transcription in subtelomeric regions and the mating-type loci (*HMR* and *HML*) (Rusche et al. 2003). Silent chromatin assembles in two steps, nucleation and spreading. The Sir complex nucleates at silencers by associating of Sir3 and Sir4 with silencer-bound proteins such as Abf1, Rap1 and ORC. Spreading of the complex occurs through the Sir2-dependent deacetylation of acetyl groups from histones of adjacent nucleosomes, which creates additional binding sites for Sir3 and Sir4 (Hoppe et al. 2002; Luo et al. 2002; Rusche et al. 2002). The group of M. R. Gartenberg showed that a chimera (Sir3-Sir2$^{243-562}$) containing Sir3 and the deacetylation core domain of Sir2 are able to silenced genes at the telomeres and both mating-type loci in a *sir2*Δ background (Chou et al. 2008). This suggests that the chimera Sir3-Sir2$^{243-562}$ is able to bind at the silencers by Sir3 and spread by the Sir2-dependent deacetylation of histone tails. Furthermore, they generated a chimera (LexA-Sir$^{278-252}$-Hos3$^{2-549}$-Sir2$^{522-562}$) where the catalytic core domain of Sir2 is replaced by the Hos3 domain, a NAD^+-independent deacetylase. They showed that this chimera is also able to silence *HMR* and *HML* in a *sir2*Δ background. These results suggest that the Sir2 N- and C-terminal region are sufficient to target a heterologous deacetylase for function within silent chromatin and that *O*-acetyl-ADP-ribose (OAADPr), which is produced during the NAD^+-dependent deacetylation reaction, are nor required for silencing in yeast (Chou et al. 2008).

For the development of an *in vivo* screen for small modulators of SirT1, we sought to create comparable chimeras of SirT1 with ySir2 or Sir3, similar to those in (Chou et al. 2008). Our rationale was that if such chimeras provide SirT1-dependent silencing in yeast, an *in vivo* silencing assay could be used to screen for SirT1 inhibitors. In a first step, we verified silencing by the chimeric constructs provided by M. R. Gartenberg (Chou et al. 2008). Telomere silencing was measured with a *URA3* reporter gene located at the telomere (TelVII-L), which is expressed when silencing is abrogated. The Ura3 protein metabolizes 5-fluoroorotic acid (5-FOA) to a toxic compound, such than Ura3 cells are unable to growth on 5-FOA-containing media. Similar to the results of the group of Gartenberg, we observed telomeric silencing with the chimera Sir3-Sir2$^{243-562}$ as well as Sir3-Hos3$^{2-549}$, but to a lesser extent. The silencing provided by the chimera LexA-Sir2$^{78-562}$ was comparable with the published results (**Figure 7.1**). We also observed slight silencing effects of the chimera LexA-Sir$^{278-252}$-Hos3$^{2-549}$-Sir2$^{522-562}$, but this effect was not shown by the group of Gartenberg.

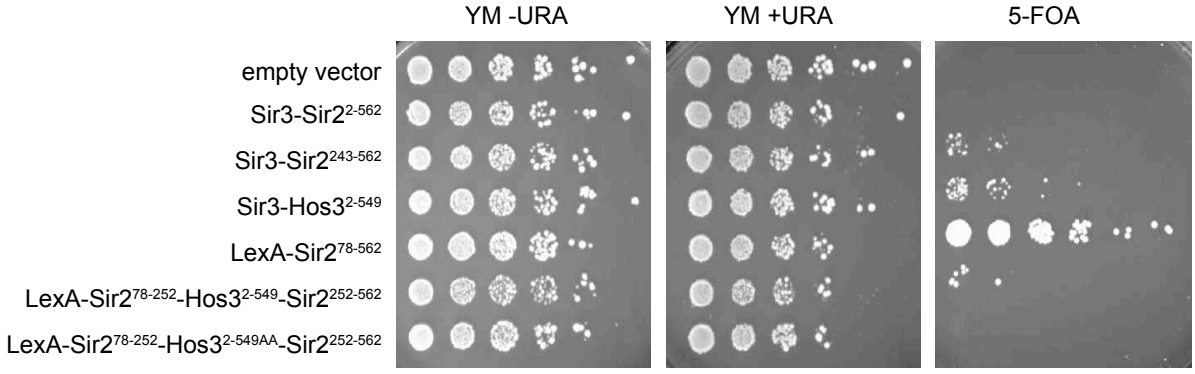

Figure 7.1: Sir2 chimeras induced telomeric silencing
Repression of *URA3* reporter was measured by growth on 5-FOA in strain AEY4017 (*sir2*Δ) transformed with empty vector or the respective plasmids. YM –URA and YM +URA plates provide loading and growth controls.

HMR silencing was measured with a patch-mating assay, where the cells are not able to mate and form diploids with a tester strain of the opposite mating-type when silencing does not occur (described in **3.3.5**). We observed that the chimeras Sir3-Sir2$^{243-562}$, Sir3-Hos3$^{2-549}$ as well as LexA-Sir2$^{78-562}$ are able to silence *HMR,* which was similar to the results of (Chou et al. 2008) (**Figure 7.2**). However, we were not able to observe *HMR* silencing of the LexA-Sir$^{278-252}$-Hos3$^{2-549}$-Sir2$^{522-562}$ chimera, unlike what was published in (Chou et al. 2008). The reason for this discrepancy is unclear. The chimera Sir3-Sir2$^{2-549}$ was also not able to silence the telomeres nor the *HMR* locus. This suggested that only the core domain of Sir2 (243-562) is able to induce silencing when it is attached to Sir3.

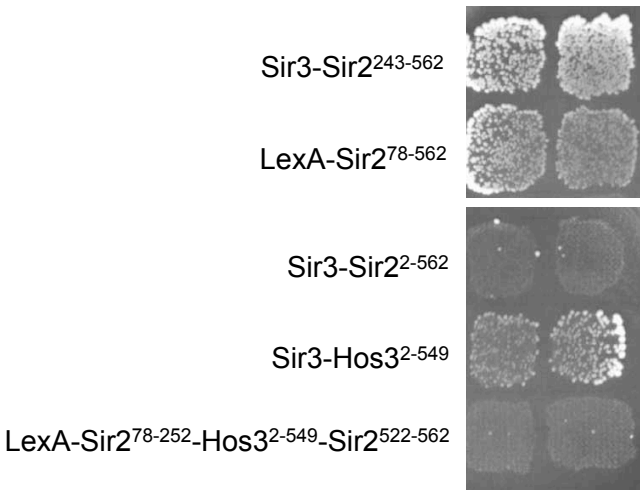

Figure 7.2: Sir2 chimeras induced *HMR* silencing
Patch mating-type assay was performed with the mating-type tester strain *MAT***a** and the yeast strain AEY4017 (*MAT*α, *sir2*Δ). *HMR* silencing was measured by selection of diploids on YM plates.

Based on the result that the chimera Sir3-Sir2$^{243-562}$ is able to silence telomeres as well as *HMR*, we sought create a similar chimera with the core domain of SirT1 in order to develop an *in vivo* screen for SirT1 modulators. For this approach, we cloned the chimeras Sir3-SirT1$^{240-500}$ as well as Sir2$^{1-252}$-SirT1$^{240-500}$-Sir2$^{522-562}$ into a yeast expression vector using

PCR-mediated plasmid gap repair (**Figure 7.3**). The fusions were chosen to be equivalent to those in Chou *et al*.

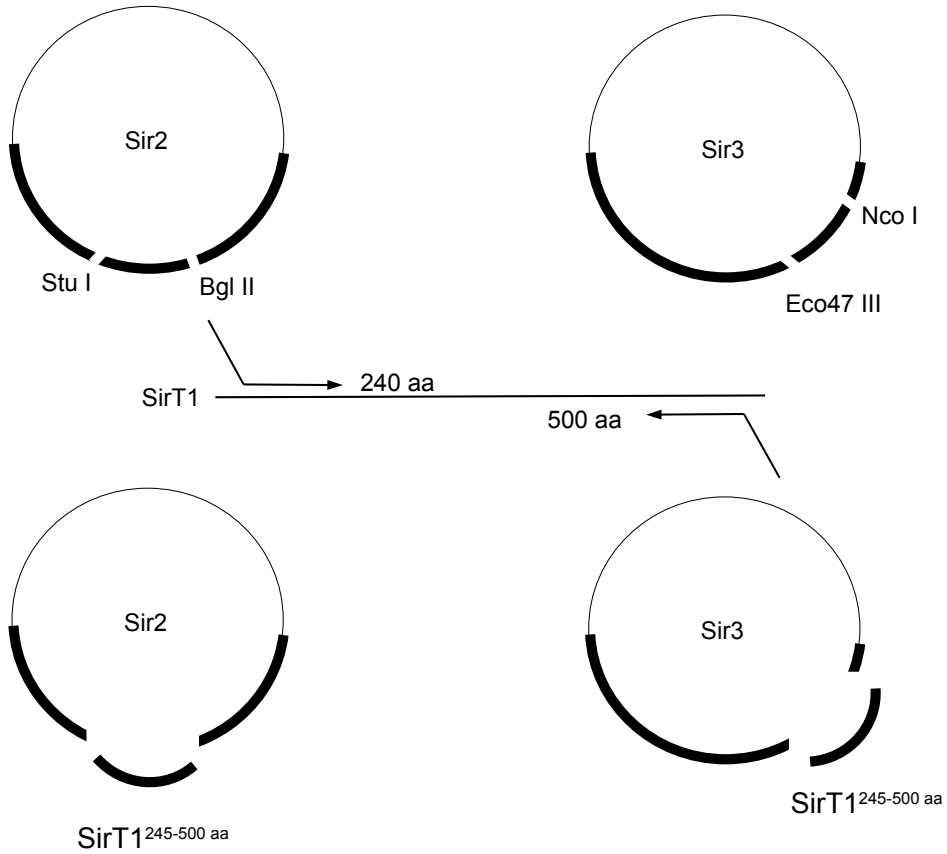

Figure 7.3: Cloning strategies of the SirT1 chimeras
The Sir2 (pAE231) and the Sir3 plasmid (pAE232) were digested by Stu I/Bgl II or by Eco47 II/Nco I. The core domain of SirT1 (244-498 aa) was amplified by PCR. The gene fusion was generated by PCR-mediated plasmid gap repair.

With these two chimeras, we performed telomeric as well as *HMR* silencing to measure the ability of the SirT1 fusion to silence both loci. As shown in **Figure 7.4**, both chimeras were unable to silence at the telomeres in comparison to the positive control, wild-type Sir2, or the chimera LexA-Sir2$^{78\text{-}562}$.

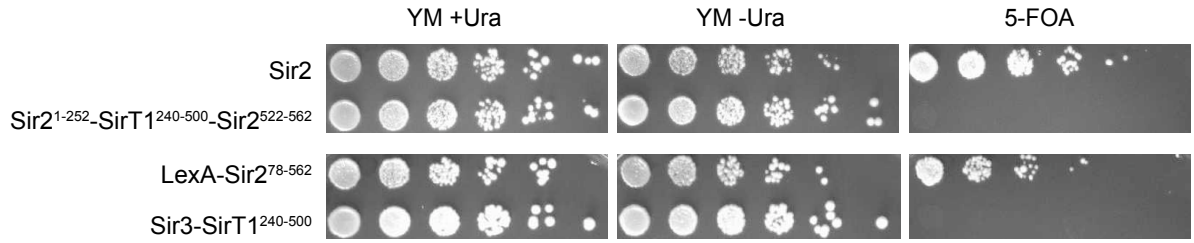

Figure 7.4: SirT1 chimeras did not induce telomeric silencing
Repression of *URA3* reporter was measured by growth on 5-FOA in strain AEY4017 (sir2Δ) transformed with wild-type Sir2 or the respective plasmids. YM –URA and YM +URA plates provide loading and growth controls.

Furthermore, both chimeras are also unable to silence the *HMR* locus (**Figure 7.5**), suggesting that the catalytic core domain of SirT1 is not sufficient to induce silencing at the telomeres or at the *HMR* locus in yeast. For this reason, we were unable to develop an *in vivo* screen for the identification of novel sirtuin modulators based on this approach.

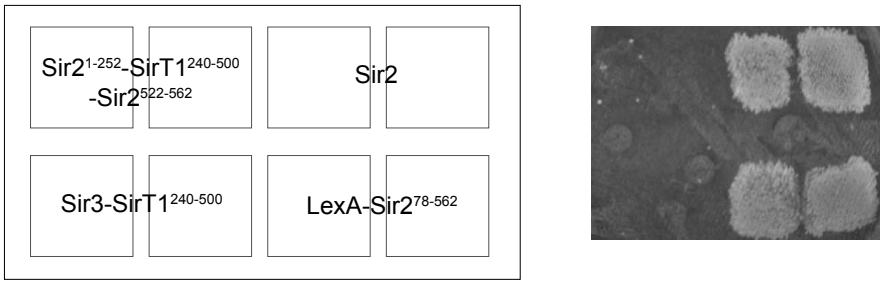

Figure 7.5: SirT1 chimeras did not induce *HMR* silencing
Patch mating-type assay was performed with the mating-type tester strain *MAT***a** and the yeast strain AEY4017 (*MAT*α, *sir2*Δ). *HMR* silencing was measured by growth on YM plates (right side). The chimeras were placed as duplicate onto the agar as indicated by the scheme on the left site. Wild-type Sir2 and the LexA-Sir2$^{78-562}$ were used as positive control.

8. Literature Cited

Ahn BH, Kim HS, Song S, Lee IH, Liu J, Vassilopoulos A, Deng CX, Finkel T. 2008. A role for the mitochondrial deacetylase Sirt3 in regulating energy homeostasis. *Proceedings of the National Academy of Sciences of the United States of America* **105**: 14447-14452.

Ahuja N, Schwer B, Carobbio S, Waltregny D, North BJ, Castronovo V, Maechler P, Verdin E. 2007. Regulation of insulin secretion by SIRT4, a mitochondrial ADP-ribosyltransferase. *The Journal of biological chemistry* **282**: 33583-33592.

Albani D, Polito L, Batelli S, De Mauro S, Fracasso C, Martelli G, Colombo L, Manzoni C, Salmona M, Caccia S et al. 2009. The SIRT1 activator resveratrol protects SK-N-BE cells from oxidative stress and against toxicity caused by alpha-synuclein or amyloid-beta (1-42) peptide. *Journal of neurochemistry* **110**: 1445-1456.

Alcain FJ, Villalba JM. 2009a. Sirtuin activators. *Expert opinion on therapeutic patents* **19**: 403-414.

-. 2009b. Sirtuin inhibitors. *Expert opinion on therapeutic patents* **19**: 283-294.

Anantharaman V, Aravind L. 2008. Analysis of DBC1 and its homologs suggests a potential mechanism for regulation of sirtuin domain deacetylases by NAD metabolites. *Cell Cycle* **7**: 1467-1472.

Anderson RM, Bitterman KJ, Wood JG, Medvedik O, Sinclair DA. 2003. Nicotinamide and PNC1 govern lifespan extension by calorie restriction in Saccharomyces cerevisiae. *Nature* **423**: 181-185.

Asensi M, Medina I, Ortega A, Carretero J, Bano MC, Obrador E, Estrela JM. 2002. Inhibition of cancer growth by resveratrol is related to its low bioavailability. *Free radical biology & medicine* **33**: 387-398.

Avalos JL, Bever KM, Wolberger C. 2005. Mechanism of sirtuin inhibition by nicotinamide: altering the NAD(+) cosubstrate specificity of a Sir2 enzyme. *Molecular cell* **17**: 855-868.

Avalos JL, Boeke JD, Wolberger C. 2004. Structural basis for the mechanism and regulation of Sir2 enzymes. *Molecular cell* **13**: 639-648.

Avalos JL, Celic I, Muhammad S, Cosgrove MS, Boeke JD, Wolberger C. 2002. Structure of a Sir2 enzyme bound to an acetylated p53 peptide. *Molecular cell* **10**: 523-535.

Back JH, Rezvani HR, Zhu Y, Guyonnet-Duperat V, Athar M, Ratner D, Kim AL. 2011. Cancer cell survival following DNA damage-mediated premature senescence is regulated by mammalian target of rapamycin (mTOR)-dependent Inhibition of sirtuin 1. *The Journal of biological chemistry* **286**: 19100-19108.

Bae NS, Swanson MJ, Vassilev A, Howard BH. 2004. Human histone deacetylase SIRT2 interacts with the homeobox transcription factor HOXA10. *Journal of biochemistry* **135**: 695-700.

Balan V, Miller GS, Kaplun L, Balan K, Chong ZZ, Li F, Kaplun A, VanBerkum MF, Arking R, Freeman DC et al. 2008. Life span extension and neuronal cell protection by Drosophila nicotinamidase. *The Journal of biological chemistry* **283**: 27810-27819.

Bao J, Lu Z, Joseph JJ, Carabenciov D, Dimond CC, Pang L, Samsel L, McCoy JP, Jr., Leclerc J, Nguyen P et al. 2010. Characterization of the murine SIRT3 mitochondrial localization sequence and comparison of mitochondrial enrichment and deacetylase activity of long and short SIRT3 isoforms. *Journal of cellular biochemistry* **110**: 238-247.

Barber MF, Michishita-Kioi E, Xi Y, Tasselli L, Kioi M, Moqtaderi Z, Tennen RI, Paredes S, Young NL, Chen K et al. 2012. SIRT7 links H3K18 deacetylation to maintenance of oncogenic transformation. *Nature* **487**: 114-118.

Baur JA, Pearson KJ, Price NL, Jamieson HA, Lerin C, Kalra A, Prabhu VV, Allard JS, Lopez-Lluch G, Lewis K et al. 2006. Resveratrol improves health and survival of mice on a high-calorie diet. *Nature* **444**: 337-342.

Bedalov A, Gatbonton T, Irvine WP, Gottschling DE, Simon JA. 2001. Identification of a small molecule inhibitor of Sir2p. *Proceedings of the National Academy of Sciences of the United States of America* **98**: 15113-15118.

Beher D, Wu J, Cumine S, Kim KW, Lu SC, Atangan L, Wang M. 2009. Resveratrol is not a direct activator of SIRT1 enzyme activity. *Chemical biology & drug design* **74**: 619-624.

Bitterman KJ, Anderson RM, Cohen HY, Latorre-Esteves M, Sinclair DA. 2002. Inhibition of silencing and accelerated aging by nicotinamide, a putative negative regulator of yeast sir2 and human SIRT1. *The Journal of biological chemistry* **277**: 45099-45107.

Bobrowska A, Donmez G, Weiss A, Guarente L, Bates G. 2012. SIRT2 ablation has no effect on tubulin acetylation in brain, cholesterol biosynthesis or the progression of Huntington's disease phenotypes in vivo. *PloS one* **7**: e34805.

Boily G, Seifert EL, Bevilacqua L, He XH, Sabourin G, Estey C, Moffat C, Crawford S, Saliba S, Jardine K et al. 2008. SirT1 regulates energy metabolism and response to caloric restriction in mice. *PloS one* **3**: e1759.

Borra MT, Denu JM. 2004. Quantitative assays for characterization of the Sir2 family of NAD(+)-dependent deacetylases. *Methods in enzymology* **376**: 171-187.

Borra MT, Langer MR, Slama JT, Denu JM. 2004. Substrate specificity and kinetic mechanism of the Sir2 family of NAD+-dependent histone/protein deacetylases. *Biochemistry* **43**: 9877-9887.

Borra MT, O'Neill FJ, Jackson MD, Marshall B, Verdin E, Foltz KR, Denu JM. 2002. Conserved enzymatic production and biological effect of O-acetyl-ADP-ribose by silent information regulator 2-like NAD+-dependent deacetylases. *The Journal of biological chemistry* **277**: 12632-12641.

Bouras T, Fu M, Sauve AA, Wang F, Quong AA, Perkins ND, Hay RT, Gu W, Pestell RG. 2005. SIRT1 deacetylation and repression of p300 involves lysine residues 1020/1024 within the cell cycle regulatory domain 1. *The Journal of biological chemistry* **280**: 10264-10276.

Braunstein M, Rose AB, Holmes SG, Allis CD, Broach JR. 1993. Transcriptional silencing in yeast is associated with reduced nucleosome acetylation. *Genes & development* **7**: 592-604.

Brunet A, Sweeney LB, Sturgill JF, Chua KF, Greer PL, Lin Y, Tran H, Ross SE, Mostoslavsky R, Cohen HY et al. 2004. Stress-dependent regulation of FOXO transcription factors by the SIRT1 deacetylase. *Science* **303**: 2011-2015.

Burnett C, Valentini S, Cabreiro F, Goss M, Somogyvari M, Piper MD, Hoddinott M, Sutphin GL, Leko V, McElwee JJ et al. 2011. Absence of effects of Sir2 overexpression on lifespan in C. elegans and Drosophila. *Nature* **477**: 482-485.

Canto C, Auwerx J. 2008. Glucose restriction: longevity SIRTainly, but without building muscle? *Developmental cell* **14**: 642-644.

-. 2009. PGC-1alpha, SIRT1 and AMPK, an energy sensing network that controls energy expenditure. *Current opinion in lipidology* **20**: 98-105.

Chen J, Zhou Y, Mueller-Steiner S, Chen LF, Kwon H, Yi S, Mucke L, Gan L. 2005. SIRT1 protects against microglia-dependent amyloid-beta toxicity through inhibiting NF-kappaB signaling. *The Journal of biological chemistry* **280**: 40364-40374.

Chen X, Yang L, Zhang N, Turpin JA, Buckheit RW, Osterling C, Oppenheim JJ, Howard OM. 2003. Shikonin, a component of chinese herbal medicine, inhibits chemokine receptor

function and suppresses human immunodeficiency virus type 1. *Antimicrobial agents and chemotherapy* **47**: 2810-2816.

Cheng HL, Mostoslavsky R, Saito S, Manis JP, Gu Y, Patel P, Bronson R, Appella E, Alt FW, Chua KF. 2003. Developmental defects and p53 hyperacetylation in Sir2 homolog (SIRT1)-deficient mice. *Proceedings of the National Academy of Sciences of the United States of America* **100**: 10794-10799.

Chou CC, Li YC, Gartenberg MR. 2008. Bypassing Sir2 and O-acetyl-ADP-ribose in transcriptional silencing. *Molecular cell* **31**: 650-659.

Cockell MM, Perrod S, Gasser SM. 2000. Analysis of Sir2p domains required for rDNA and telomeric silencing in Saccharomyces cerevisiae. *Genetics* **154**: 1069-1083.

Cohen HY, Miller C, Bitterman KJ, Wall NR, Hekking B, Kessler B, Howitz KT, Gorospe M, de Cabo R, Sinclair DA. 2004. Calorie restriction promotes mammalian cell survival by inducing the SIRT1 deacetylase. *Science* **305**: 390-392.

Contreras A, Hale TK, Stenoien DL, Rosen JM, Mancini MA, Herrera RE. 2003. The dynamic mobility of histone H1 is regulated by cyclin/CDK phosphorylation. *Molecular and cellular biology* **23**: 8626-8636.

Crujeiras AB, Parra D, Goyenechea E, Martinez JA. 2008. Sirtuin gene expression in human mononuclear cells is modulated by caloric restriction. *European journal of clinical investigation* **38**: 672-678.

Csiszar A, Labinskyy N, Podlutsky A, Kaminski PM, Wolin MS, Zhang C, Mukhopadhyay P, Pacher P, Hu F, de Cabo R et al. 2008. Vasoprotective effects of resveratrol and SIRT1: attenuation of cigarette smoke-induced oxidative stress and proinflammatory phenotypic alterations. *American journal of physiology Heart and circulatory physiology* **294**: H2721-2735.

Cuperus G, Shafaatian R, Shore D. 2000. Locus specificity determinants in the multifunctional yeast silencing protein Sir2. *The EMBO journal* **19**: 2641-2651.

Dephoure N, Zhou C, Villen J, Beausoleil SA, Bakalarski CE, Elledge SJ, Gygi SP. 2008. A quantitative atlas of mitotic phosphorylation. *Proceedings of the National Academy of Sciences of the United States of America* **105**: 10762-10767.

Dryden SC, Nahhas FA, Nowak JE, Goustin AS, Tainsky MA. 2003. Role for human SIRT2 NAD-dependent deacetylase activity in control of mitotic exit in the cell cycle. *Molecular and cellular biology* **23**: 3173-3185.

Du J, Zhou Y, Su X, Yu JJ, Khan S, Jiang H, Kim J, Woo J, Kim JH, Choi BH et al. 2011. Sirt5 is a NAD-dependent protein lysine demalonylase and desuccinylase. *Science* **334**: 806-809.

El Mohsen MA, Marks J, Kuhnle G, Moore K, Debnam E, Kaila Srai S, Rice-Evans C, Spencer JP. 2006. Absorption, tissue distribution and excretion of pelargonidin and its metabolites following oral administration to rats. *The British journal of nutrition* **95**: 51-58.

Finnin MS, Donigian JR, Pavletich NP. 2001. Structure of the histone deacetylase SIRT2. *Nature structural biology* **8**: 621-625.

Flick F, Luscher B. 2012. Regulation of sirtuin function by posttranslational modifications. *Frontiers in pharmacology* **3**: 29.

Ford E, Voit R, Liszt G, Magin C, Grummt I, Guarente L. 2006. Mammalian Sir2 homolog SIRT7 is an activator of RNA polymerase I transcription. *Genes & development* **20**: 1075-1080.

Ford J, Jiang M, Milner J. 2005. Cancer-specific functions of SIRT1 enable human epithelial cancer cell growth and survival. *Cancer research* **65**: 10457-10463.

Fraga MF, Esteller M. 2007. Epigenetics and aging: the targets and the marks. *Trends in genetics : TIG* **23**: 413-418.

Frye RA. 1999. Characterization of five human cDNAs with homology to the yeast SIR2 gene: Sir2-like proteins (sirtuins) metabolize NAD and may have protein ADP-ribosyltransferase activity. *Biochemical and biophysical research communications* **260**: 273-279.

-. 2000. Phylogenetic classification of prokaryotic and eukaryotic Sir2-like proteins. *Biochemical and biophysical research communications* **273**: 793-798.

Gagliardi AR, Taylor MF, Collins DC. 1998. Uptake of suramin by human microvascular endothelial cells. *Cancer letters* **125**: 97-102.

Gallo CM, Smith DL, Jr., Smith JS. 2004. Nicotinamide clearance by Pnc1 directly regulates Sir2-mediated silencing and longevity. *Molecular and cellular biology* **24**: 1301-1312.

Garcia-Salcedo JA, Gijon P, Nolan DP, Tebabi P, Pays E. 2003. A chromosomal SIR2 homologue with both histone NAD-dependent ADP-ribosyltransferase and deacetylase activities is involved in DNA repair in Trypanosoma brucei. *The EMBO journal* **22**: 5851-5862.

Gelb DJ, Oliver E, Gilman S. 1999. Diagnostic criteria for Parkinson disease. *Archives of neurology* **56**: 33-39.

Greer EL, Dowlatshahi D, Banko MR, Villen J, Hoang K, Blanchard D, Gygi SP, Brunet A. 2007. An AMPK-FOXO pathway mediates longevity induced by a novel method of dietary restriction in C. elegans. *Current biology : CB* **17**: 1646-1656.

Grob A, Roussel P, Wright JE, McStay B, Hernandez-Verdun D, Sirri V. 2009. Involvement of SIRT7 in resumption of rDNA transcription at the exit from mitosis. *Journal of cell science* **122**: 489-498.

Grozinger CM, Chao ED, Blackwell HE, Moazed D, Schreiber SL. 2001. Identification of a class of small molecule inhibitors of the sirtuin family of NAD-dependent deacetylases by phenotypic screening. *The Journal of biological chemistry* **276**: 38837-38843.

Grubisha O, Rafty LA, Takanishi CL, Xu X, Tong L, Perraud AL, Scharenberg AM, Denu JM. 2006. Metabolite of SIR2 reaction modulates TRPM2 ion channel. *The Journal of biological chemistry* **281**: 14057-14065.

Gschwendt M, Muller HJ, Kielbassa K, Zang R, Kittstein W, Rincke G, Marks F. 1994. Rottlerin, a novel protein kinase inhibitor. *Biochemical and biophysical research communications* **199**: 93-98.

Guarente L, Kenyon C. 2000. Genetic pathways that regulate ageing in model organisms. *Nature* **408**: 255-262.

Guarente L, Picard F. 2005. Calorie restriction--the SIR2 connection. *Cell* **120**: 473-482.

Haigis MC, Mostoslavsky R, Haigis KM, Fahie K, Christodoulou DC, Murphy AJ, Valenzuela DM, Yancopoulos GD, Karow M, Blander G et al. 2006. SIRT4 inhibits glutamate dehydrogenase and opposes the effects of calorie restriction in pancreatic beta cells. *Cell* **126**: 941-954.

Haigis MC, Sinclair DA. 2010. Mammalian sirtuins: biological insights and disease relevance. *Annual review of pathology* **5**: 253-295.

Hajji N, Wallenborg K, Vlachos P, Fullgrabe J, Hermanson O, Joseph B. 2010. Opposing effects of hMOF and SIRT1 on H4K16 acetylation and the sensitivity to the topoisomerase II inhibitor etoposide. *Oncogene* **29**: 2192-2204.

Hallows WC, Lee S, Denu JM. 2006. Sirtuins deacetylate and activate mammalian acetyl-CoA synthetases. *Proceedings of the National Academy of Sciences of the United States of America* **103**: 10230-10235.

Hamaguchi M, Meth JL, von Klitzing C, Wei W, Esposito D, Rodgers L, Walsh T, Welcsh P, King MC, Wigler MH. 2002. DBC2, a candidate for a tumor suppressor gene involved in

breast cancer. *Proceedings of the National Academy of Sciences of the United States of America* **99**: 13647-13652.

Han Y, Jin YH, Kim YJ, Kang BY, Choi HJ, Kim DW, Yeo CY, Lee KY. 2008. Acetylation of Sirt2 by p300 attenuates its deacetylase activity. *Biochemical and biophysical research communications* **375**: 576-580.

Hande KR. 1998. Etoposide: four decades of development of a topoisomerase II inhibitor. *Eur J Cancer* **34**: 1514-1521.

Heltweg B, Dequiedt F, Verdin E, Jung M. 2003. Nonisotopic substrate for assaying both human zinc and NAD+-dependent histone deacetylases. *Analytical biochemistry* **319**: 42-48.

Heltweg B, Gatbonton T, Schuler AD, Posakony J, Li H, Goehle S, Kollipara R, Depinho RA, Gu Y, Simon JA et al. 2006. Antitumor activity of a small-molecule inhibitor of human silent information regulator 2 enzymes. *Cancer research* **66**: 4368-4377.

Heltweg B, Jung M. 2003. A homogeneous nonisotopic histone deacetylase activity assay. *Journal of biomolecular screening* **8**: 89-95.

Hendrie HC, Ogunniyi A, Hall KS, Baiyewu O, Unverzagt FW, Gureje O, Gao S, Evans RM, Ogunseyinde AO, Adeyinka AO et al. 2001. Incidence of dementia and Alzheimer disease in 2 communities: Yoruba residing in Ibadan, Nigeria, and African Americans residing in Indianapolis, Indiana. *JAMA : the journal of the American Medical Association* **285**: 739-747.

Hirao M, Posakony J, Nelson M, Hruby H, Jung M, Simon JA, Bedalov A. 2003. Identification of selective inhibitors of NAD+-dependent deacetylases using phenotypic screens in yeast. *The Journal of biological chemistry* **278**: 52773-52782.

Hirschey MD, Shimazu T, Goetzman E, Jing E, Schwer B, Lombard DB, Grueter CA, Harris C, Biddinger S, Ilkayeva OR et al. 2010. SIRT3 regulates mitochondrial fatty-acid oxidation by reversible enzyme deacetylation. *Nature* **464**: 121-125.

Hoffmann K, Brosch G, Loidl P, Jung M. 1999. A non-isotopic assay for histone deacetylase activity. *Nucleic acids research* **27**: 2057-2058.

Hoppe GJ, Tanny JC, Rudner AD, Gerber SA, Danaie S, Gygi SP, Moazed D. 2002. Steps in assembly of silent chromatin in yeast: Sir3-independent binding of a Sir2/Sir4 complex to silencers and role for Sir2-dependent deacetylation. *Molecular and cellular biology* **22**: 4167-4180.

Howitz KT, Bitterman KJ, Cohen HY, Lamming DW, Lavu S, Wood JG, Zipkin RE, Chung P, Kisielewski A, Zhang LL et al. 2003. Small molecule activators of sirtuins extend Saccharomyces cerevisiae lifespan. *Nature* **425**: 191-196.

Huang J, Gan Q, Han L, Li J, Zhang H, Sun Y, Zhang Z, Tong T. 2008. SIRT1 overexpression antagonizes cellular senescence with activated ERK/S6k1 signaling in human diploid fibroblasts. *PloS one* **3**: e1710.

Imai S, Armstrong CM, Kaeberlein M, Guarente L. 2000. Transcriptional silencing and longevity protein Sir2 is an NAD-dependent histone deacetylase. *Nature* **403**: 795-800.

Inoue T, Hiratsuka M, Osaki M, Oshimura M. 2007. The molecular biology of mammalian SIRT proteins: SIRT2 in cell cycle regulation. *Cell Cycle* **6**: 1011-1018.

Jackson MD, Denu JM. 2002. Structural identification of 2'- and 3'-O-acetyl-ADP-ribose as novel metabolites derived from the Sir2 family of beta -NAD+-dependent histone/protein deacetylases. *The Journal of biological chemistry* **277**: 18535-18544.

Jenuwein T, Allis CD. 2001. Translating the histone code. *Science* **293**: 1074-1080.

Jiang W, Wang S, Xiao M, Lin Y, Zhou L, Lei Q, Xiong Y, Guan KL, Zhao S. 2011. Acetylation regulates gluconeogenesis by promoting PEPCK1 degradation via recruiting the UBR5 ubiquitin ligase. *Molecular cell* **43**: 33-44.

Jin L, Galonek H, Israelian K, Choy W, Morrison M, Xia Y, Wang X, Xu Y, Yang Y, Smith JJ et al. 2009. Biochemical characterization, localization, and tissue distribution of the longer form of mouse SIRT3. *Protein science : a publication of the Protein Society* **18**: 514-525.

Kaeberlein M, Kirkland KT, Fields S, Kennedy BK. 2004. Sir2-independent life span extension by calorie restriction in yeast. *PLoS biology* **2**: E296.

Kaeberlein M, McDonagh T, Heltweg B, Hixon J, Westman EA, Caldwell SD, Napper A, Curtis R, DiStefano PS, Fields S et al. 2005. Substrate-specific activation of sirtuins by resveratrol. *The Journal of biological chemistry* **280**: 17038-17045.

Kaeberlein M, McVey M, Guarente L. 1999. The SIR2/3/4 complex and SIR2 alone promote longevity in Saccharomyces cerevisiae by two different mechanisms. *Genes & development* **13**: 2570-2580.

Kamakaka RT, Rine J. 1998. Sir- and silencer-independent disruption of silencing in Saccharomyces by Sas10p. *Genetics* **149**: 903-914.

Kang H, Jung JW, Kim MK, Chung JH. 2009. CK2 is the regulator of SIRT1 substrate-binding affinity, deacetylase activity and cellular response to DNA-damage. *PloS one* **4**: e6611.

Kang H, Suh JY, Jung YS, Jung JW, Kim MK, Chung JH. 2011. Peptide switch is essential for Sirt1 deacetylase activity. *Molecular cell* **44**: 203-213.

Kawahara TL, Michishita E, Adler AS, Damian M, Berber E, Lin M, McCord RA, Ongaigui KC, Boxer LD, Chang HY et al. 2009. SIRT6 links histone H3 lysine 9 deacetylation to NF-kappaB-dependent gene expression and organismal life span. *Cell* **136**: 62-74.

Kawahara TL, Rapicavoli NA, Wu AR, Qu K, Quake SR, Chang HY. 2011. Dynamic chromatin localization of Sirt6 shapes stress- and aging-related transcriptional networks. *PLoS genetics* **7**: e1002153.

Kim D, Nguyen MD, Dobbin MM, Fischer A, Sananbenesi F, Rodgers JT, Delalle I, Baur JA, Sui G, Armour SM et al. 2007a. SIRT1 deacetylase protects against neurodegeneration in models for Alzheimer's disease and amyotrophic lateral sclerosis. *The EMBO journal* **26**: 3169-3179.

Kim EJ, Kho JH, Kang MR, Um SJ. 2007b. Active regulator of SIRT1 cooperates with SIRT1 and facilitates suppression of p53 activity. *Molecular cell* **28**: 277-290.

Kim HS, Patel K, Muldoon-Jacobs K, Bisht KS, Aykin-Burns N, Pennington JD, van der Meer R, Nguyen P, Savage J, Owens KM et al. 2010. SIRT3 is a mitochondria-localized tumor suppressor required for maintenance of mitochondrial integrity and metabolism during stress. *Cancer cell* **17**: 41-52.

Kim HS, Vassilopoulos A, Wang RH, Lahusen T, Xiao Z, Xu X, Li C, Veenstra TD, Li B, Yu H et al. 2011. SIRT2 maintains genome integrity and suppresses tumorigenesis through regulating APC/C activity. *Cancer cell* **20**: 487-499.

Kim JE, Chen J, Lou Z. 2008. DBC1 is a negative regulator of SIRT1. *Nature* **451**: 583-586.

Kojima K, Ohhashi R, Fujita Y, Hamada N, Akao Y, Nozawa Y, Deguchi T, Ito M. 2008. A role for SIRT1 in cell growth and chemoresistance in prostate cancer PC3 and DU145 cells. *Biochemical and biophysical research communications* **373**: 423-428.

Kolle D, Brosch G, Lechner T, Lusser A, Loidl P. 1998. Biochemical methods for analysis of histone deacetylases. *Methods* **15**: 323-331.

Kornberg MD, Sen N, Hara MR, Juluri KR, Nguyen JV, Snowman AM, Law L, Hester LD, Snyder SH. 2010. GAPDH mediates nitrosylation of nuclear proteins. *Nature cell biology* **12**: 1094-1100.

Kornberg RD. 1974. Chromatin structure: a repeating unit of histones and DNA. *Science* **184**: 868-871.

Kustatscher G, Hothorn M, Pugieux C, Scheffzek K, Ladurner AG. 2005. Splicing regulates NAD metabolite binding to histone macroH2A. *Nature structural & molecular biology* **12**: 624-625.

Lagouge M, Argmann C, Gerhart-Hines Z, Meziane H, Lerin C, Daussin F, Messadeq N, Milne J, Lambert P, Elliott P et al. 2006. Resveratrol improves mitochondrial function and protects against metabolic disease by activating SIRT1 and PGC-1alpha. *Cell* **127**: 1109-1122.

Lain S, Hollick JJ, Campbell J, Staples OD, Higgins M, Aoubala M, McCarthy A, Appleyard V, Murray KE, Baker L et al. 2008. Discovery, in vivo activity, and mechanism of action of a small-molecule p53 activator. *Cancer cell* **13**: 454-463.

Lamming DW, Latorre-Esteves M, Medvedik O, Wong SN, Tsang FA, Wang C, Lin SJ, Sinclair DA. 2005. HST2 mediates SIR2-independent life-span extension by calorie restriction. *Science* **309**: 1861-1864.

Landry J, Sutton A, Tafrov ST, Heller RC, Stebbins J, Pillus L, Sternglanz R. 2000. The silencing protein SIR2 and its homologs are NAD-dependent protein deacetylases. *Proceedings of the National Academy of Sciences of the United States of America* **97**: 5807-5811.

Lara E, Mai A, Calvanese V, Altucci L, Lopez-Nieva P, Martinez-Chantar ML, Varela-Rey M, Rotili D, Nebbioso A, Ropero S et al. 2009. Salermide, a Sirtuin inhibitor with a strong cancer-specific proapoptotic effect. *Oncogene* **28**: 781-791.

Lee DS, Lee SH, Noh JG, Hong SD. 1999. Antibacterial activities of cryptotanshinone and dihydrotanshinone I from a medicinal herb, Salvia miltiorrhiza Bunge. *Bioscience, biotechnology, and biochemistry* **63**: 2236-2239.

Lee S, Tong L, Denu JM. 2008. Quantification of endogenous sirtuin metabolite O-acetyl-ADP-ribose. *Analytical biochemistry* **383**: 174-179.

Levine AJ. 1997. p53, the cellular gatekeeper for growth and division. *Cell* **88**: 323-331.

Li K, Luo J. 2011. The role of SIRT1 in tumorigenesis. *North American journal of medicine & science* **4**: 104-106.

Li Y, Matsumori H, Nakayama Y, Osaki M, Kojima H, Kurimasa A, Ito H, Mori S, Katoh M, Oshimura M et al. 2011. SIRT2 down-regulation in HeLa can induce p53 accumulation via p38 MAPK activation-dependent p300 decrease, eventually leading to apoptosis. *Genes to cells : devoted to molecular & cellular mechanisms* **16**: 34-45.

Lim CS. 2006. SIRT1: tumor promoter or tumor suppressor? *Medical hypotheses* **67**: 341-344.

Lin SJ, Defossez PA, Guarente L. 2000. Requirement of NAD and SIR2 for life-span extension by calorie restriction in Saccharomyces cerevisiae. *Science* **289**: 2126-2128.

Liszt G, Ford E, Kurtev M, Guarente L. 2005. Mouse Sir2 homolog SIRT6 is a nuclear ADP-ribosyltransferase. *The Journal of biological chemistry* **280**: 21313-21320.

Littlewood TD, Hancock DC, Danielian PS, Parker MG, Evan GI. 1995. A modified oestrogen receptor ligand-binding domain as an improved switch for the regulation of heterologous proteins. *Nucleic acids research* **23**: 1686-1690.

Liu X, Wang D, Zhao Y, Tu B, Zheng Z, Wang L, Wang H, Gu W, Roeder RG, Zhu WG. 2011. Methyltransferase Set7/9 regulates p53 activity by interacting with Sirtuin 1 (SIRT1). *Proceedings of the National Academy of Sciences of the United States of America* **108**: 1925-1930.

Liu Y, Gerber R, Wu J, Tsuruda T, McCarter JD. 2008. High-throughput assays for sirtuin enzymes: a microfluidic mobility shift assay and a bioluminescence assay. *Analytical biochemistry* **378**: 53-59.

Lombard DB, Alt FW, Cheng HL, Bunkenborg J, Streeper RS, Mostoslavsky R, Kim J, Yancopoulos G, Valenzuela D, Murphy A et al. 2007. Mammalian Sir2 homolog SIRT3

regulates global mitochondrial lysine acetylation. *Molecular and cellular biology* **27**: 8807-8814.

Longo VD, Kennedy BK. 2006. Sirtuins in aging and age-related disease. *Cell* **126**: 257-268.

Luchsinger JA, Tang MX, Shea S, Mayeux R. 2002. Caloric intake and the risk of Alzheimer disease. *Archives of neurology* **59**: 1258-1263.

Luger K, Mader AW, Richmond RK, Sargent DF, Richmond TJ. 1997. Crystal structure of the nucleosome core particle at 2.8 A resolution. *Nature* **389**: 251-260.

Luo J, Nikolaev AY, Imai S, Chen D, Su F, Shiloh A, Guarente L, Gu W. 2001. Negative control of p53 by Sir2alpha promotes cell survival under stress. *Cell* **107**: 137-148.

Luo K, Vega-Palas MA, Grunstein M. 2002. Rap1-Sir4 binding independent of other Sir, yKu, or histone interactions initiates the assembly of telomeric heterochromatin in yeast. *Genes & development* **16**: 1528-1539.

Mai A, Massa S, Lavu S, Pezzi R, Simeoni S, Ragno R, Mariotti FR, Chiani F, Camilloni G, Sinclair DA. 2005. Design, synthesis, and biological evaluation of sirtinol analogues as class III histone/protein deacetylase (Sirtuin) inhibitors. *Journal of medicinal chemistry* **48**: 7789-7795.

Manuyakorn A, Paulus R, Farrell J, Dawson NA, Tze S, Cheung-Lau G, Hines OJ, Reber H, Seligson DB, Horvath S et al. 2010. Cellular histone modification patterns predict prognosis and treatment response in resectable pancreatic adenocarcinoma: results from RTOG 9704. *Journal of clinical oncology : official journal of the American Society of Clinical Oncology* **28**: 1358-1365.

Marcotte PA, Richardson PL, Guo J, Barrett LW, Xu N, Gunasekera A, Glaser KB. 2004. Fluorescence assay of SIRT protein deacetylases using an acetylated peptide substrate and a secondary trypsin reaction. *Analytical biochemistry* **332**: 90-99.

Matsushita N, Yonashiro R, Ogata Y, Sugiura A, Nagashima S, Fukuda T, Inatome R, Yanagi S. 2011. Distinct regulation of mitochondrial localization and stability of two human Sirt5 isoforms. *Genes to cells : devoted to molecular & cellular mechanisms* **16**: 190-202.

Mattson MP. 2003. Will caloric restriction and folate protect against AD and PD? *Neurology* **60**: 690-695.

Mattson MP, Duan W, Guo Z. 2003. Meal size and frequency affect neuronal plasticity and vulnerability to disease: cellular and molecular mechanisms. *Journal of neurochemistry* **84**: 417-431.

McCord RA, Michishita E, Hong T, Berber E, Boxer LD, Kusumoto R, Guan S, Shi X, Gozani O, Burlingame AL et al. 2009. SIRT6 stabilizes DNA-dependent protein kinase at chromatin for DNA double-strand break repair. *Aging* **1**: 109-121.

McGuinness D, McGuinness DH, McCaul JA, Shiels PG. 2011. Sirtuins, bioageing, and cancer. *Journal of aging research* **2011**: 235754.

Michishita E, McCord RA, Berber E, Kioi M, Padilla-Nash H, Damian M, Cheung P, Kusumoto R, Kawahara TL, Barrett JC et al. 2008. SIRT6 is a histone H3 lysine 9 deacetylase that modulates telomeric chromatin. *Nature* **452**: 492-496.

Michishita E, Park JY, Burneskis JM, Barrett JC, Horikawa I. 2005. Evolutionarily conserved and nonconserved cellular localizations and functions of human SIRT proteins. *Molecular biology of the cell* **16**: 4623-4635.

Milne JC, Denu JM. 2008. The Sirtuin family: therapeutic targets to treat diseases of aging. *Current opinion in chemical biology* **12**: 11-17.

Milne JC, Lambert PD, Schenk S, Carney DP, Smith JJ, Gagne DJ, Jin L, Boss O, Perni RB, Vu CB et al. 2007. Small molecule activators of SIRT1 as therapeutics for the treatment of type 2 diabetes. *Nature* **450**: 712-716.

Min J, Landry J, Sternglanz R, Xu RM. 2001. Crystal structure of a SIR2 homolog-NAD complex. *Cell* **105**: 269-279.

Nahhas F, Dryden SC, Abrams J, Tainsky MA. 2007. Mutations in SIRT2 deacetylase which regulate enzymatic activity but not its interaction with HDAC6 and tubulin. *Molecular and cellular biochemistry* **303**: 221-230.

Nakagawa T, Lomb DJ, Haigis MC, Guarente L. 2009. SIRT5 Deacetylates carbamoyl phosphate synthetase 1 and regulates the urea cycle. *Cell* **137**: 560-570.

Nakamura Y, Ogura M, Tanaka D, Inagaki N. 2008. Localization of mouse mitochondrial SIRT proteins: shift of SIRT3 to nucleus by co-expression with SIRT5. *Biochemical and biophysical research communications* **366**: 174-179.

Napper AD, Hixon J, McDonagh T, Keavey K, Pons JF, Barker J, Yau WT, Amouzegh P, Flegg A, Hamelin E et al. 2005. Discovery of indoles as potent and selective inhibitors of the deacetylase SIRT1. *Journal of medicinal chemistry* **48**: 8045-8054.

Nare B, Allocco JJ, Kuningas R, Galuska S, Myers RW, Bednarek MA, Schmatz DM. 1999. Development of a scintillation proximity assay for histone deacetylase using a biotinylated peptide derived from histone-H4. *Analytical biochemistry* **267**: 390-396.

Nasrin N, Kaushik VK, Fortier E, Wall D, Pearson KJ, de Cabo R, Bordone L. 2009. JNK1 phosphorylates SIRT1 and promotes its enzymatic activity. *PloS one* **4**: e8414.

Nathan D, Ingvarsdottir K, Sterner DE, Bylebyl GR, Dokmanovic M, Dorsey JA, Whelan KA, Krsmanovic M, Lane WS, Meluh PB et al. 2006. Histone sumoylation is a negative regulator in Saccharomyces cerevisiae and shows dynamic interplay with positive-acting histone modifications. *Genes & development* **20**: 966-976.

Neugebauer RC, Uchiechowska U, Meier R, Hruby H, Valkov V, Verdin E, Sippl W, Jung M. 2008. Structure-activity studies on splitomicin derivatives as sirtuin inhibitors and computational prediction of binding mode. *Journal of medicinal chemistry* **51**: 1203-1213.

North BJ, Marshall BL, Borra MT, Denu JM, Verdin E. 2003. The human Sir2 ortholog, SIRT2, is an NAD+-dependent tubulin deacetylase. *Molecular cell* **11**: 437-444.

North BJ, Verdin E. 2007. Interphase nucleo-cytoplasmic shuttling and localization of SIRT2 during mitosis. *PloS one* **2**: e784.

Oberdoerffer P, Michan S, McVay M, Mostoslavsky R, Vann J, Park SK, Hartlerode A, Stegmuller J, Hafner A, Loerch P et al. 2008. SIRT1 redistribution on chromatin promotes genomic stability but alters gene expression during aging. *Cell* **135**: 907-918.

Ogura M, Nakamura Y, Tanaka D, Zhuang X, Fujita Y, Obara A, Hamasaki A, Hosokawa M, Inagaki N. 2010. Overexpression of SIRT5 confirms its involvement in deacetylation and activation of carbamoyl phosphate synthetase 1. *Biochemical and biophysical research communications* **393**: 73-78.

Olsen JV, Vermeulen M, Santamaria A, Kumar C, Miller ML, Jensen LJ, Gnad F, Cox J, Jensen TS, Nigg EA et al. 2010. Quantitative phosphoproteomics reveals widespread full phosphorylation site occupancy during mitosis. *Science signaling* **3**: ra3.

Onyango P, Celic I, McCaffery JM, Boeke JD, Feinberg AP. 2002. SIRT3, a human SIR2 homologue, is an NAD-dependent deacetylase localized to mitochondria. *Proceedings of the National Academy of Sciences of the United States of America* **99**: 13653-13658.

Ota H, Tokunaga E, Chang K, Hikasa M, Iijima K, Eto M, Kozaki K, Akishita M, Ouchi Y, Kaneki M. 2006. Sirt1 inhibitor, Sirtinol, induces senescence-like growth arrest with attenuated Ras-MAPK signaling in human cancer cells. *Oncogene* **25**: 176-185.

Outeiro TF, Kontopoulos E, Altmann SM, Kufareva I, Strathearn KE, Amore AM, Volk CB, Maxwell MM, Rochet JC, McLean PJ et al. 2007. Sirtuin 2 inhibitors rescue alpha-synuclein-mediated toxicity in models of Parkinson's disease. *Science* **317**: 516-519.

Pacholec M, Bleasdale JE, Chrunyk B, Cunningham D, Flynn D, Garofalo RS, Griffith D, Griffor M, Loulakis P, Pabst B et al. 2010. SRT1720, SRT2183, SRT1460, and resveratrol are not direct activators of SIRT1. *The Journal of biological chemistry* **285**: 8340-8351.

Pagans S, Pedal A, North BJ, Kaehlcke K, Marshall BL, Dorr A, Hetzer-Egger C, Henklein P, Frye R, McBurney MW et al. 2005. SIRT1 regulates HIV transcription via Tat deacetylation. *PLoS biology* **3**: e41.

Pan M, Yuan H, Brent M, Ding EC, Marmorstein R. 2012. SIRT1 contains N- and C-terminal regions that potentiate deacetylase activity. *The Journal of biological chemistry* **287**: 2468-2476.

Pandithage R, Lilischkis R, Harting K, Wolf A, Jedamzik B, Luscher-Firzlaff J, Vervoorts J, Lasonder E, Kremmer E, Knoll B et al. 2008. The regulation of SIRT2 function by cyclin-dependent kinases affects cell motility. *The Journal of cell biology* **180**: 915-929.

Patel NV, Gordon MN, Connor KE, Good RA, Engelman RW, Mason J, Morgan DG, Morgan TE, Finch CE. 2005. Caloric restriction attenuates Abeta-deposition in Alzheimer transgenic models. *Neurobiology of aging* **26**: 995-1000.

Peck B, Chen CY, Ho KK, Di Fruscia P, Myatt SS, Coombes RC, Fuchter MJ, Hsiao CD, Lam EW. 2010. SIRT inhibitors induce cell death and p53 acetylation through targeting both SIRT1 and SIRT2. *Molecular cancer therapeutics* **9**: 844-855.

Peltier AC, Russell JW. 2002. Recent advances in drug-induced neuropathies. *Current opinion in neurology* **15**: 633-638.

Perabo FG, Muller SC. 2005. New agents in intravesical chemotherapy of superficial bladder cancer. *Scandinavian journal of urology and nephrology* **39**: 108-116.

Perrod S, Cockell MM, Laroche T, Renauld H, Ducrest AL, Bonnard C, Gasser SM. 2001. A cytosolic NAD-dependent deacetylase, Hst2p, can modulate nucleolar and telomeric silencing in yeast. *The EMBO journal* **20**: 197-209.

Pfluger PT, Herranz D, Velasco-Miguel S, Serrano M, Tschop MH. 2008. Sirt1 protects against high-fat diet-induced metabolic damage. *Proceedings of the National Academy of Sciences of the United States of America* **105**: 9793-9798.

Piperno G, LeDizet M, Chang XJ. 1987. Microtubules containing acetylated alpha-tubulin in mammalian cells in culture. *The Journal of cell biology* **104**: 289-302.

Posakony J, Hirao M, Stevens S, Simon JA, Bedalov A. 2004. Inhibitors of Sir2: evaluation of splitomicin analogues. *Journal of medicinal chemistry* **47**: 2635-2644.

Prives C, Hall PA. 1999. The p53 pathway. *The Journal of pathology* **187**: 112-126.

Qiu X, Brown K, Hirschey MD, Verdin E, Chen D. 2010. Calorie restriction reduces oxidative stress by SIRT3-mediated SOD2 activation. *Cell metabolism* **12**: 662-667.

Revollo JR, Grimm AA, Imai S. 2004. The NAD biosynthesis pathway mediated by nicotinamide phosphoribosyltransferase regulates Sir2 activity in mammalian cells. *The Journal of biological chemistry* **279**: 50754-50763.

Rine J, Herskowitz I. 1987. Four genes responsible for a position effect on expression from HML and HMR in Saccharomyces cerevisiae. *Genetics* **116**: 9-22.

Robson SJ, Burgoyne RD. 1989. Differential localisation of tyrosinated, detyrosinated, and acetylated alpha-tubulins in neurites and growth cones of dorsal root ganglion neurons. *Cell motility and the cytoskeleton* **12**: 273-282.

Rodgers JT, Lerin C, Haas W, Gygi SP, Spiegelman BM, Puigserver P. 2005. Nutrient control of glucose homeostasis through a complex of PGC-1alpha and SIRT1. *Nature* **434**: 113-118.

Rogina B, Helfand SL. 2004. Sir2 mediates longevity in the fly through a pathway related to calorie restriction. *Proceedings of the National Academy of Sciences of the United States of America* **101**: 15998-16003.

Rongvaux A, Shea RJ, Mulks MH, Gigot D, Urbain J, Leo O, Andris F. 2002. Pre-B-cell colony-enhancing factor, whose expression is up-regulated in activated lymphocytes, is a nicotinamide phosphoribosyltransferase, a cytosolic enzyme involved in NAD biosynthesis. *European journal of immunology* **32**: 3225-3234.

Rossmann MG, Argos P. 1978. The taxonomy of binding sites in proteins. *Molecular and cellular biochemistry* **21**: 161-182.

Rusche LN, Kirchmaier AL, Rine J. 2002. Ordered nucleation and spreading of silenced chromatin in Saccharomyces cerevisiae. *Molecular biology of the cell* **13**: 2207-2222.

-. 2003. The establishment, inheritance, and function of silenced chromatin in Saccharomyces cerevisiae. *Annual review of biochemistry* **72**: 481-516.

Sanders BD, Jackson B, Brent M, Taylor AM, Dang W, Berger SL, Schreiber SL, Howitz K, Marmorstein R. 2009. Identification and characterization of novel sirtuin inhibitor scaffolds. *Bioorganic & medicinal chemistry* **17**: 7031-7041.

Sanders BD, Jackson B, Marmorstein R. 2010. Structural basis for sirtuin function: what we know and what we don't. *Biochimica et biophysica acta* **1804**: 1604-1616.

Sasaki T, Maier B, Koclega KD, Chruszcz M, Gluba W, Stukenberg PT, Minor W, Scrable H. 2008. Phosphorylation regulates SIRT1 function. *PloS one* **3**: e4020.

Sauve AA, Celic I, Avalos J, Deng H, Boeke JD, Schramm VL. 2001. Chemistry of gene silencing: the mechanism of NAD+-dependent deacetylation reactions. *Biochemistry* **40**: 15456-15463.

Sauve AA, Schramm VL. 2003. Sir2 regulation by nicotinamide results from switching between base exchange and deacetylation chemistry. *Biochemistry* **42**: 9249-9256.

Sauve AA, Wolberger C, Schramm VL, Boeke JD. 2006. The biochemistry of sirtuins. *Annual review of biochemistry* **75**: 435-465.

Schuetz A, Min J, Antoshenko T, Wang CL, Allali-Hassani A, Dong A, Loppnau P, Vedadi M, Bochkarev A, Sternglanz R et al. 2007. Structural basis of inhibition of the human NAD+-dependent deacetylase SIRT5 by suramin. *Structure* **15**: 377-389.

Schwer B, Bunkenborg J, Verdin RO, Andersen JS, Verdin E. 2006. Reversible lysine acetylation controls the activity of the mitochondrial enzyme acetyl-CoA synthetase 2. *Proceedings of the National Academy of Sciences of the United States of America* **103**: 10224-10229.

Schwer B, North BJ, Frye RA, Ott M, Verdin E. 2002. The human silent information regulator (Sir)2 homologue hSIRT3 is a mitochondrial nicotinamide adenine dinucleotide-dependent deacetylase. *The Journal of cell biology* **158**: 647-657.

Schwer B, Verdin E. 2008. Conserved metabolic regulatory functions of sirtuins. *Cell metabolism* **7**: 104-112.

Shimazu T, Hirschey MD, Hua L, Dittenhafer-Reed KE, Schwer B, Lombard DB, Li Y, Bunkenborg J, Alt FW, Denu JM et al. 2010. SIRT3 deacetylates mitochondrial 3-hydroxy-3-methylglutaryl CoA synthase 2 and regulates ketone body production. *Cell metabolism* **12**: 654-661.

Shin DS, Kim HN, Shin KD, Yoon YJ, Kim SJ, Han DC, Kwon BM. 2009. Cryptotanshinone inhibits constitutive signal transducer and activator of transcription 3 function through blocking the dimerization in DU145 prostate cancer cells. *Cancer research* **69**: 193-202.

Sinclair DA. 2005. Toward a unified theory of caloric restriction and longevity regulation. *Mechanisms of ageing and development* **126**: 987-1002.

Sinclair DA, Guarente L. 1997. Extrachromosomal rDNA circles--a cause of aging in yeast. *Cell* **91**: 1033-1042.

Smith BC, Denu JM. 2006. Sir2 protein deacetylases: evidence for chemical intermediates and functions of a conserved histidine. *Biochemistry* **45**: 272-282.

Smith BC, Settles B, Hallows WC, Craven MW, Denu JM. 2011. SIRT3 substrate specificity determined by peptide arrays and machine learning. *ACS chemical biology* **6**: 146-157.

Smith JS, Brachmann CB, Celic I, Kenna MA, Muhammad S, Starai VJ, Avalos JL, Escalante-Semerena JC, Grubmeyer C, Wolberger C et al. 2000. A phylogenetically conserved NAD+-dependent protein deacetylase activity in the Sir2 protein family. *Proceedings of the National Academy of Sciences of the United States of America* **97**: 6658-6663.

Solomon JM, Pasupuleti R, Xu L, McDonagh T, Curtis R, DiStefano PS, Huber LJ. 2006. Inhibition of SIRT1 catalytic activity increases p53 acetylation but does not alter cell survival following DNA damage. *Molecular and cellular biology* **26**: 28-38.

Someya S, Yu W, Hallows WC, Xu J, Vann JM, Leeuwenburgh C, Tanokura M, Denu JM, Prolla TA. 2010. Sirt3 mediates reduction of oxidative damage and prevention of age-related hearing loss under caloric restriction. *Cell* **143**: 802-812.

Spillantini MG, Schmidt ML, Lee VM, Trojanowski JQ, Jakes R, Goedert M. 1997. Alpha-synuclein in Lewy bodies. *Nature* **388**: 839-840.

Stone EM, Pillus L. 1998. Silent chromatin in yeast: an orchestrated medley featuring Sir3p [corrected]. *BioEssays : news and reviews in molecular, cellular and developmental biology* **20**: 30-40.

Stunkel W, Peh BK, Tan YC, Nayagam VM, Wang X, Salto-Tellez M, Ni B, Entzeroth M, Wood J. 2007. Function of the SIRT1 protein deacetylase in cancer. *Biotechnology journal* **2**: 1360-1368.

Tanner KG, Landry J, Sternglanz R, Denu JM. 2000. Silent information regulator 2 family of NAD- dependent histone/protein deacetylases generates a unique product, 1-O-acetyl-ADP-ribose. *Proceedings of the National Academy of Sciences of the United States of America* **97**: 14178-14182.

Tanno M, Sakamoto J, Miura T, Shimamoto K, Horio Y. 2007. Nucleocytoplasmic shuttling of the NAD+-dependent histone deacetylase SIRT1. *The Journal of biological chemistry* **282**: 6823-6832.

Tanny JC, Moazed D. 2001. Coupling of histone deacetylation to NAD breakdown by the yeast silencing protein Sir2: Evidence for acetyl transfer from substrate to an NAD breakdown product. *Proceedings of the National Academy of Sciences of the United States of America* **98**: 415-420.

Tao R, Coleman MC, Pennington JD, Ozden O, Park SH, Jiang H, Kim HS, Flynn CR, Hill S, Hayes McDonald W et al. 2010. Sirt3-mediated deacetylation of evolutionarily conserved lysine 122 regulates MnSOD activity in response to stress. *Molecular cell* **40**: 893-904.

Tennen RI, Berber E, Chua KF. 2010. Functional dissection of SIRT6: identification of domains that regulate histone deacetylase activity and chromatin localization. *Mechanisms of ageing and development* **131**: 185-192.

Tissenbaum HA, Guarente L. 2001. Increased dosage of a sir-2 gene extends lifespan in Caenorhabditis elegans. *Nature* **410**: 227-230.

Trapp J, Meier R, Hongwiset D, Kassack MU, Sippl W, Jung M. 2007. Structure-activity studies on suramin analogues as inhibitors of NAD+-dependent histone deacetylases (sirtuins). *ChemMedChem* **2**: 1419-1431.

Tsai SL, Suk FM, Wang CI, Liu DZ, Hou WC, Lin PJ, Hung LF, Liang YC. 2007. Anti-tumor potential of 15,16-dihydrotanshinone I against breast adenocarcinoma through inducing G1 arrest and apoptosis. *Biochemical pharmacology* **74**: 1575-1586.

Tsang AW, Escalante-Semerena JC. 1998. CobB, a new member of the SIR2 family of eucaryotic regulatory proteins, is required to compensate for the lack of nicotinate mononucleotide:5,6-dimethylbenzimidazole phosphoribosyltransferase activity in cobT

mutants during cobalamin biosynthesis in Salmonella typhimurium LT2. *The Journal of biological chemistry* **273**: 31788-31794.

Tsuchiya M, Dang N, Kerr EO, Hu D, Steffen KK, Oakes JA, Kennedy BK, Kaeberlein M. 2006. Sirtuin-independent effects of nicotinamide on lifespan extension from calorie restriction in yeast. *Aging cell* **5**: 505-514.

Turner BM. 1991. Histone acetylation and control of gene expression. *Journal of cell science* **99 (Pt 1)**: 13-20.

Vakhrusheva O, Smolka C, Gajawada P, Kostin S, Boettger T, Kubin T, Braun T, Bober E. 2008. Sirt7 increases stress resistance of cardiomyocytes and prevents apoptosis and inflammatory cardiomyopathy in mice. *Circulation research* **102**: 703-710.

Vaquero A, Scher M, Lee D, Erdjument-Bromage H, Tempst P, Reinberg D. 2004. Human SirT1 interacts with histone H1 and promotes formation of facultative heterochromatin. *Molecular cell* **16**: 93-105.

Vaquero A, Scher MB, Lee DH, Sutton A, Cheng HL, Alt FW, Serrano L, Sternglanz R, Reinberg D. 2006. SirT2 is a histone deacetylase with preference for histone H4 Lys 16 during mitosis. *Genes & development* **20**: 1256-1261.

Vaziri H, Dessain SK, Ng Eaton E, Imai SI, Frye RA, Pandita TK, Guarente L, Weinberg RA. 2001. hSIR2(SIRT1) functions as an NAD-dependent p53 deacetylase. *Cell* **107**: 149-159.

Vempati RK, Jayani RS, Notani D, Sengupta A, Galande S, Haldar D. 2010. p300-mediated acetylation of histone H3 lysine 56 functions in DNA damage response in mammals. *The Journal of biological chemistry* **285**: 28553-28564.

Voelter-Mahlknecht S, Ho AD, Mahlknecht U. 2005. FISH-mapping and genomic organization of the NAD-dependent histone deacetylase gene, Sirtuin 2 (Sirt2). *International journal of oncology* **27**: 1187-1196.

Voelter-Mahlknecht S, Mahlknecht U. 2006. Cloning, chromosomal characterization and mapping of the NAD-dependent histone deacetylases gene sirtuin 1. *International journal of molecular medicine* **17**: 59-67.

Walter RD. 1979. Inhibition of lactate dehydrogenase activity from Dirofilaria immitis by suramin. *Tropenmedizin und Parasitologie* **30**: 463-465.

Walter RD, Schulz-Key H. 1980. Onchocerca volvulus: effect of suramin on lactate dehydrogenase and malate dehydrogenase. *Tropenmedizin und Parasitologie* **31**: 55-58.

Wang C, Wheeler CT, Alberico T, Sun X, Seeberger J, Laslo M, Spangler E, Kern B, de Cabo R, Zou S. 2011. The effect of resveratrol on lifespan depends on both gender and dietary nutrient composition in Drosophila melanogaster. *Age (Dordr)*.

Wang F, Nguyen M, Qin FX, Tong Q. 2007. SIRT2 deacetylates FOXO3a in response to oxidative stress and caloric restriction. *Aging cell* **6**: 505-514.

Wang F, Tong Q. 2009. SIRT2 suppresses adipocyte differentiation by deacetylating FOXO1 and enhancing FOXO1's repressive interaction with PPARgamma. *Molecular biology of the cell* **20**: 801-808.

Wang J, Ho L, Qin W, Rocher AB, Seror I, Humala N, Maniar K, Dolios G, Wang R, Hof PR et al. 2005. Caloric restriction attenuates beta-amyloid neuropathology in a mouse model of Alzheimer's disease. *FASEB journal : official publication of the Federation of American Societies for Experimental Biology* **19**: 659-661.

Wang RH, Sengupta K, Li C, Kim HS, Cao L, Xiao C, Kim S, Xu X, Zheng Y, Chilton B et al. 2008. Impaired DNA damage response, genome instability, and tumorigenesis in SIRT1 mutant mice. *Cancer cell* **14**: 312-323.

Wegener D, Wirsching F, Riester D, Schwienhorst A. 2003. A Fluorogenic Histone Deacetylase Assay Well Suited for High-Throughput Activity Screening. *Chemistry & Biology* **10**: 61-68.

Wood JG, Rogina B, Lavu S, Howitz K, Helfand SL, Tatar M, Sinclair D. 2004. Sirtuin activators mimic caloric restriction and delay ageing in metazoans. *Nature* **430**: 686-689.

Wu Z, Wu L, Li L, Tashiro S, Onodera S, Ikejima T. 2004a. p53-mediated cell cycle arrest and apoptosis induced by shikonin via a caspase-9-dependent mechanism in human malignant melanoma A375-S2 cells. *J Pharmacol Sci* **94**: 166-176.

Wu Z, Wu LJ, Li LH, Tashiro S, Onodera S, Ikejima T. 2004b. Shikonin regulates HeLa cell death via caspase-3 activation and blockage of DNA synthesis. *Journal of Asian natural products research* **6**: 155-166.

Yang B, Zwaans BM, Eckersdorff M, Lombard DB. 2009. The sirtuin SIRT6 deacetylates H3 K56Ac in vivo to promote genomic stability. *Cell Cycle* **8**: 2662-2663.

Yang H, Lavu S, Sinclair DA. 2006. Nampt/PBEF/Visfatin: a regulator of mammalian health and longevity? *Experimental gerontology* **41**: 718-726.

Yang Y, Fu W, Chen J, Olashaw N, Zhang X, Nicosia SV, Bhalla K, Bai W. 2007. SIRT1 sumoylation regulates its deacetylase activity and cellular response to genotoxic stress. *Nature cell biology* **9**: 1253-1262.

Yeung F, Hoberg JE, Ramsey CS, Keller MD, Jones DR, Frye RA, Mayo MW. 2004. Modulation of NF-kappaB-dependent transcription and cell survival by the SIRT1 deacetylase. *The EMBO journal* **23**: 2369-2380.

Yu LR, Zhu Z, Chan KC, Issaq HJ, Dimitrov DS, Veenstra TD. 2007. Improved titanium dioxide enrichment of phosphopeptides from HeLa cells and high confident phosphopeptide identification by cross-validation of MS/MS and MS/MS/MS spectra. *Journal of proteome research* **6**: 4150-4162.

Yuan H, Marmorstein R. 2012. Structural Basis for Sirtuin Activity and Inhibition. *The Journal of biological chemistry*.

Yuan Z, Zhang X, Sengupta N, Lane WS, Seto E. 2007. SIRT1 regulates the function of the Nijmegen breakage syndrome protein. *Molecular cell* **27**: 149-162.

Zannini L, Buscemi G, Kim JE, Fontanella E, Delia D. 2012. DBC1 phosphorylation by ATM/ATR inhibits SIRT1 deacetylase in response to DNA damage. *Journal of molecular cell biology*.

Zhang Y, Au Q, Zhang M, Barber JR, Ng SC, Zhang B. 2009. Identification of a small molecule SIRT2 inhibitor with selective tumor cytotoxicity. *Biochemical and biophysical research communications* **386**: 729-733.

Zhao K, Chai X, Clements A, Marmorstein R. 2003a. Structure and autoregulation of the yeast Hst2 homolog of Sir2. *Nature structural biology* **10**: 864-871.

Zhao K, Chai X, Marmorstein R. 2003b. Structure of the yeast Hst2 protein deacetylase in ternary complex with 2'-O-acetyl ADP ribose and histone peptide. *Structure* **11**: 1403-1411.

-. 2004a. Structure and substrate binding properties of cobB, a Sir2 homolog protein deacetylase from Escherichia coli. *Journal of molecular biology* **337**: 731-741.

Zhao K, Harshaw R, Chai X, Marmorstein R. 2004b. Structural basis for nicotinamide cleavage and ADP-ribose transfer by NAD(+)-dependent Sir2 histone/protein deacetylases. *Proceedings of the National Academy of Sciences of the United States of America* **101**: 8563-8568.

Zhao W, Kruse JP, Tang Y, Jung SY, Qin J, Gu W. 2008. Negative regulation of the deacetylase SIRT1 by DBC1. *Nature* **451**: 587-590.

Zschoernig B, Mahlknecht U. 2009. Carboxy-terminal phosphorylation of SIRT1 by protein kinase CK2. *Biochemical and biophysical research communications* **381**: 372-377.

Danksagung

Mein besonderer Dank gilt Frau Prof. Ann Ehrenhofer-Murray für die Bereitstellung dieses großartigen Projekts. Ebenso dafür, dass sie sich immer die Zeit genommen hat, um mich bei der Projektplanung sowie Problemen und Versuchen zu beraten und zu unterstützen. Des Weiteren danke ich ihr für die Möglichkeit mein fachliches Wissen, sowie meine sozialen Kontakte auf Tagungen und Weiterbildungen zu erweitern.

Ein großer Dank geht nach Berlin, an die Screening-Unit vom FMP, die einen sehr großen Beitrag zur Etablierung des Fluoreszenz-Assays geleistet haben. Besonders bedanke ich mich bei Carola Seyffarth und Martin Neuenschwander, die mich bei der Durchführung des Screens der ChemBioNet Bank tatkräftig unterstütz haben, sowie Edgar Specker, der mir bei der Validierung der Substanzen zur Seite stand.

Ich bedanke mich bei Prof. Martin Schuler und Dr. Frank Breitenbücher für die Möglichkeit die *in vivo* Experimente in ihrem Labor durchzuführen, sowie für die Bereitstellung der Zelllinien und die Unterstützung bei der Versuchsplanung und Auswertung. Außerdem danke ich allen Mitgliedern der AG Schuler, dass sie mich während meiner Besuche so herzlich empfangen und aufgenommen haben.

Weiterhin möchte ich mich bei Prof. Markus Kaiser für seinen persönlichen Rat bedanken.

Den ehemaligen und derzeitigen Mitarbeitern der AG Genetik danke ich für die gute Zusammenarbeit und das angenehme Arbeitsklima. Martina, Rolf, Anda und Nina danke ich für die technische Unterstützung im Labor. Besonders danke ich der „Mittagsgruppe“ Rita, Karolin, Maria, Tanja, Chrissi sowie Anke für die interessanten und abwechslungsreichen Diskussionen über aktuelle Themen des Alltags aber auch über Probleme und Schwierigkeiten im Labor.

Abschließend möchte ich mich von ganzem Herzen bei meinen Eltern bedanken, die mir das Studium ermöglicht haben und mich auch während der Promotion in jeglicher Hinsicht unterstützt haben. Roberto danke ich für die abwechslungsreichen und lustigen Skype-Abende, die mich immer wieder aufgebaut haben, wenn ich demotiviert und schlecht gelaunt war.